



Topological aspects in solid state chemistry



© Nature

Claudia Felser



Topology



\mathbb{R}^2



\mathbb{R}^2



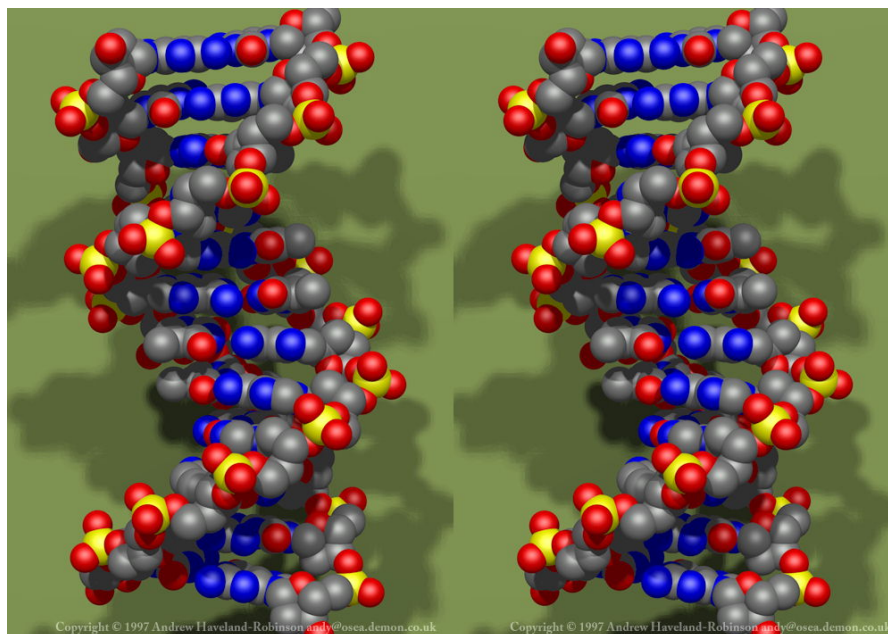
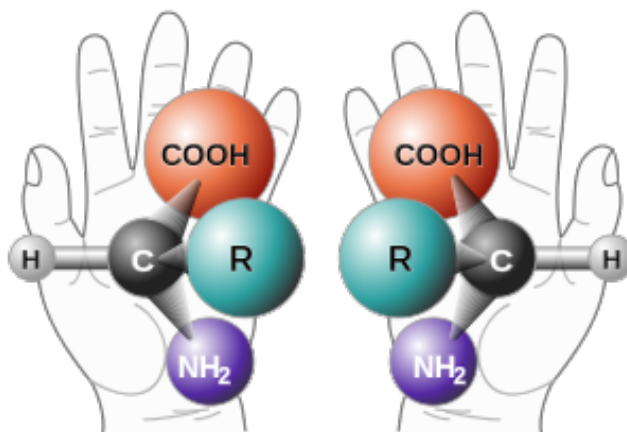
\mathbb{R}^2





Topology in Chemistry

Molecules with different chiralities can have different physical and chemical properties

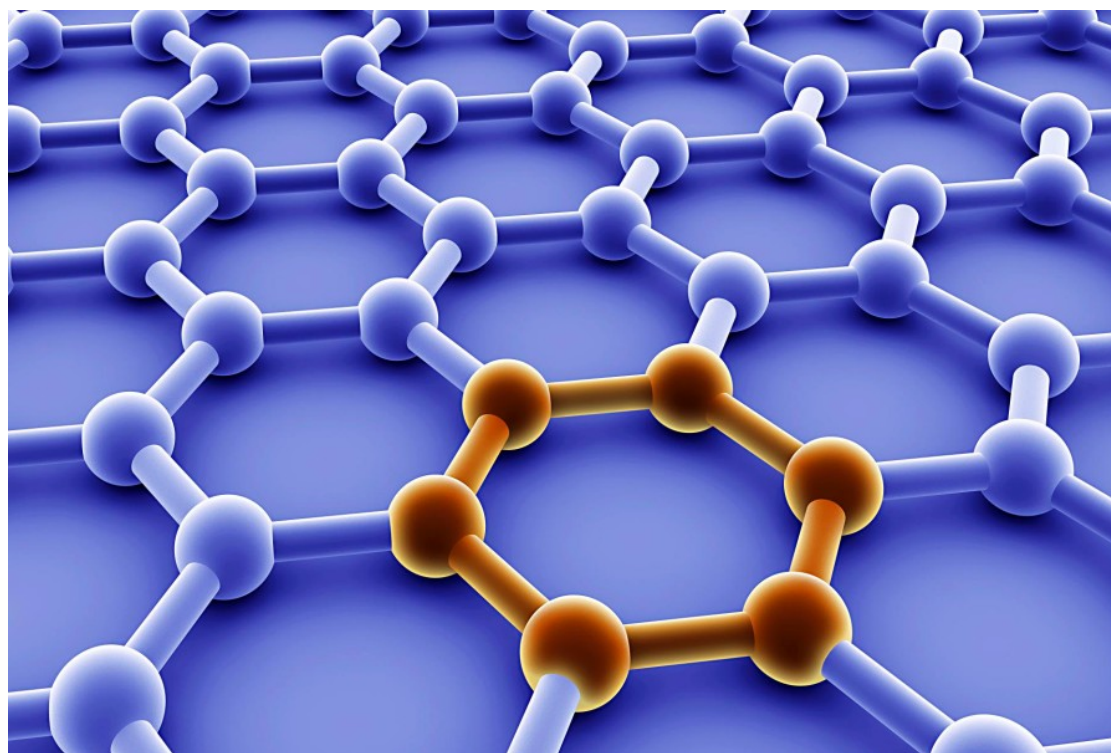
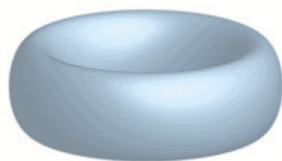
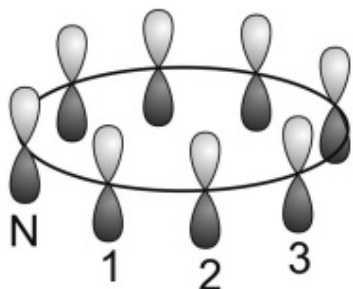
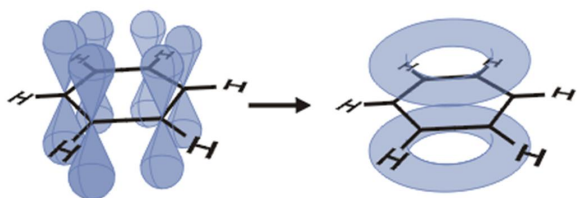
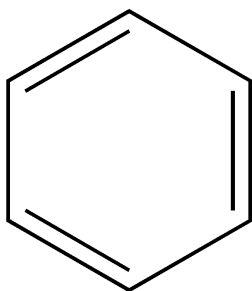




Topology in Chemistry

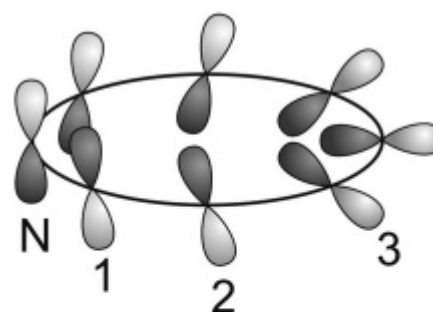
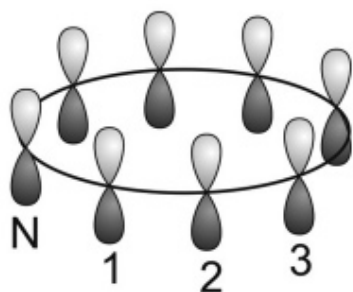
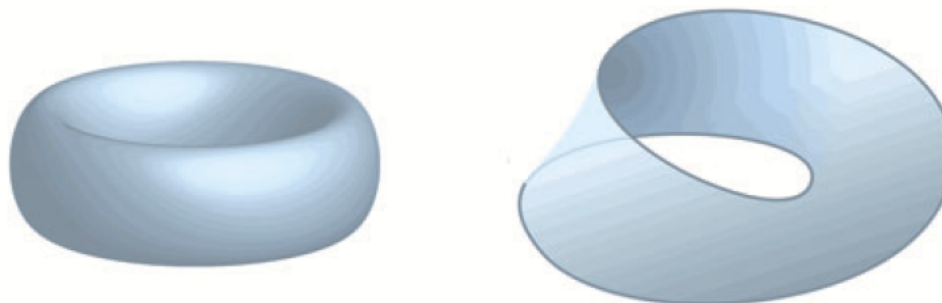
Aromatic compounds

- Aromatic with $(4n + 2)$ π -electrons
- The symmetry counts





Topology in Chemistry



Magic electron numbers of π -electrons

Hückel:

$4n+2$ aromatic

$4n$ antiaromatic

Möbius

$4n$ aromatic

$4n+2$ antiaromatic



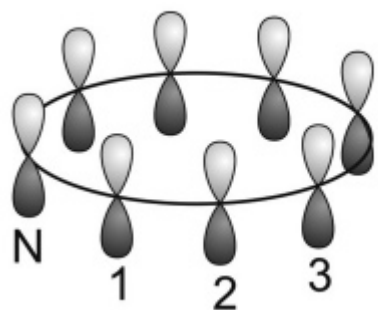
Hückel and Möbius Aromaticity

ORGANIC CHEMISTRY

Aromatics with a twist

Rainer Herges

The properties of flat aromatic molecules are well known to chemists, but some non-planar aromatics remain a mystery. A molecule that can twist into a Möbius band on command might shed light on their features.



Möbius Annulenes

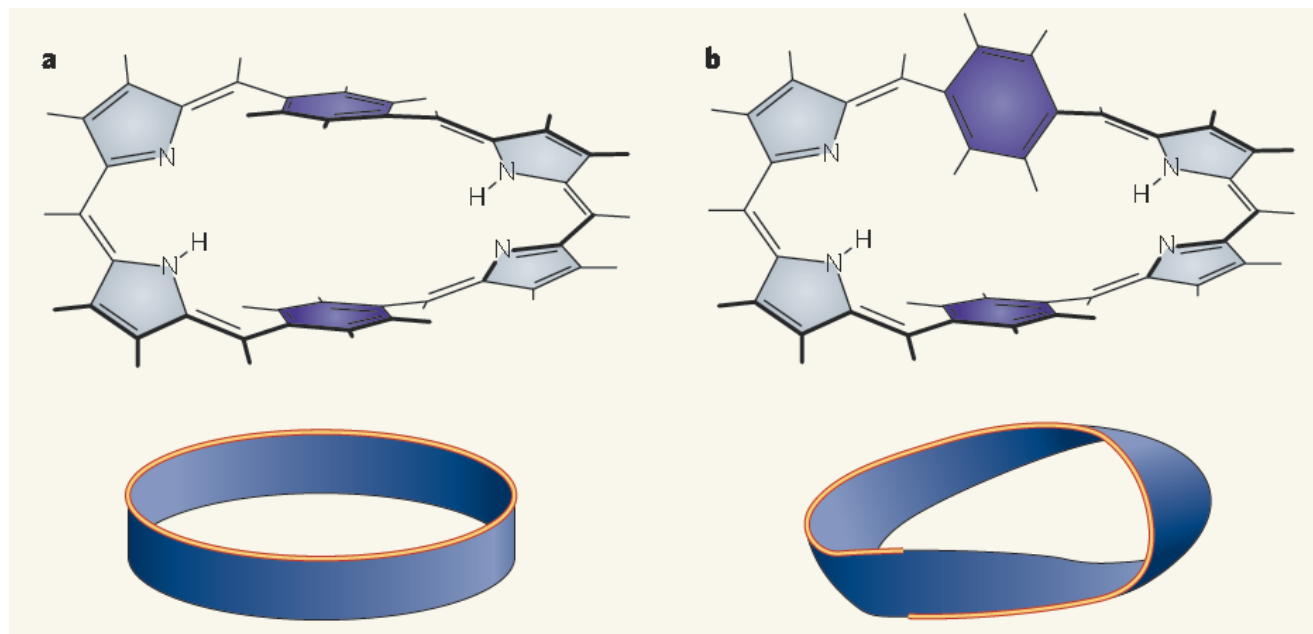
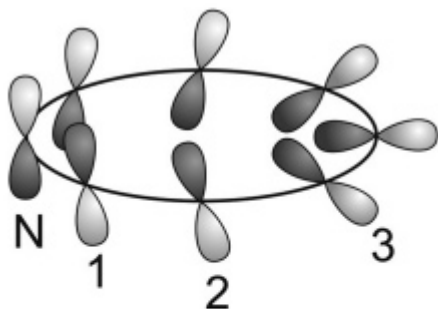
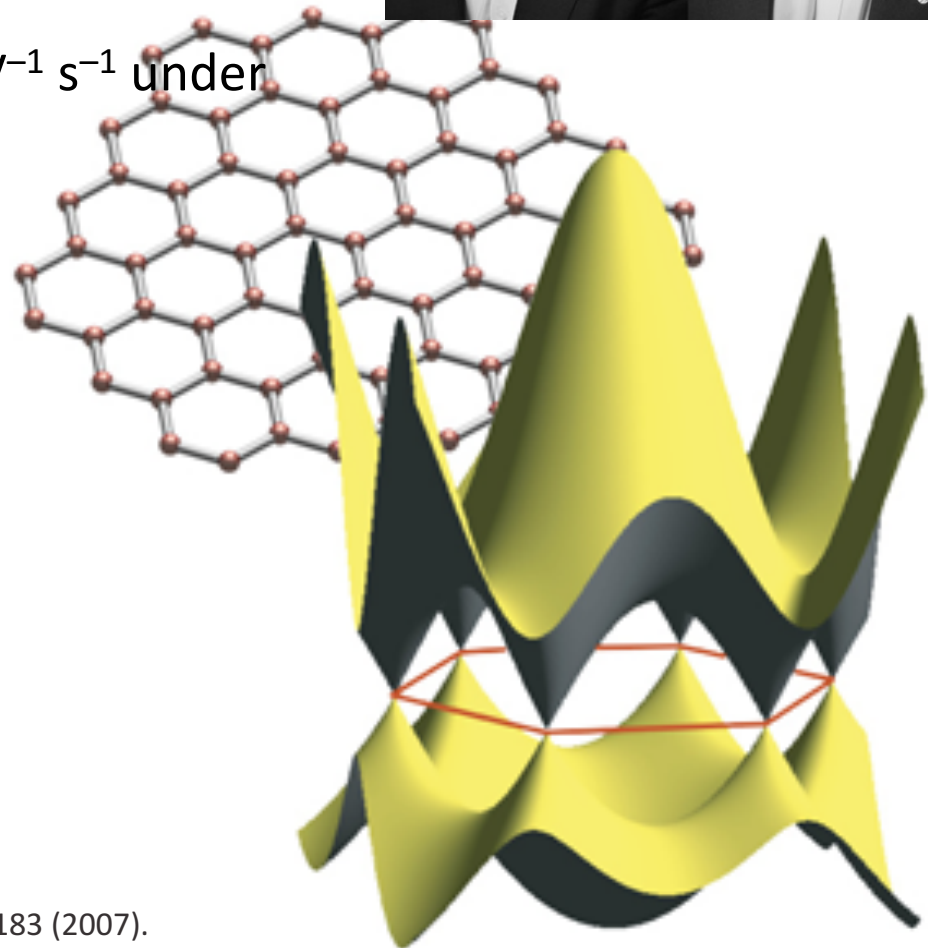
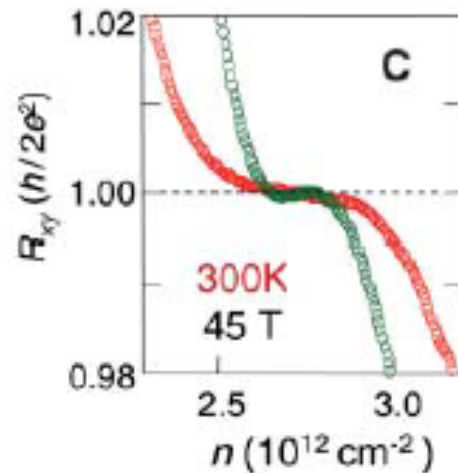


Figure 2 | A molecular topological switch. Latos-Grażyński and colleagues¹ have made a compound that is antiaromatic in nonpolar solvents, but not in polar solvents. **a**, In nonpolar solvents, the two benzene rings (purple) in the molecule are parallel, and the molecule is a two-sided, non-twisted band. **b**, In polar solvents, the upper benzene ring twists by 90°, so that the molecule becomes a one-sided, Möbius structure. This conformational change alters the aromaticity of the molecule.



Graphene

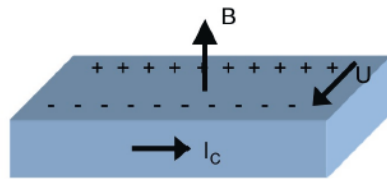
- Graphene's conductivity exhibits values close to the conductivity quantum e^2/h per carrier type
- Graphene's charge carriers can be tuned continuously between electrons and holes in concentrations $n = 10^{13} \text{ cm}^{-2}$
- Mobilities μ can exceed $15,000 \text{ cm}^2 \text{ V}^{-1} \text{ s}^{-1}$ under ambient conditions
- InSb has $\mu \approx 77,000 \text{ cm}^2 \text{ V}^{-1} \text{ s}^{-1}$



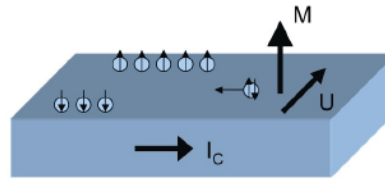


Family of Quantum Hall Effects

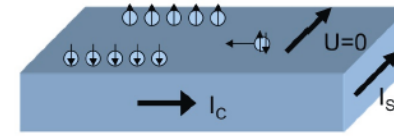
Hall effect
1879



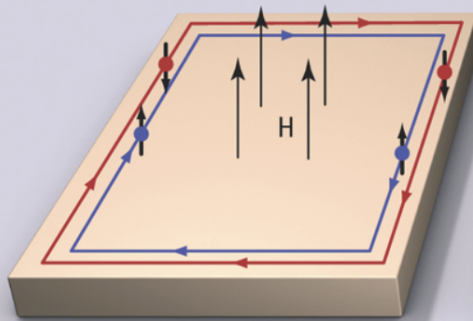
Anomalous Hall effect
1881



Spin Hall effect
2004

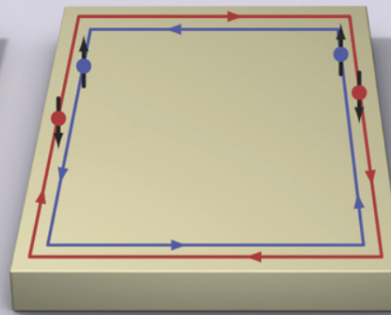


Quantum Hall
(1980)



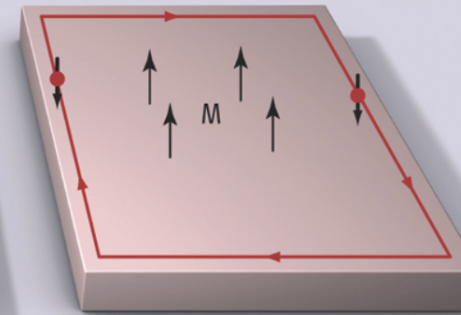
Quantum Hall

Quantum spin Hall
(2007)



Quantum spin Hall

Quantum anomalous Hall
(2013)



Quantum anomalous Hall



1985

Klaus von Klitzing

1998

Horst Ludwig Störmer and Daniel Tsui

2010

Andre Geim and Konstantin Novoselov

2016

David Thouless, Duncan Haldane und Michael Kosterlitz



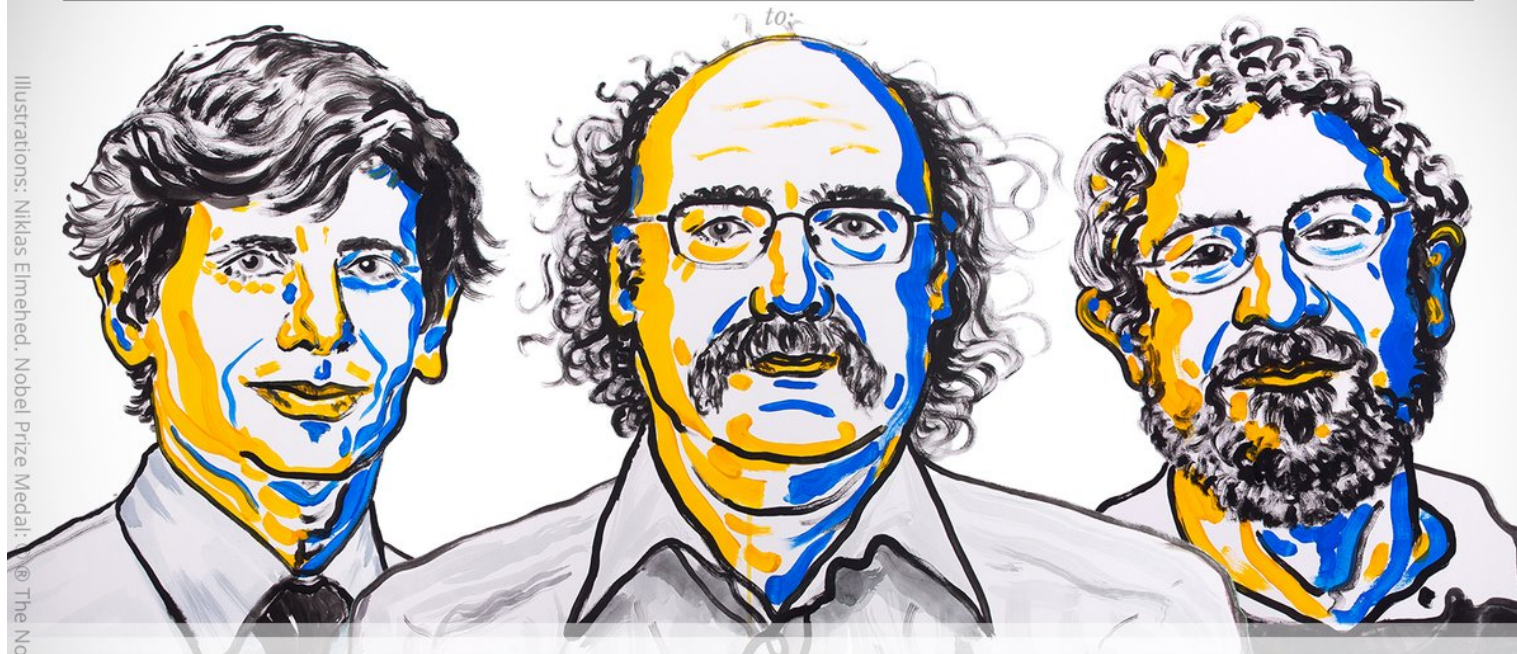
"For the greatest benefit to mankind"
Alfred Nobel



The Royal Swedish Academy of Sciences has decided to award the

2016 NOBEL PRIZE IN PHYSICS

Illustrations: Niklas Elmehed, Nobel Prize Medal: © The Nobel Foundation, Photo: Lovisa Engblom.



David J. Thouless
F. Duncan M. Haldane
J. Michael Kosterlitz

*"for theoretical discoveries of topological phase transitions
and topological phases of matter"*

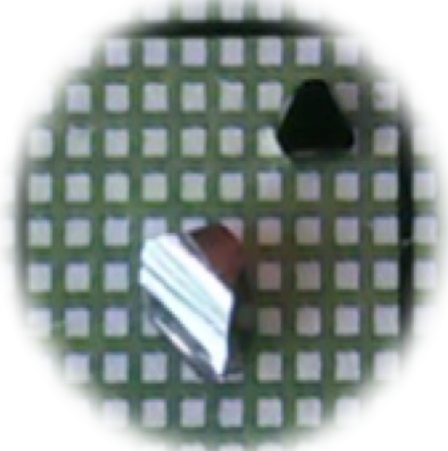


Particles – Universe – Condensed matter

Quantum field theory – Berry curvature

Dirac

Cd_3As_2
Guido Kreiner



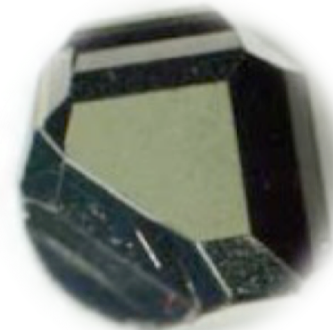
Higgs

YMnO_3
Lichtenberg Spaldin



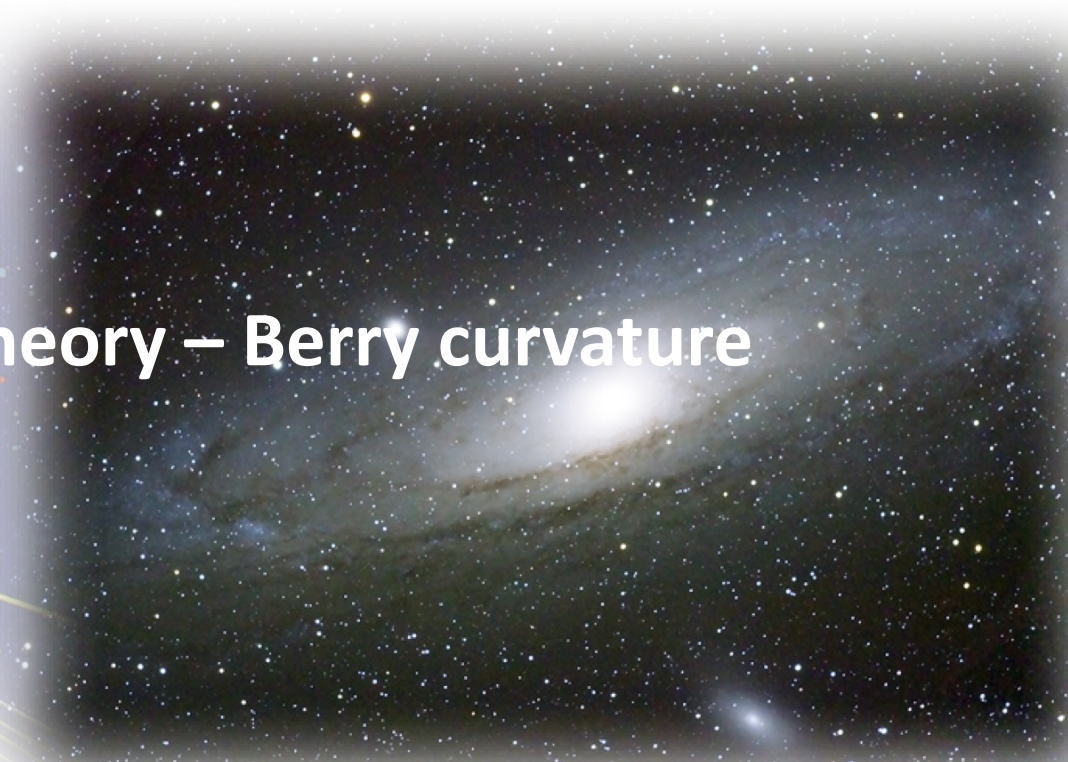
Weyl

TaAs
Vicky Süß, Marcus Schmidt



Majorana

YPtBi
Chandra Shekhar





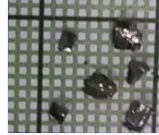
Topology - Electronic structure



Topology – interdisciplinary

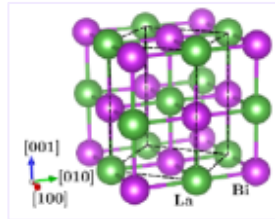
Chemistry

Real space - local
Crystals



LaBi

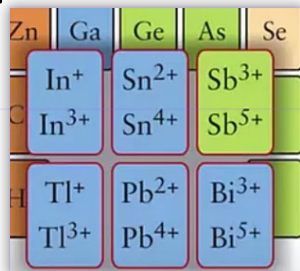
Crystal structure



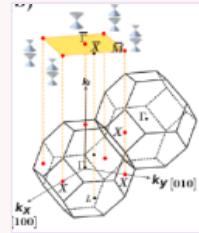
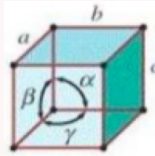
Position of the atoms
Orbitals

Check	WP	Representative
<input type="checkbox"/>	8g	x,y,z
<input type="checkbox"/>	4f	x,1/2,z
<input type="checkbox"/>	4e	x,0,z
<input checked="" type="checkbox"/>	4d	x,x,z
<input checked="" type="checkbox"/>	2c	1/2,0,z
<input type="checkbox"/>	1b	1/2,1/2,z
<input checked="" type="checkbox"/>	1a	0,0,z

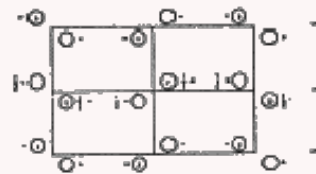
Inert pair effect



Symmetry



Local symmetry

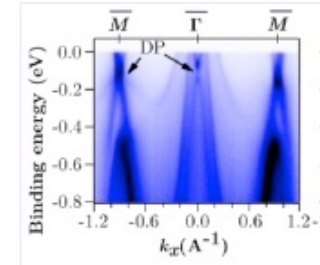
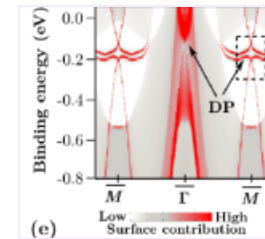


Relativistic effects

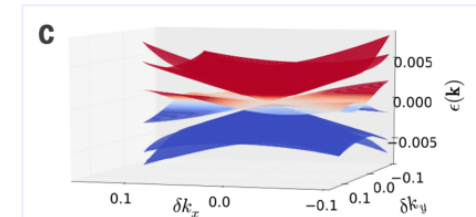
Physics

Recipro. space - delocalized
Brillouin zone

Electronic structure



Band connectivity

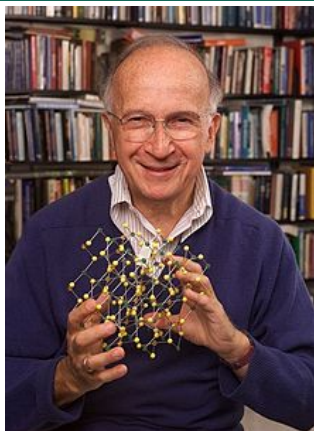


Darwin term

$$H_{\text{Darwin}} = \frac{\hbar^2}{8m_e^2 c^2} (\Delta V)$$

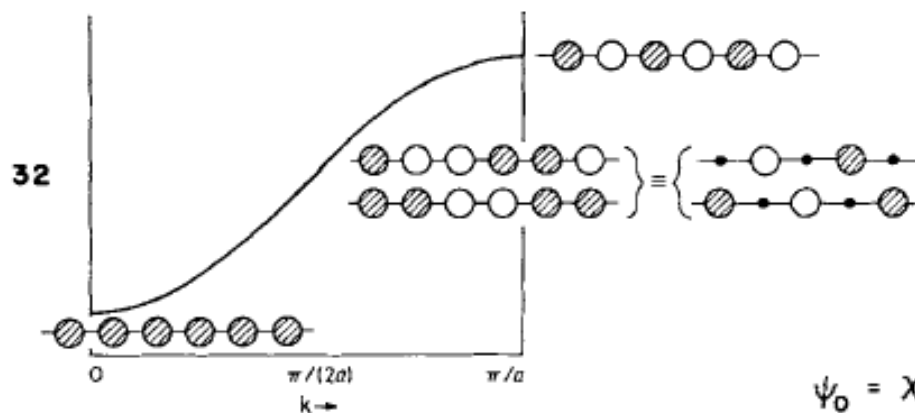
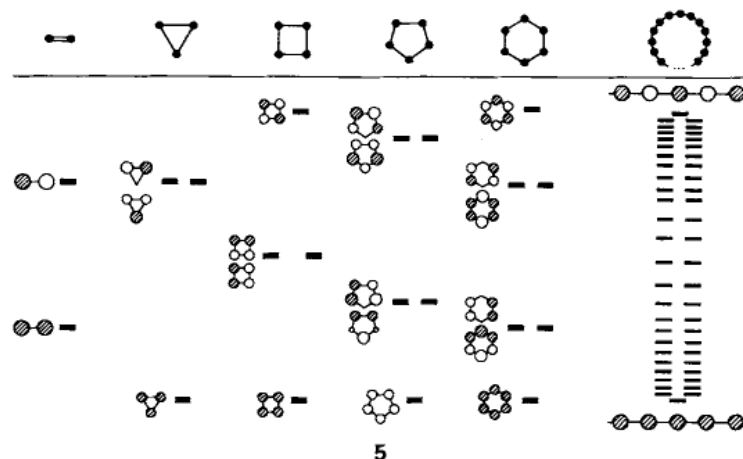


How to find a band structure



How Chemistry and Physics Meet in the Solid State

By Roald Hoffmann*



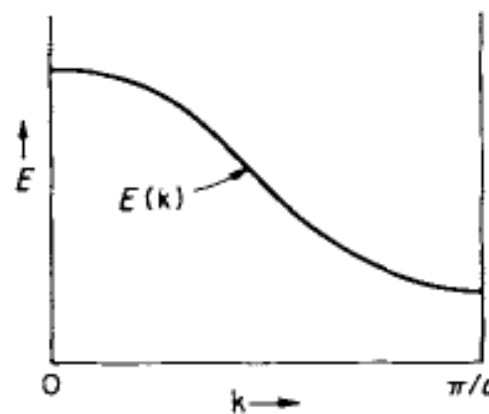
$$\psi_0 = \chi_0 + \chi_1 + \chi_2 + \chi_3 + \dots$$



$$\psi_{\pi/a} = \chi_0 - \chi_1 + \chi_2 - \chi_3 + \dots$$



9



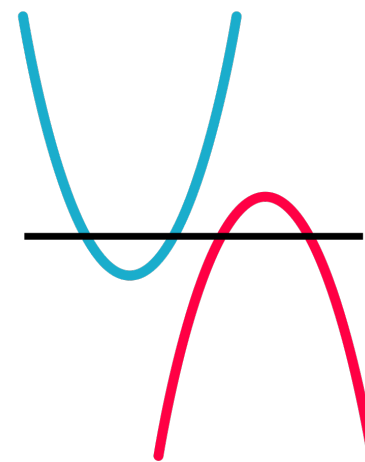
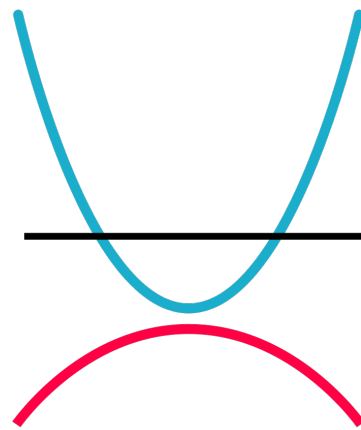
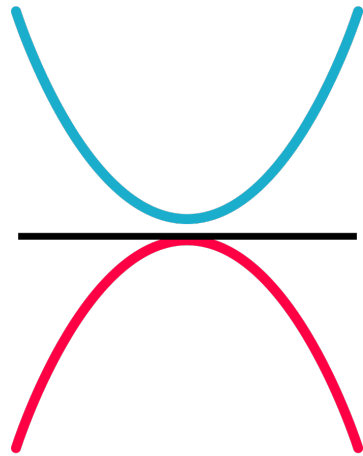


Insulator – Semiconductor – Metal

Insulator/Semiconductor

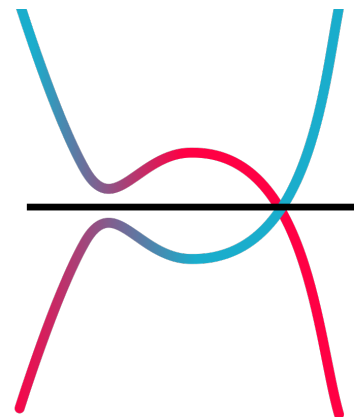
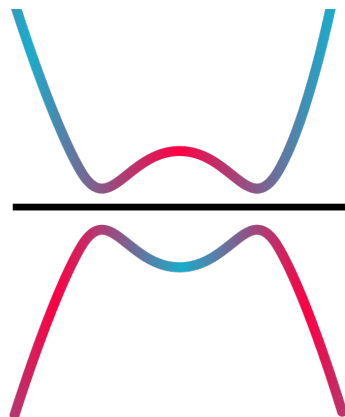
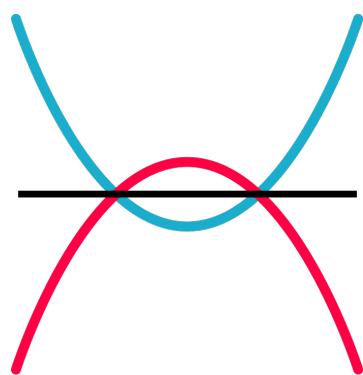
Metal

Semimetal



Topological Insulator/Semiconductor

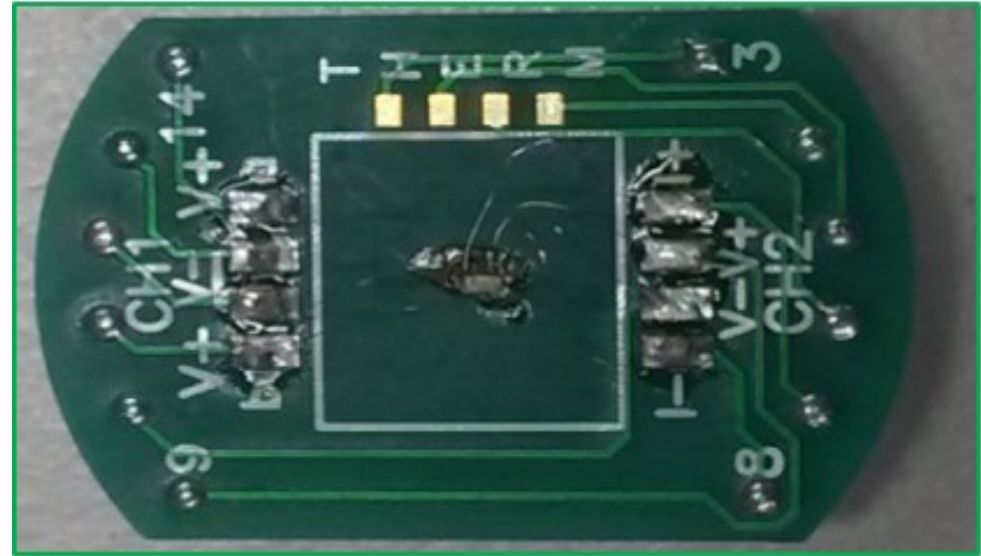
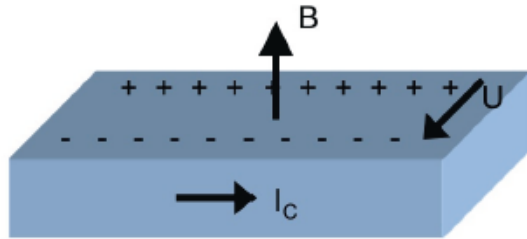
Dirac/Weyl-Semimetal





Resistance Measurement

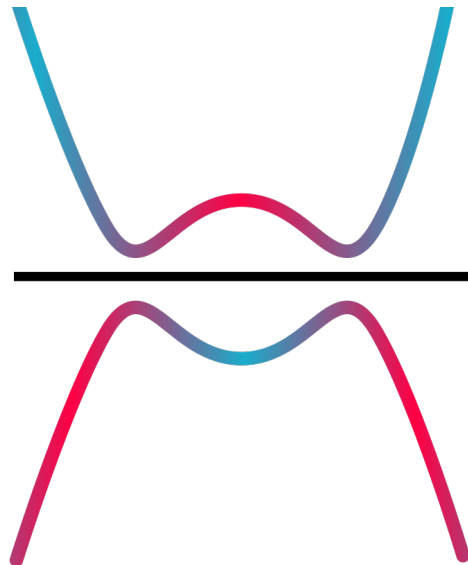
Hall effect
1879



- We measure the resistance without and with a magnetic field
- ? Metal, semiconductor, or insulator
 - ? Electron or hole conductivity
 - ? Resistance in a magnetic field: Magnetoresistance



Topological Insulators



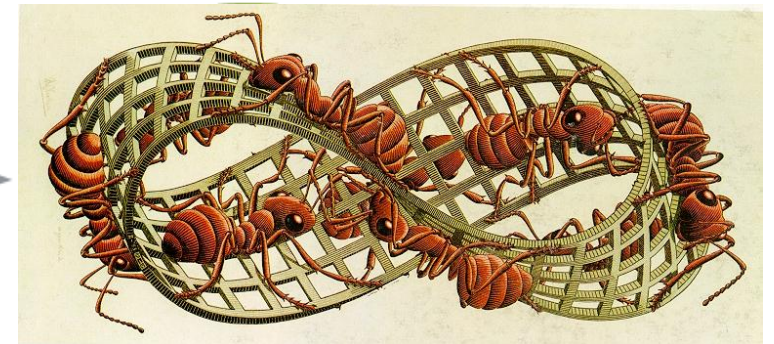
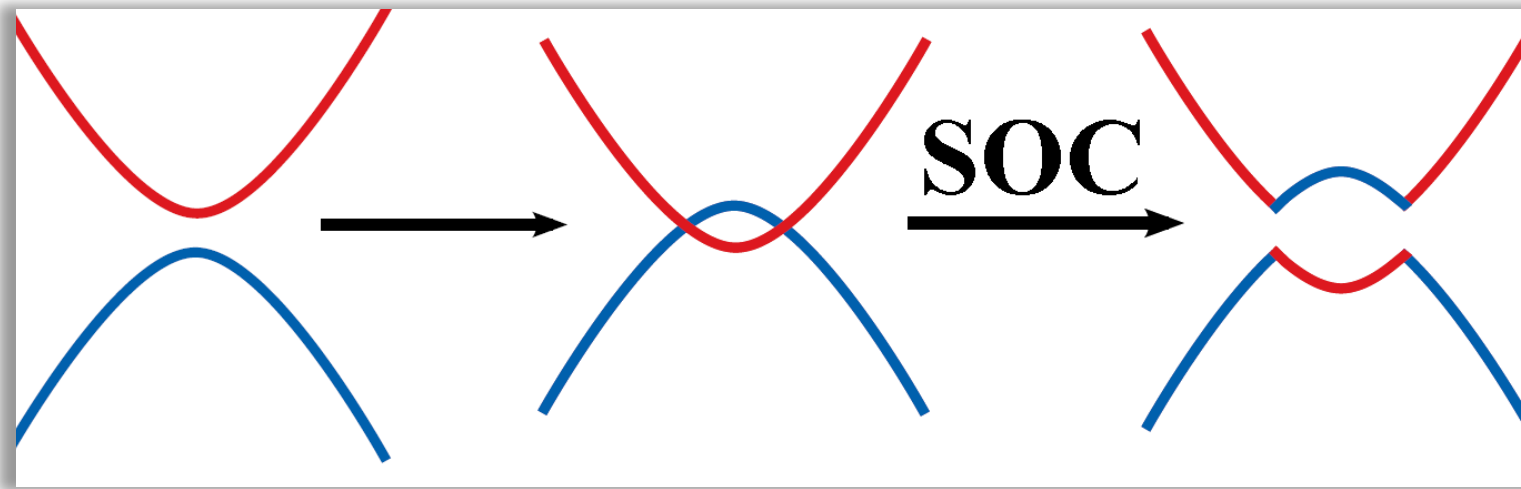


Trivial and Topological Insulators

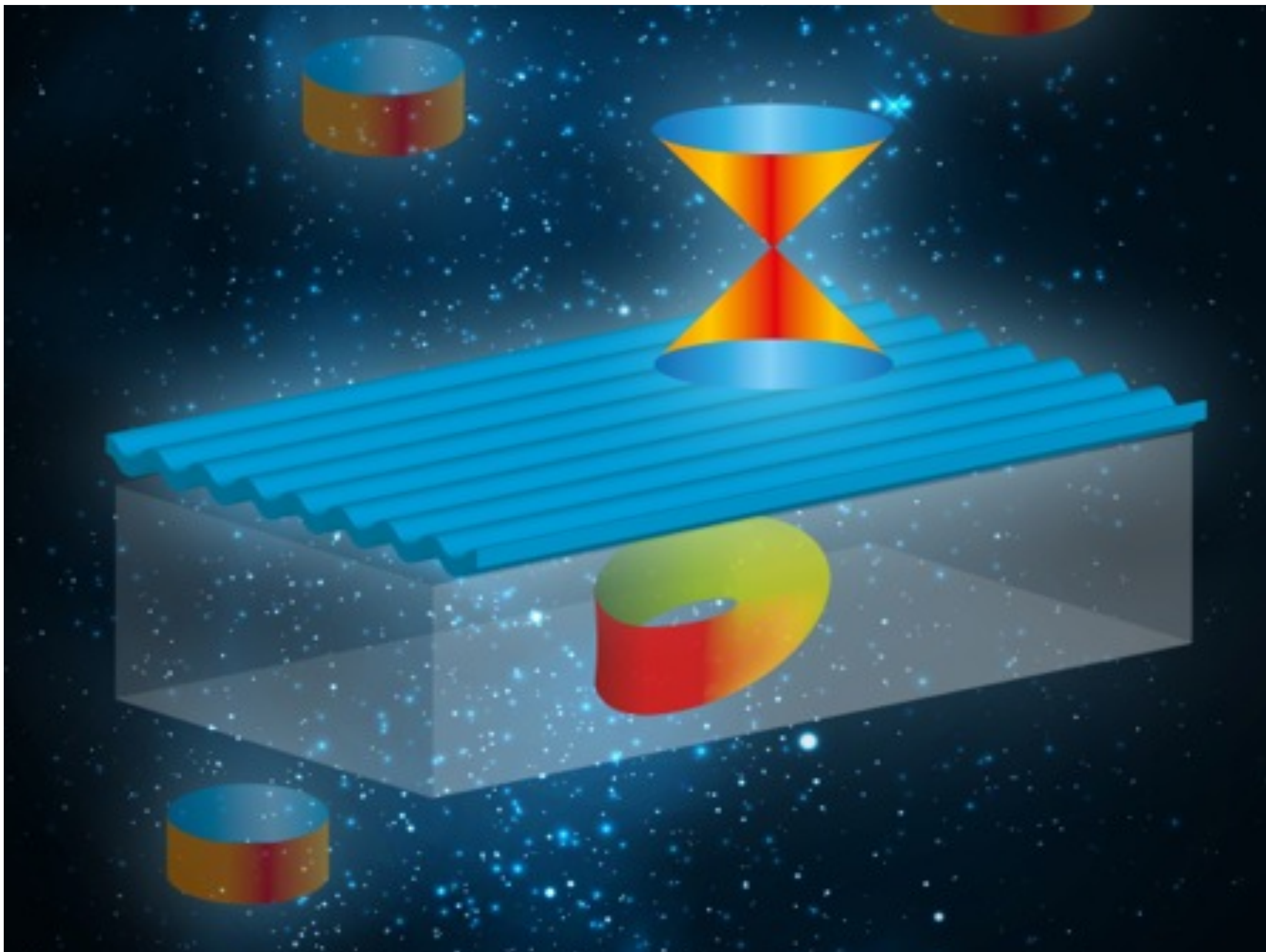
Trivial semiconductor
CdS

Topological Insulator
Without spin orbit coupling

Topological Insulator
With spin orbit coupling



M. C. Escher





Topological Insulators

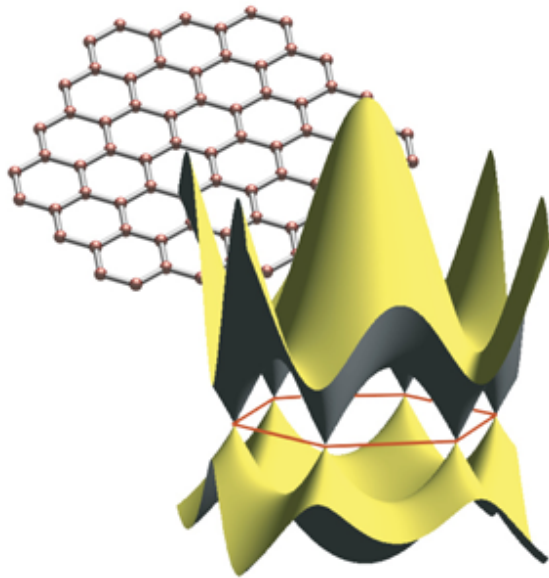
Z₂ Topological Order and the Quantum Spin Hall Effect

C.L. Kane and E.J. Mele

Department of Physics and Astronomy, University of Pennsylvania, Philadelphia, Pennsylvania 19104, USA
(Received 22 June 2005; published 28 September 2005)

The quantum spin Hall (QSH) phase is a time reversal invariant electronic state with a bulk electronic band gap that supports the transport of charge and spin in gapless edge states. We show that this phase is associated with a novel Z₂ topological invariant, which distinguishes it from an ordinary insulator. The Z₂ classification, which is defined for time reversal invariant Hamiltonians, is analogous to the Chern number classification of the quantum Hall effect. We establish the Z₂ order of the QSH phase in the two band model of graphene and propose a generalization of the formalism applicable to multiband and interacting systems.

Heavy insulating elements



First prediction in graphene by Kane

H 2.20																	He
Li 0.98	Be 1.57											B 2.04	C 2.55	N 3.04	O 3.44	F 3.98	Ne
Na 0.93	Mg 1.31											Al 1.61	Si 1.90	P 2.19	S 2.58	Cl 3.16	Ar
K 0.82	Ca 1.00	Sc 1.36	Ti 1.54	V 1.63	Cr 1.66	Mn 1.55	Fe 1.83	Co 1.88	Ni 1.91	Cu 1.90	Zn 1.65	Ga 1.81	Ge 2.01	As 2.18	Se 2.55	Br 2.96	Kr 3.00
Rb 0.82	Sr 0.95	Y 1.22	Zr 1.33	Nb 1.60	Mo 2.16	Tc 1.90	Ru 2.20	Rh 2.28	Pd 2.20	Ag 1.93	Cd 1.69	In 1.78	Sn 1.96	Sb 2.05	Te 2.10	I 2.66	Xe 2.60
Cs 0.79	Ba 0.89																
Fr 0.70	Ra 0.90	Hf 1.30	Ta 1.50	W 1.70	Re 1.90	Os 2.20	Ir 2.20	Pt 2.20	Au 2.40	Hg 1.90	Tl 1.80	Pb 1.80	Bi 1.90	Po 2.00	At 2.20	Rn	
		La 1.10	Ce 1.12	Pr 1.13	Nd 1.14	Pm 1.13	Sm 1.17	Eu 1.20	Gd 1.20	Tb 1.10	Dy 1.22	Ho 1.23	Er 1.24	Tm 1.25	Yb 1.10	Lu 1.27	
		Ac 1.10	Th 1.30	Pa 1.50	U 1.70	Np 1.30	Pu 1.28	Am 1.13	Cm 1.28	Bk 1.30	Cf 1.30	Es 1.30	Fm 1.30	Md 1.30	No 1.30	Lr 1.30	

$$\lambda_{\text{SOC}} \sim Z^2 \text{ for valence shells}$$



Topological Insulators

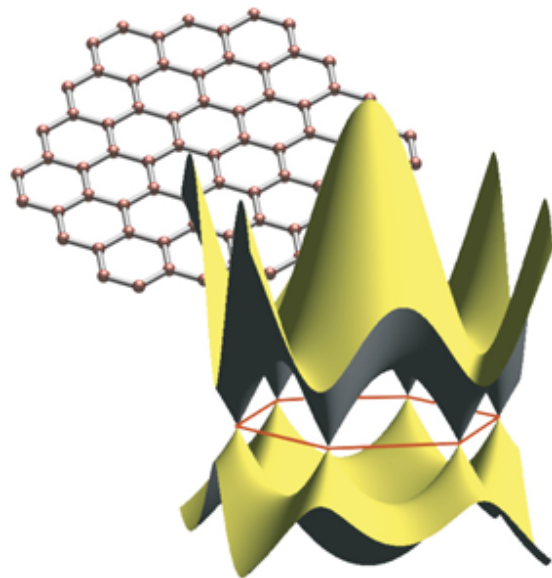
Z₂ Topological Order and the Quantum Spin Hall Effect

C. L. Kane and E. J. Mele

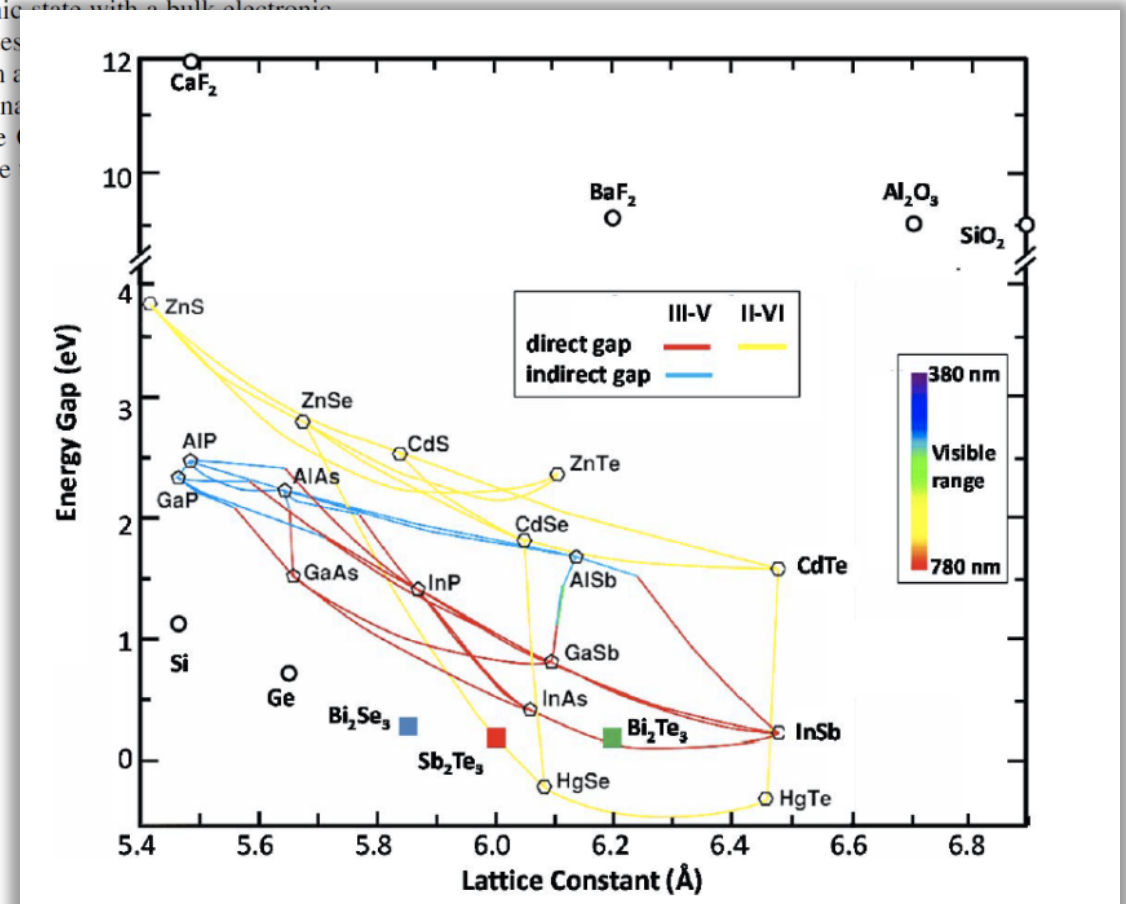
Department of Physics and Astronomy, University of Pennsylvania, Philadelphia, Pennsylvania 19104, USA
(Received 22 June 2005; published 28 September 2005)

Heavy insulating binaries

The quantum spin Hall (QSH) phase is a time reversal invariant electronic state with a bulk electronic band gap that supports the transport of charge and spin in gapless edge states associated with a novel Z₂ topological invariant, which distinguishes it from a conventional insulator. This classification, which is defined for time reversal invariant Hamiltonians, is analogous to the classification of the quantum Hall effect. We establish the Z₂ order of the QSH phase in a model of graphene and propose a generalization of the formalism applicable to other two-dimensional systems.



First prediction in graphene by Kane



Kane and Mele, PRL 95, 146802 (2005)
 Bernevig, et al., Science 314, 1757 (2006)
 Bernevig, S.C. Zhang, PRL 96, 106802 (2006)
 König, et al. Science 318, 766 (2007)

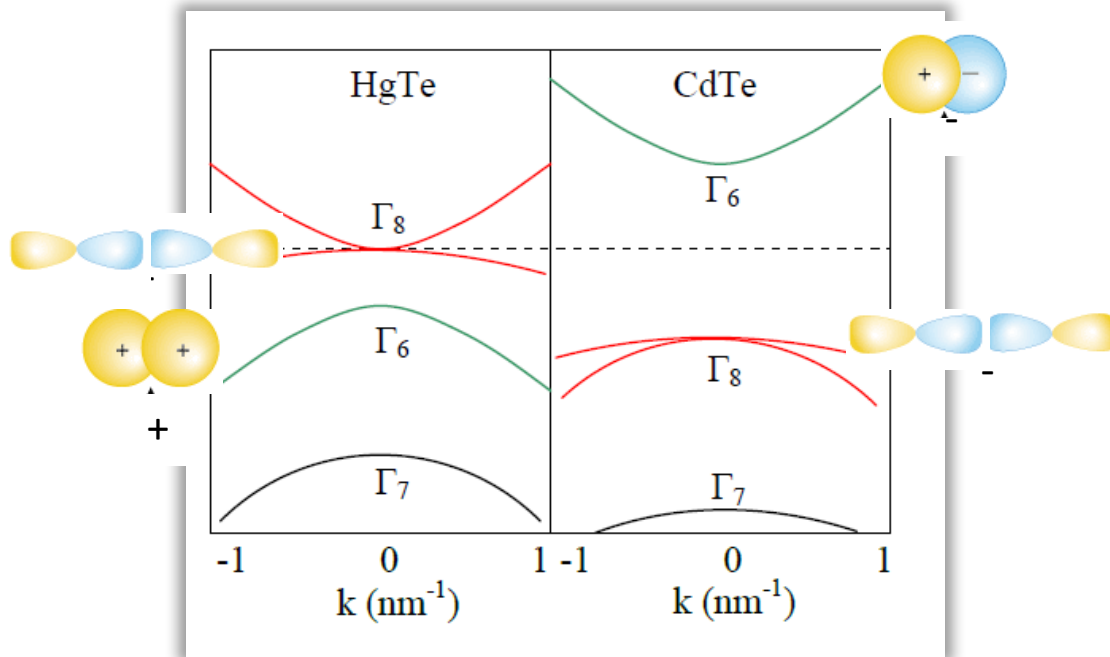


Quantum Spin Hall

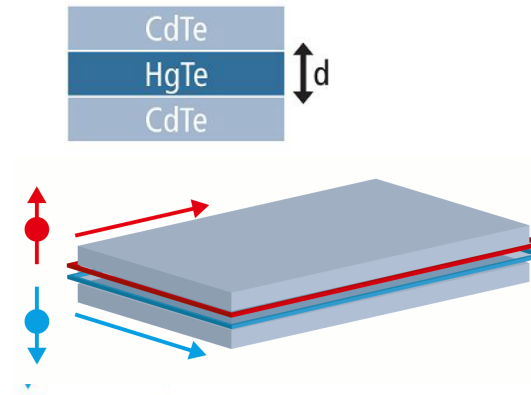


Quantum Spin Hall Effect and Topological Phase Transition in HgTe Quantum Wells

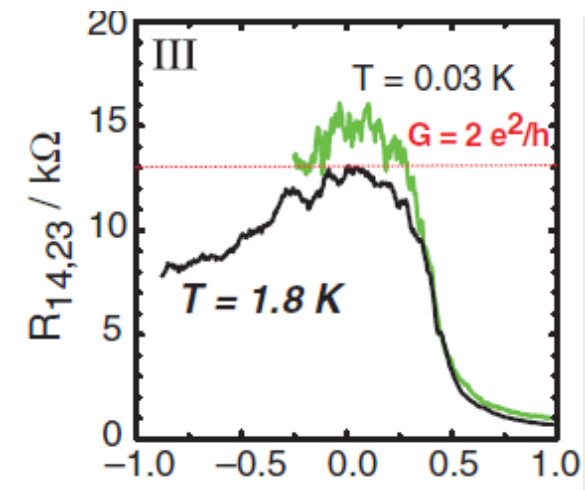
B. Andrei Bernevig, *et al.*
Science **314**, 1757 (2006);
DOI: 10.1126/science.1133734



Inert pair effect



3D: Dirac cone on the surface
2D: Dirac cone in quantum well



Bernevig, *et al.*, *Science* 314, 1757 (2006)
Bernevig, S.C. Zhang, *PRL* 96, 106802 (2006)
König, *et al.* *Science* 318, 766 (2007)



Stau im Mikrochip heute



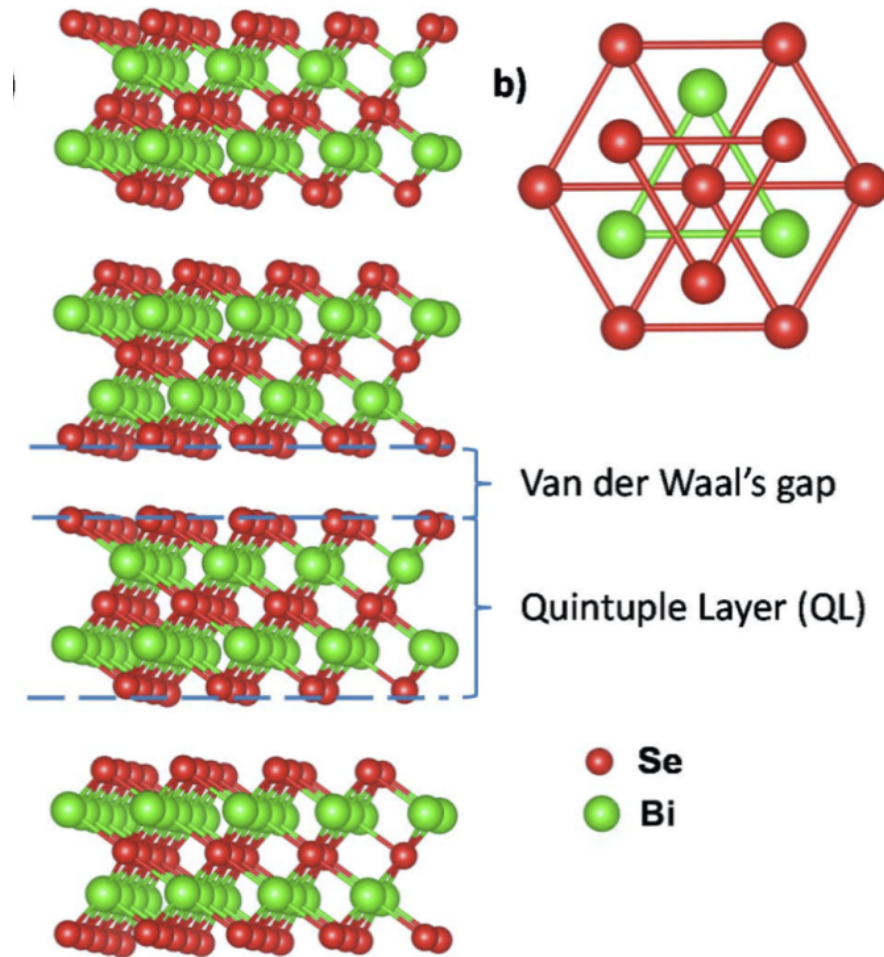
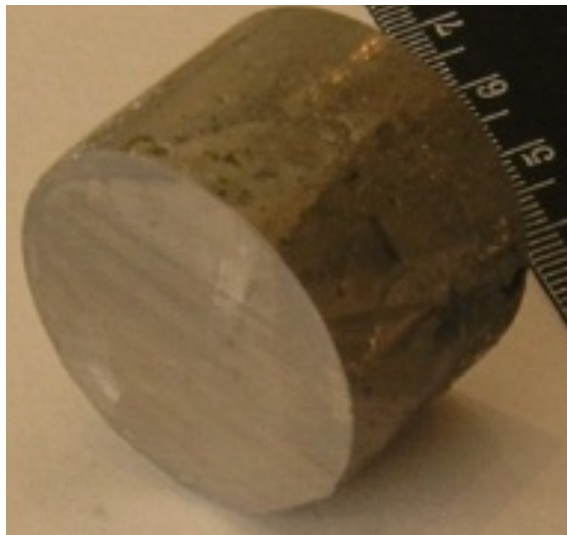
Chip-Autobahn in der Zukunft



Topologische Isolatoren

Bi-Sb Legierungen

Bi_2Se_3 und verwandte Strukturen



Moore and Balents, PRB 75, 121306(R) (2007)

Fu and Kane, PRB 76, 045302 (2007)

Murakami, New J. Phys. 9, 356 (2007)

Hsieh, et al., Science 323, 919 (2009)

Xia, et al., Nature Phys. 5, 398 (2009); Zhang, et al., Nature Phys. 5, 438 (2009)

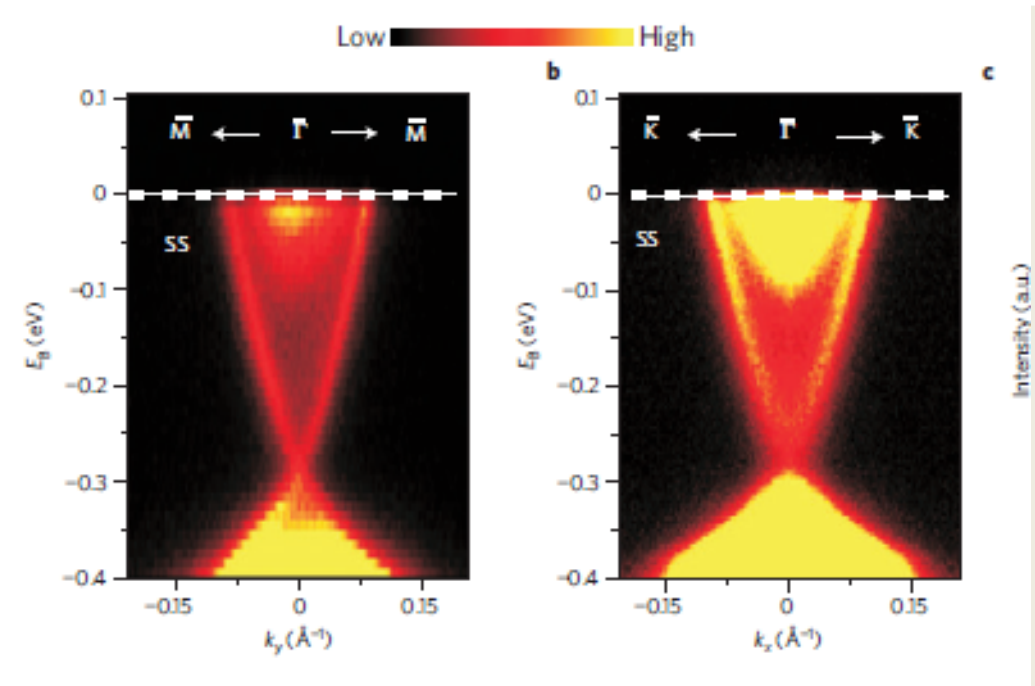
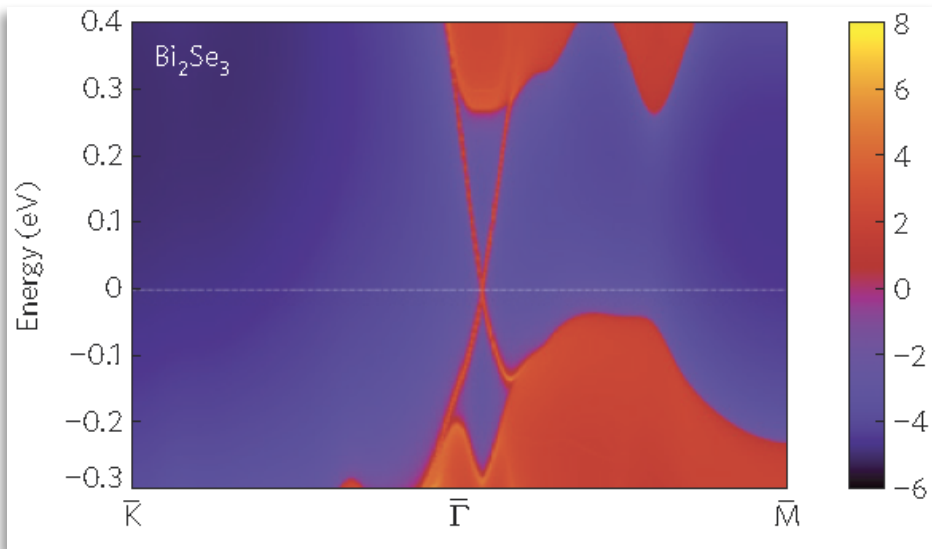
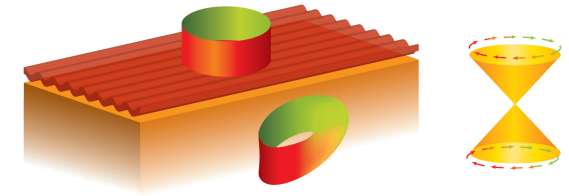
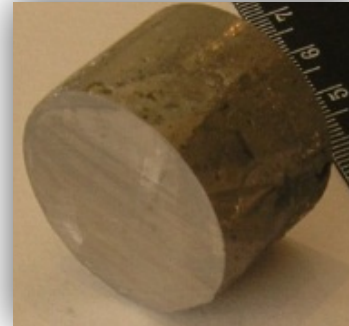


3D Topological Insulator

3D topological insulators

Bi-Sb alloy

Bi_2Se_3 and relatives



Moore and Balents, PRB 75, 121306(R) (2007)

Fu and Kane, PRB 76, 045302 (2007)

Murakami, New J. Phys. 9, 356 (2007)

Hsieh, et al., Science 323, 919 (2009)

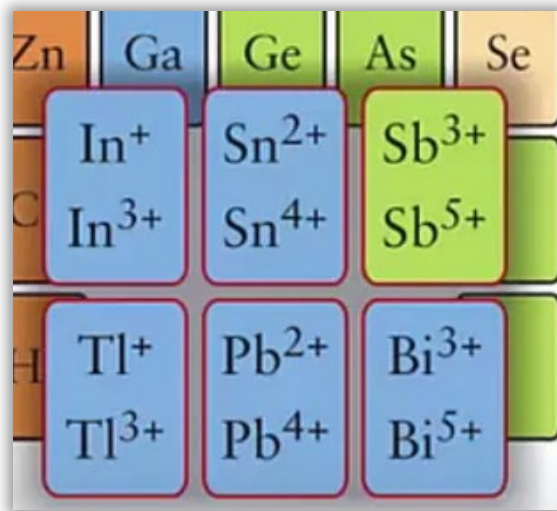
Xia, et al., Nature Phys. 5, 398 (2009); Zhang, et al., Nature Phys. 5, 438 (2009)



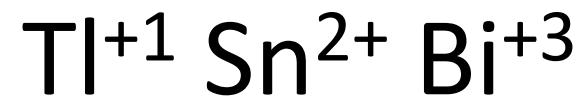
Materials

Table I. Proposed topological insulator materials grouped into several different material classes.^{4,12,13,19,23-29}

HgTe-type	Bi ₂ Se ₃ -type	Honey Comb Lattice	Bismuth-Alloys	NaCl Structure	Oxides	Correlated Materials	Super-conductors
HgTe	Bi ₂ Se ₃ , Bi ₂ Te ₃ , and Sb ₂ Te ₃	Graphene	Bi-Sb	SnTe PbTe	Doped BaBiO ₃	Iridates	Cu _x Bi ₂ Se ₃
Half-Heuslers such as LaPtBi	Bi ₂ Te ₂ Se	LiAuTe		PuTe AmN	Iridates	SmB ₆	LaPtBi YPtBi LuPtBi
α -Sn, HgSe β -HgS	(Bi _x Sb _{1-x}) ₂ Te ₃					YbPtBi	TiBiSe ₂ TiBiTe ₂
Chalco-pyrites	TiBiSe ₂ and TiBiTe ₂					Skutterudites	
AlSb/InAs/GaSb	Bi ₁₄ Rh ₃ I ₉					PuTe, AmN	



Claudia Felser and Xiao-Liang Qi , Guest Editors, MRS Bull. 39 (2014) 843.



Inert pair effect

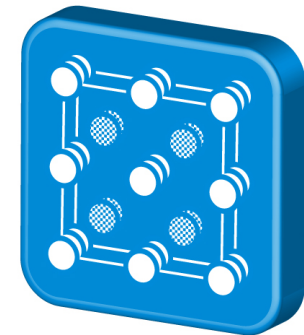


Design scheme: topological insulator

- Semiconductor or Insulator
- Band inversion – e.g. inert pair effect



The „Designer“-Material





Concept

Rational design

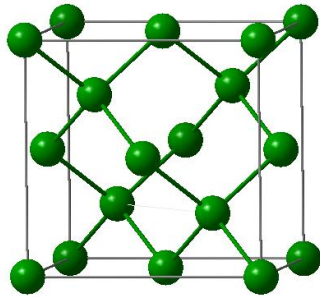
X₂YZ Heusler compounds

H																	He										
2.20																											
Li	Be											B	C	N	O	F	Ne										
0.98	1.57											2.04	2.55	3.04	3.44	3.98											
Na	Mg											Al	Si	P	S	Cl	Ar										
0.93	1.31											1.61	1.90	2.19	2.58	3.16											
K	Ca	Sc	Ti	V	Cr	Mn	Fe	Co	Ni	Cu	Zn	Ga	Ge	As	Se	Br	Kr										
0.82	1.00	1.36	1.54	1.63	1.66	1.55	1.83	1.88	1.91	1.90	1.65	1.81	2.01	2.18	2.55	2.96	3.00										
Rb	Sr	Y	Zr	Nb	Mo	Tc	Ru	Rh	Pd	Ag	Cd	In	Sn	Sb	Te	I	Xe										
0.82	0.95	1.22	1.33	1.60	2.16	1.90	2.20	2.28	2.20	1.93	1.69	1.78	1.96	2.05	2.10	2.66	2.60										
Cs	Ba											Hf	Ta	W	Re	Os	Ir	Pt	Au	Hg	Tl	Pb	Bi	Po	At	Rn	
0.79	0.89											1.30	1.50	1.70	1.90	2.20	2.20	2.40	1.90	1.80	1.80	1.90	2.00	2.20			
Fr	Ra																										
0.70	0.90																										
		La	Ce	Pr	Nd	Pm	Sm	Eu	Gd	Tb	Dy	Ho	Er	Tm	Yb	Lu											
		1.10	1.12	1.13	1.14	1.13	1.17	1.20	1.20	1.10	1.22	1.23	1.24	1.25	1.10	1.27											
		Ac	Th	Pa	U	Np	Pu	Am	Cm	Bk	Cf	Es	Fm	Md	No	Lr											
		1.10	1.30	1.50	1.70	1.30	1.28	1.13	1.28	1.30	1.30	1.30	1.30	1.30	1.30	1.30											

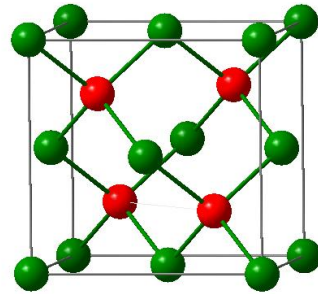


Heusler compounds

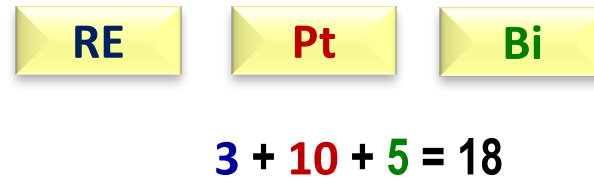
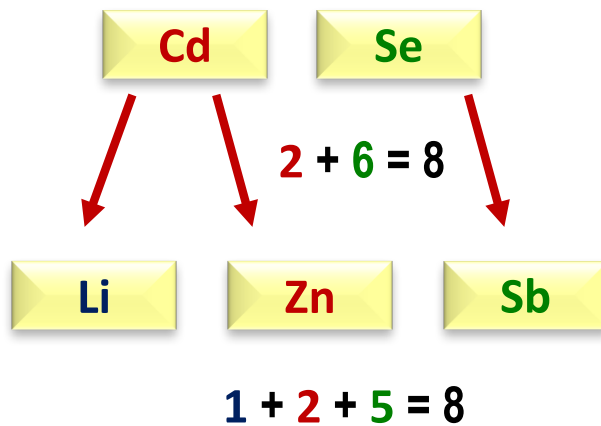
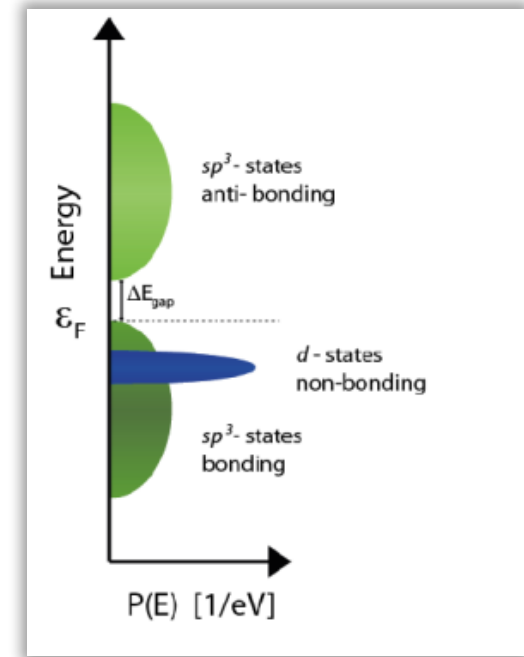
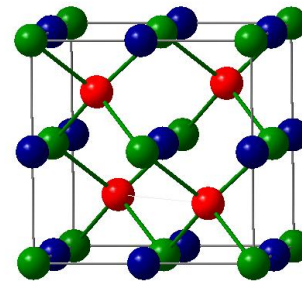
Diamond



ZnS



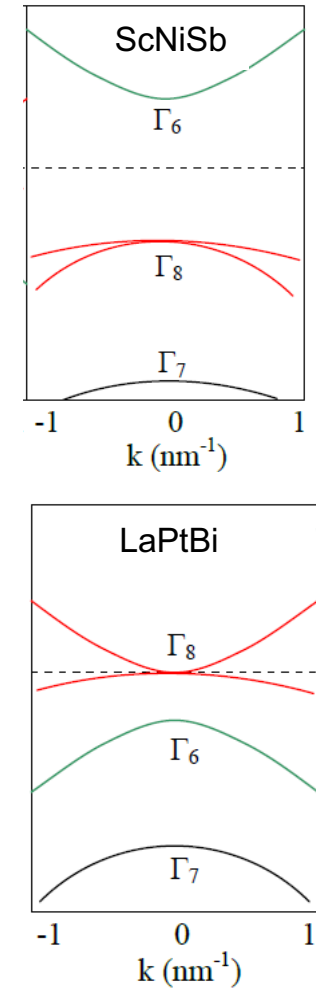
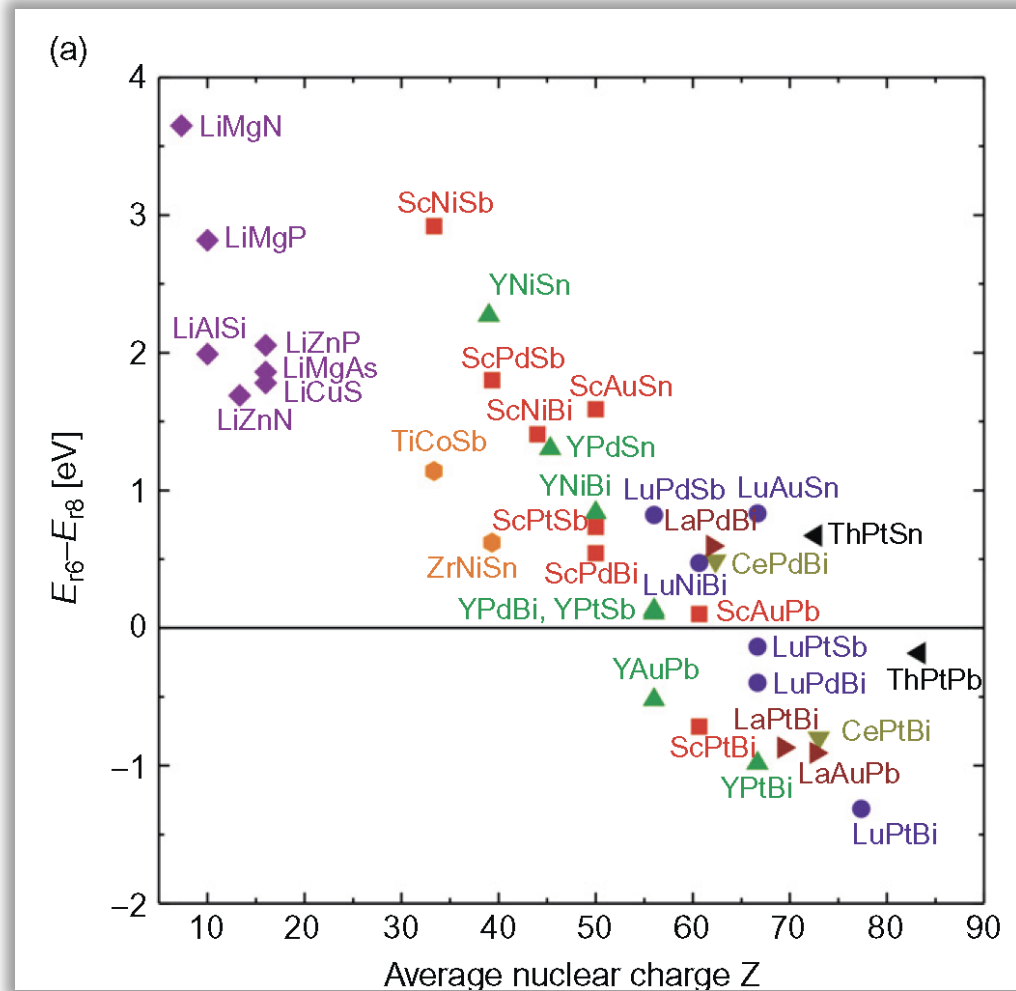
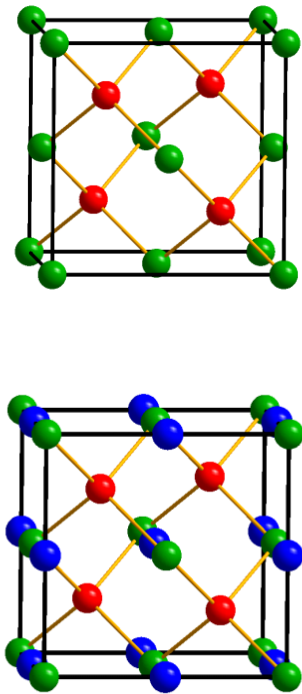
Heusler XYZ C1_b







Predicting new compounds



S. Chadov et al., Nat. Mater. 9, 541 (2010).

H. Lin et al., Nat. Mater. 9, 546 (2010).



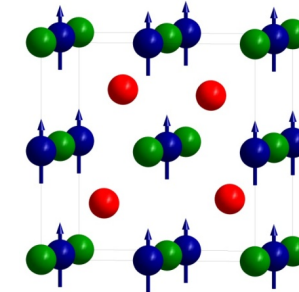
REPtBi... multifunctional topologic insulators

Magnetism and heavy fermion-like behavior in the RBiPt series

P. C. Canfield, J. D. Thompson, W. P. Beyermann, A. Lacerda, M. F. Hundley, E. Peterson, and Z. Fisk
Los Alamos National Laboratory, Los Alamos, New Mexico 87545

H. R. Ott
ETH, Zurich, Switzerland

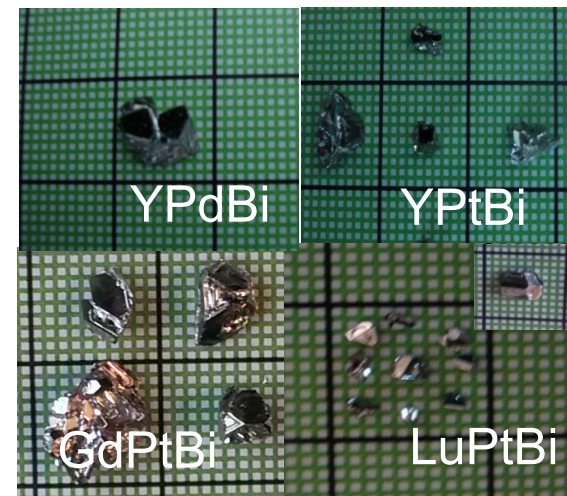
J. Appl. Phys. **70** (10), 15 November 1991



$$10 + 3 (+f^n) + 5 = 18$$

Multifunctional properties

- RE: Y, La, Lu, Er, ... superconductivity
RE: Gd, Tb, Sm Magnetism and TI
 - Antiferromagnetism with GdPtBi
- RE: Ce
 - complex behaviour of the Fermi surface
- RE: Yb Kondo insulator and TI
 - YbPtBi is a super heavy fermion with the highest γ value

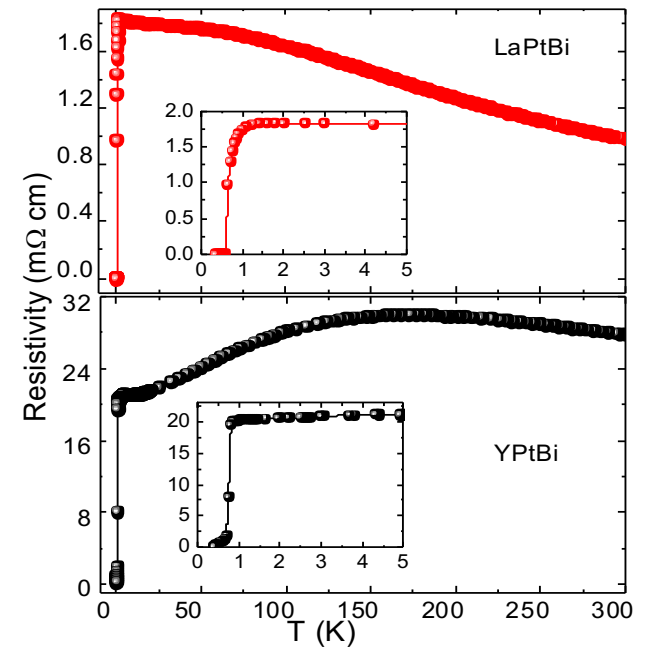
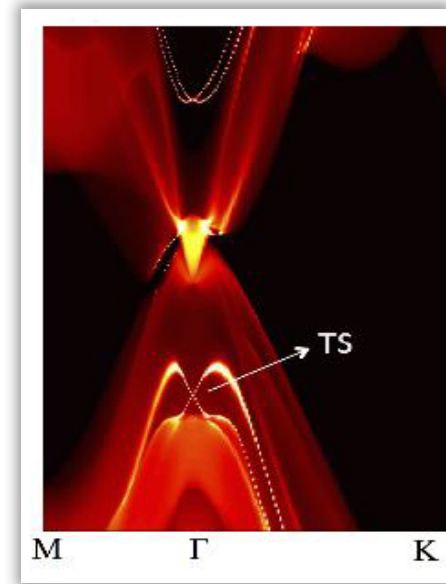
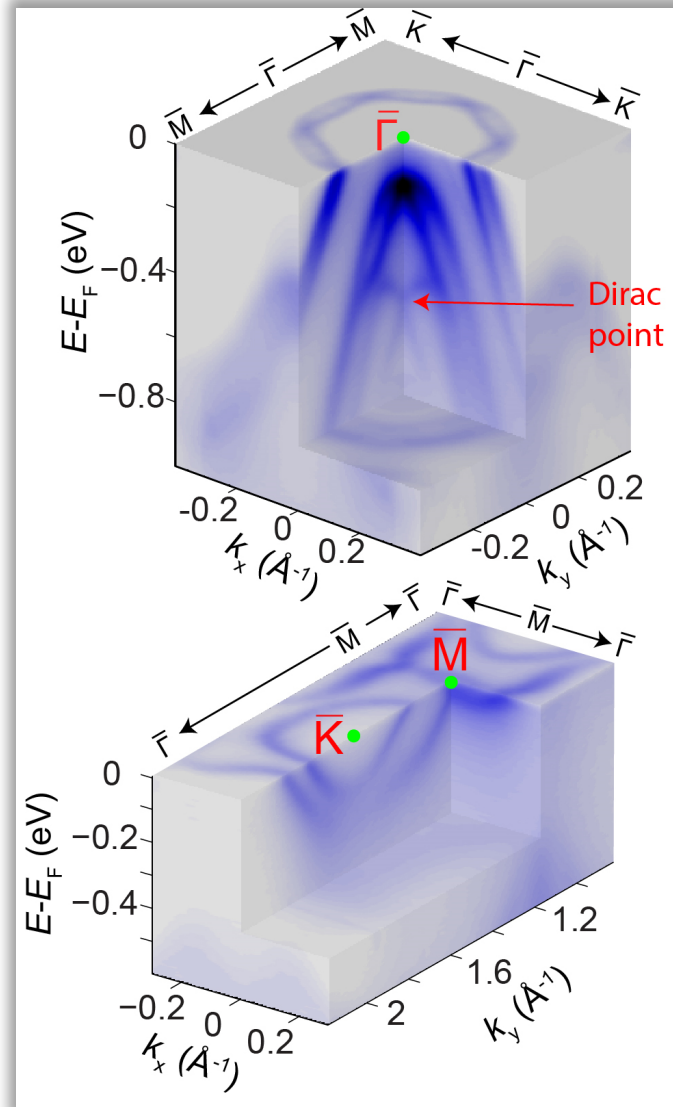
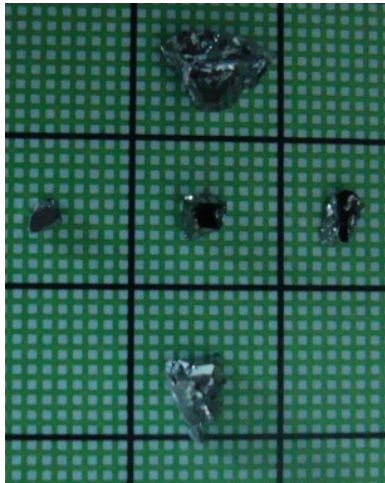


S. Chadov et al., Nat. Mater. 9, 541 (2010).

H. Lin et al., Nat. Mater. 9, 546 (2010).

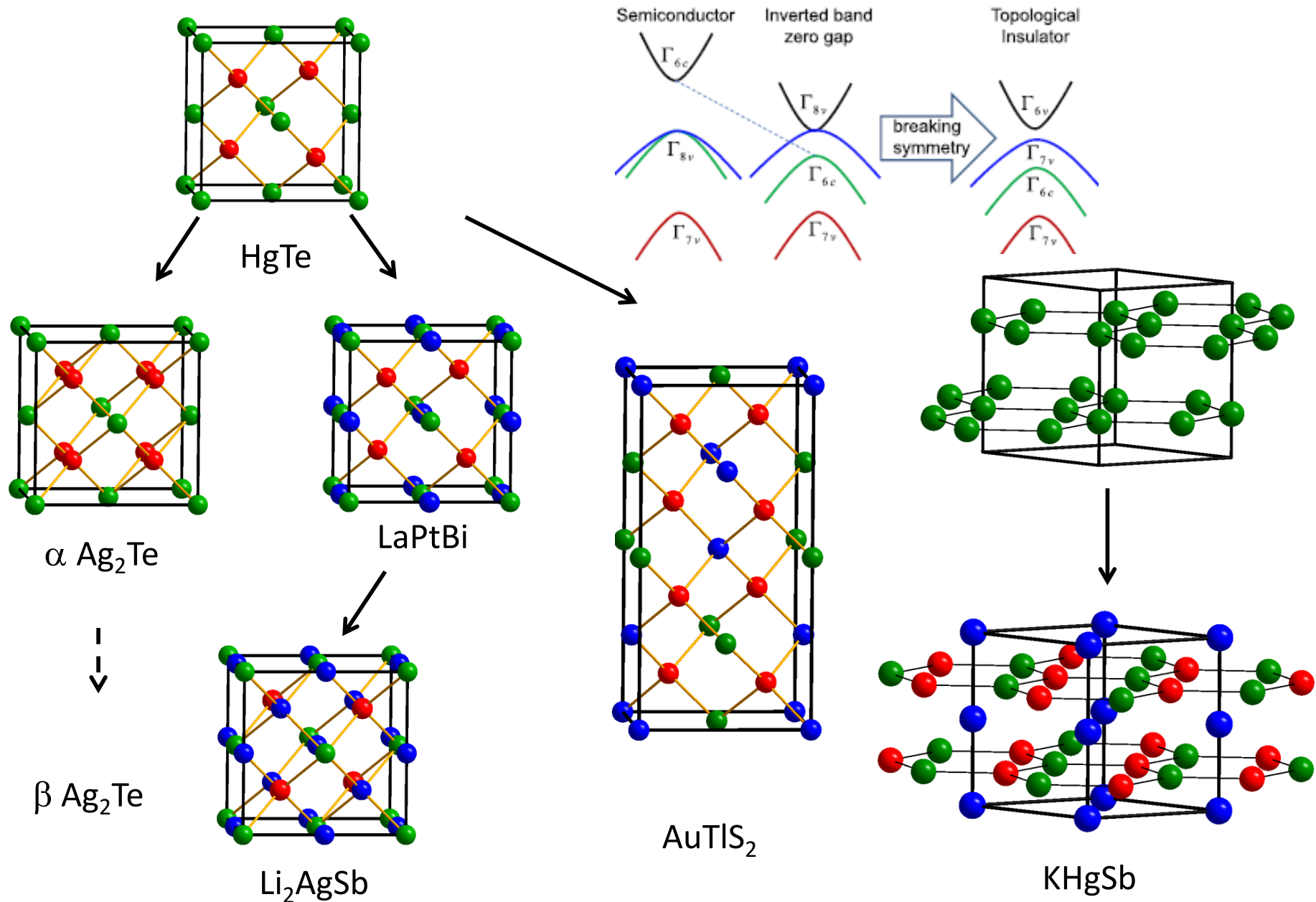


ARPES of LnPtBi



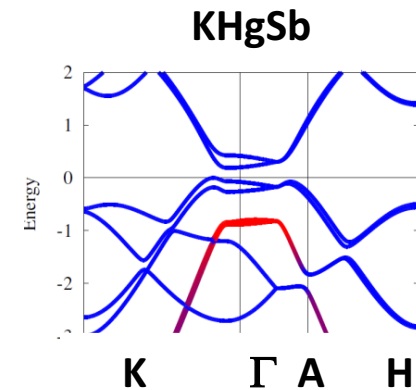
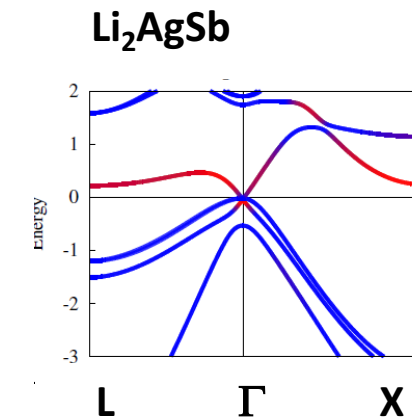
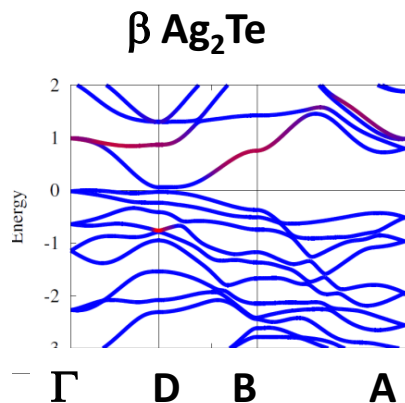
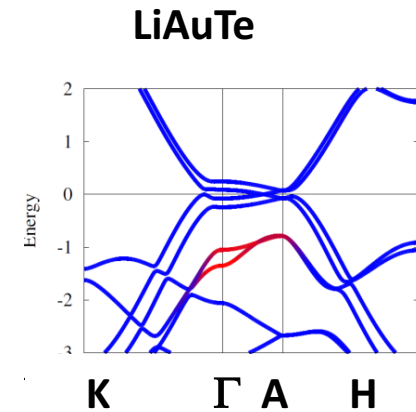
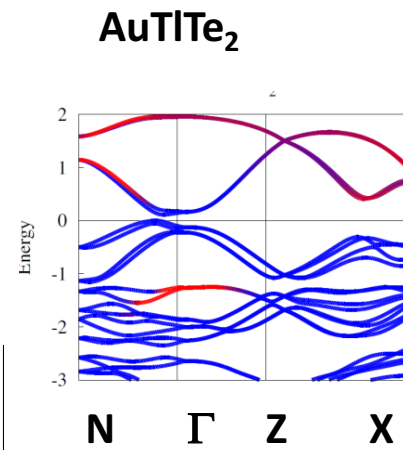
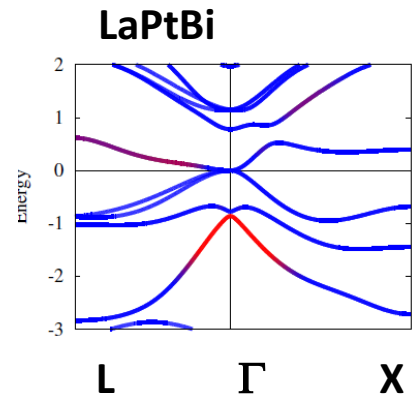
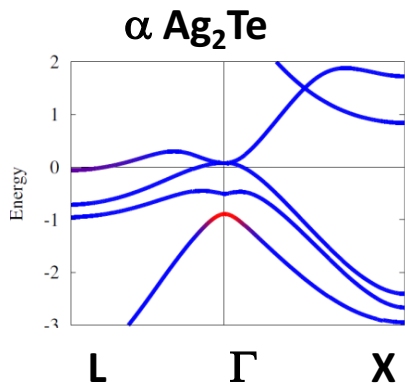
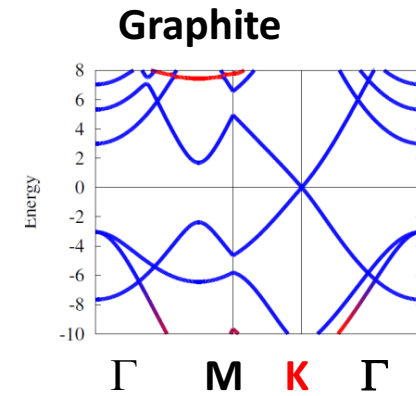
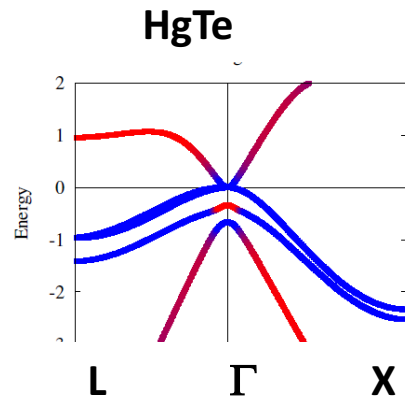


Structure to Property



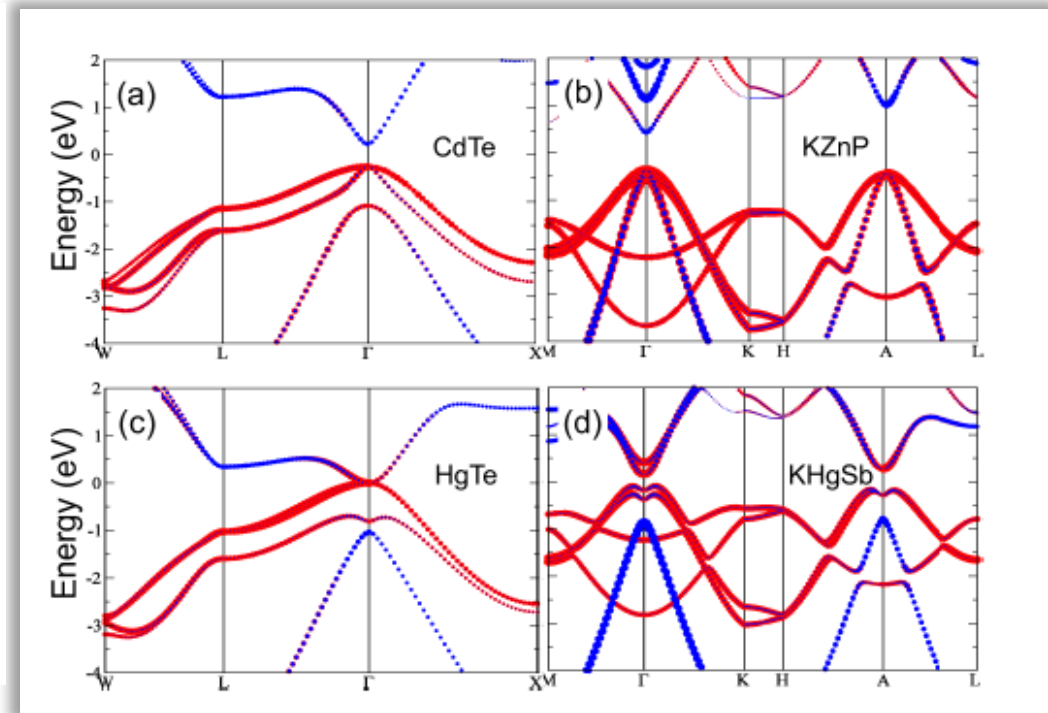
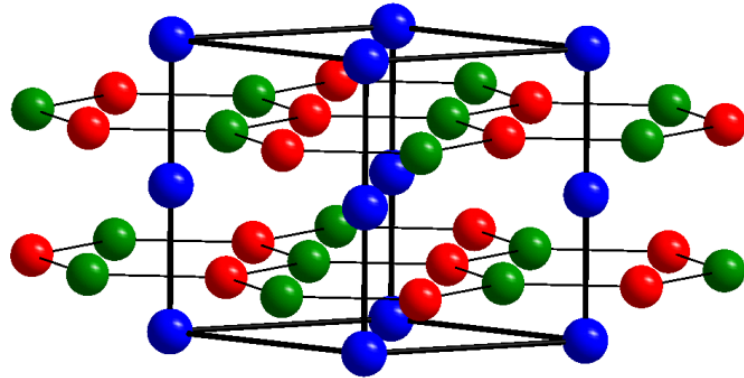


Struktur und elektronische Struktur





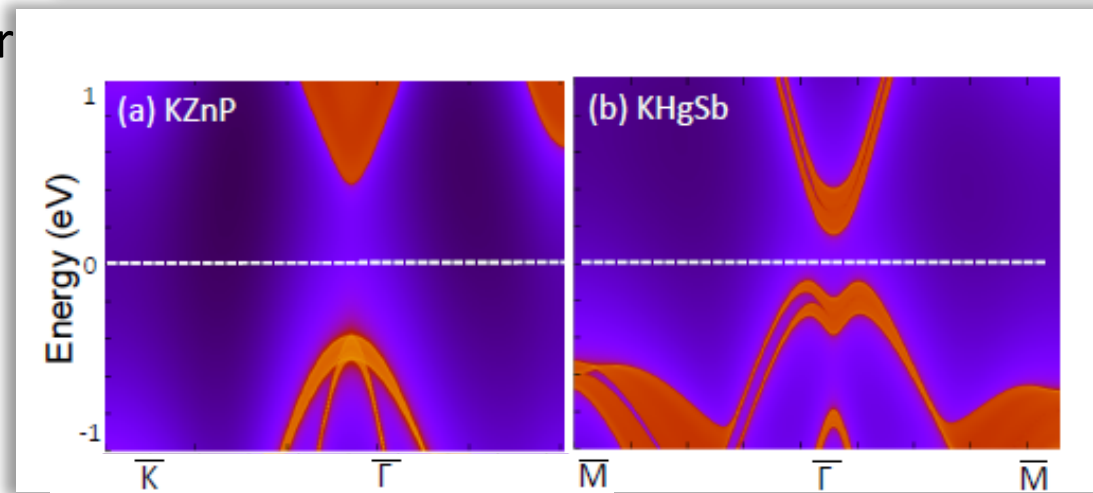
Honeycomb from sp^3 to sp^2



Band inversion is found in the heavier compounds

No surface state? Why?

→ Interaction between the two layers in the unit cell and two Dirac Cones



a)

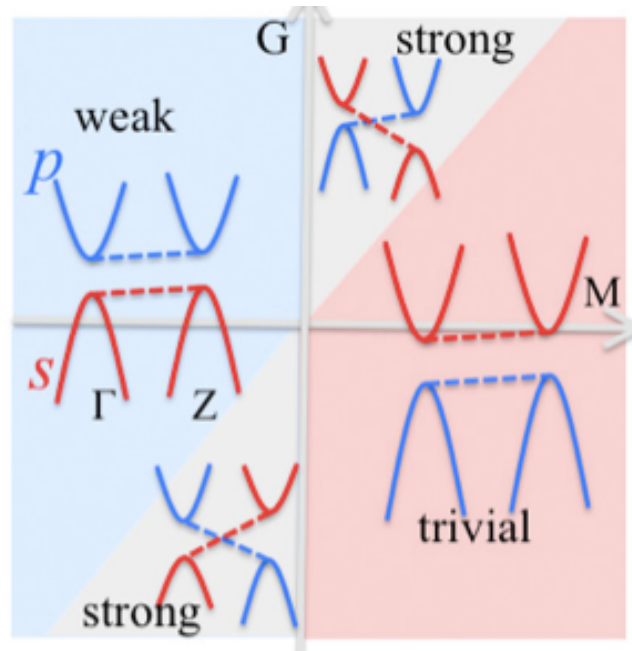
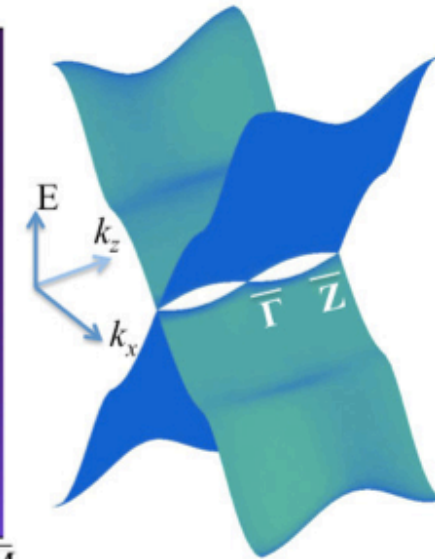
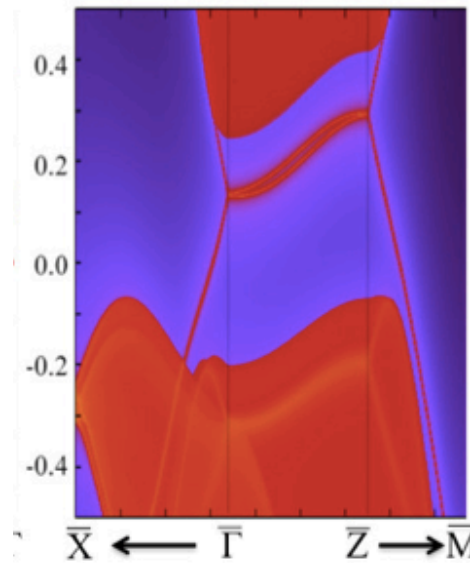
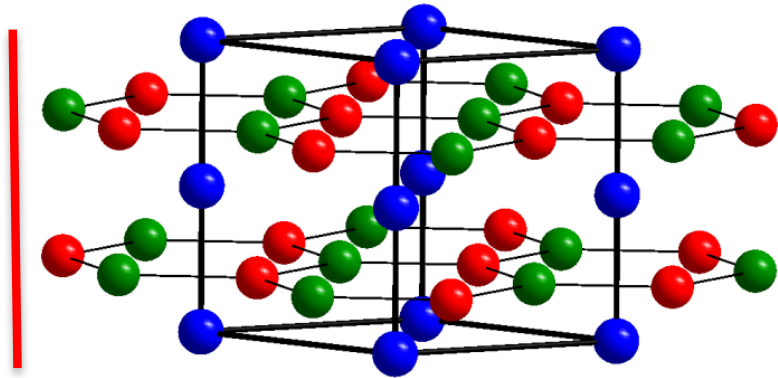


b)





Honeycomb: Weak TI



KHgSb	KHgAs	KHgP
NaHgSb	NaHgAs	NaHgP
LiHgSb	LiHgAs	LiHgP
KCdSb	KCdAs	KCdP
NaCdSb	NaCdAs	NaCdP
LiCdSb	LiCdAs	LiCdP

KAuTe	KAuSe
NaAuTe	NaAuSe
LiAuTe	LiAuSe
KAgTe	KAgSe
NaAgTe	NaAgSe
LiAgTe	LiAgSe



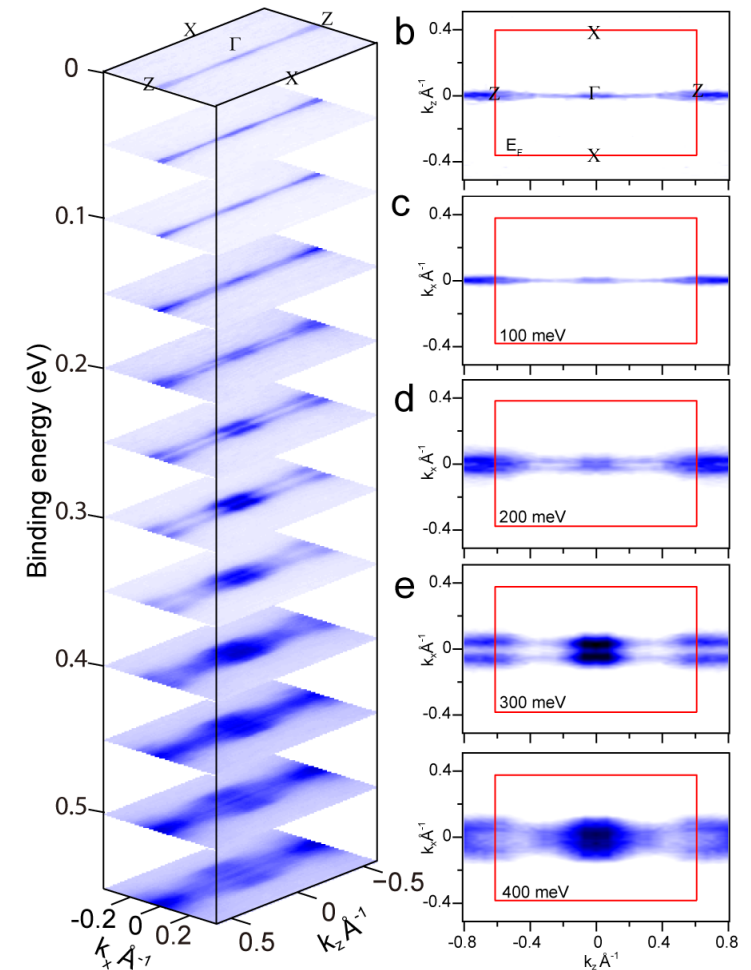
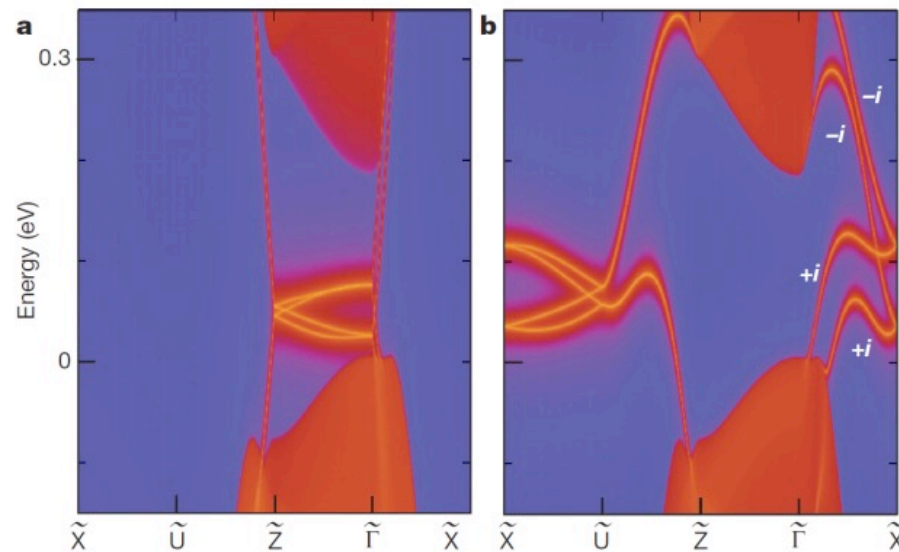
Hourglass



ARTICLE

Hourglass fermions

Zhijun Wang^{1*}, A. Alexandradinata^{1,2*}, R. J. Cava³ & B. Andrei Bernevig¹



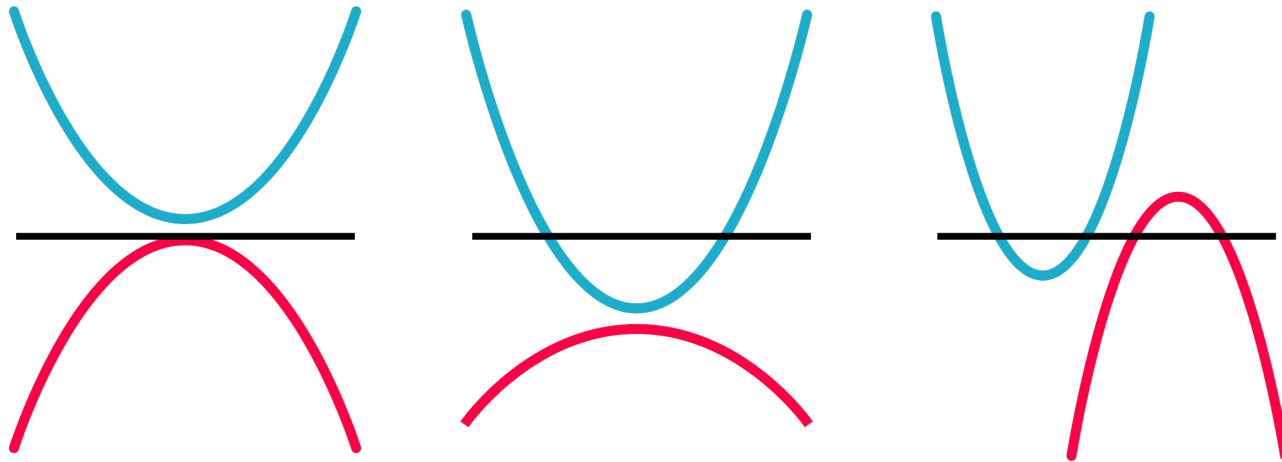


Dirac - Weyl Semimetals

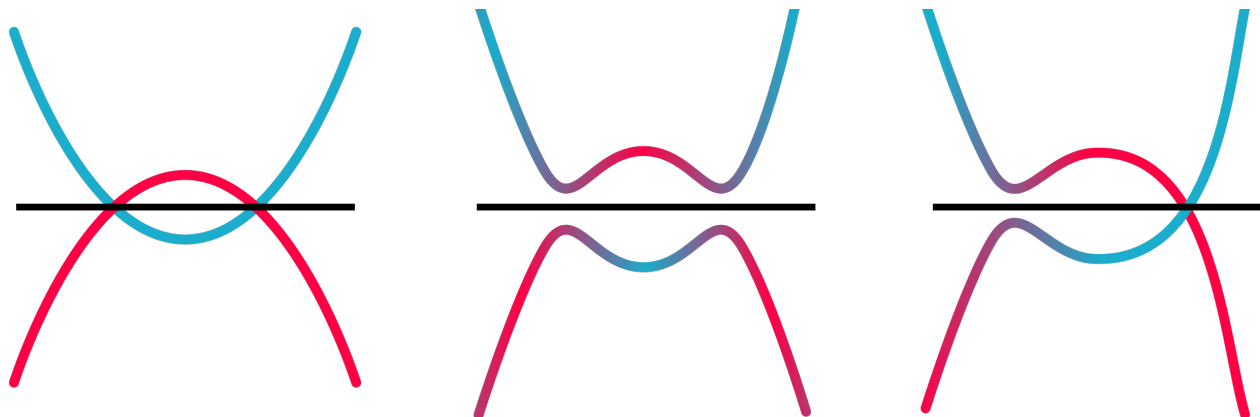


Insulator – semiconductor – Metal

Insulator/Semiconductor – Metal – Semimetal

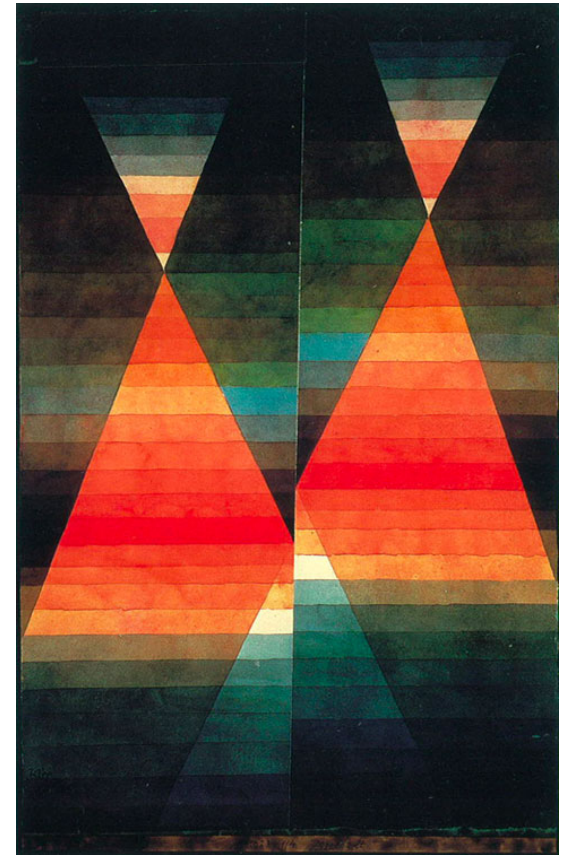
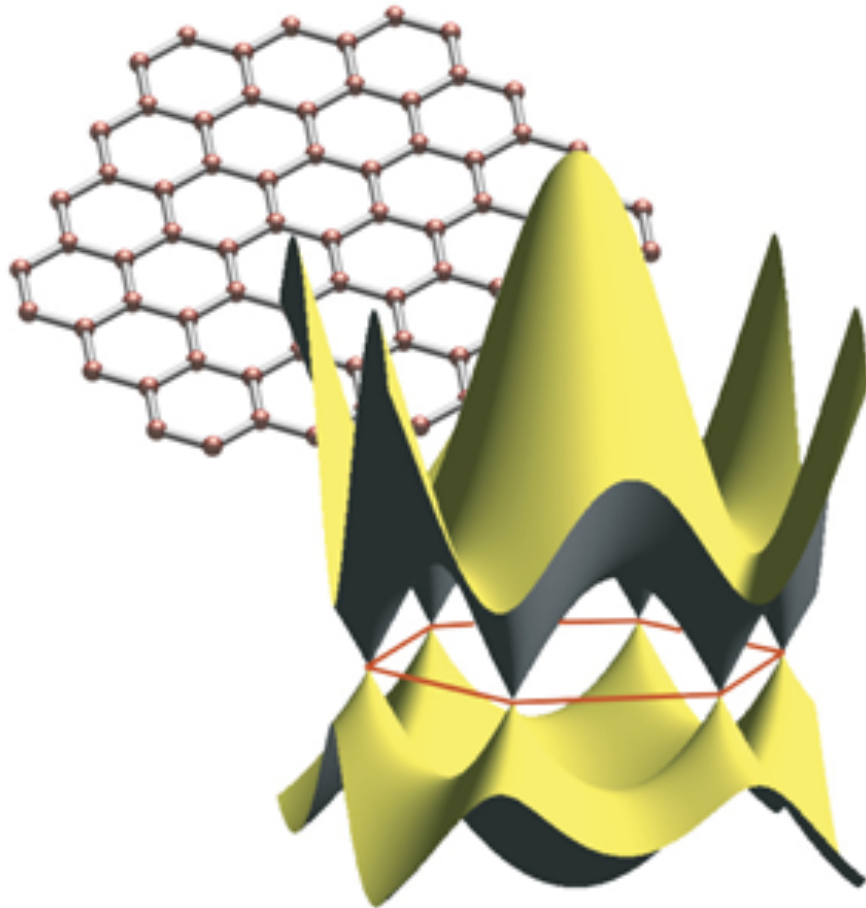


Topological Insulator/Semiconductor – Dirac/Weyl Semimetal





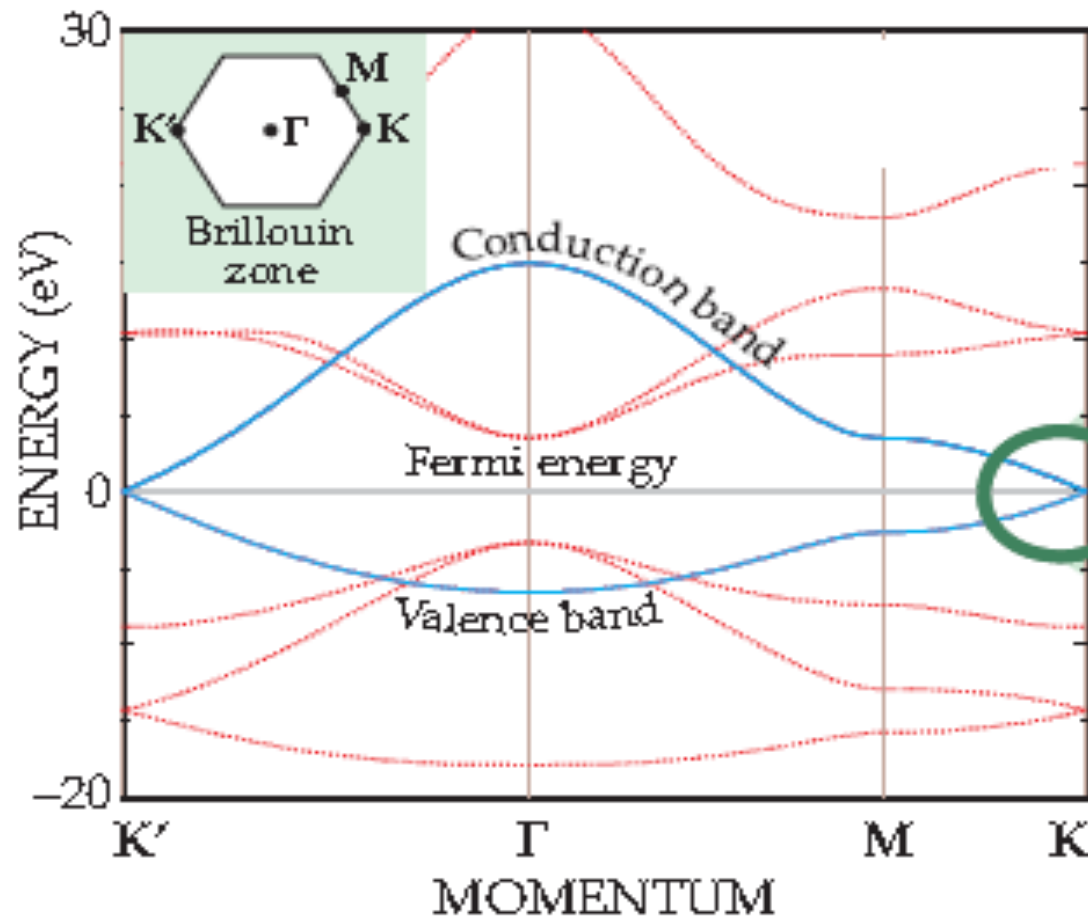
Dirac and Weyl semimetals



Paul Klee



Graphene

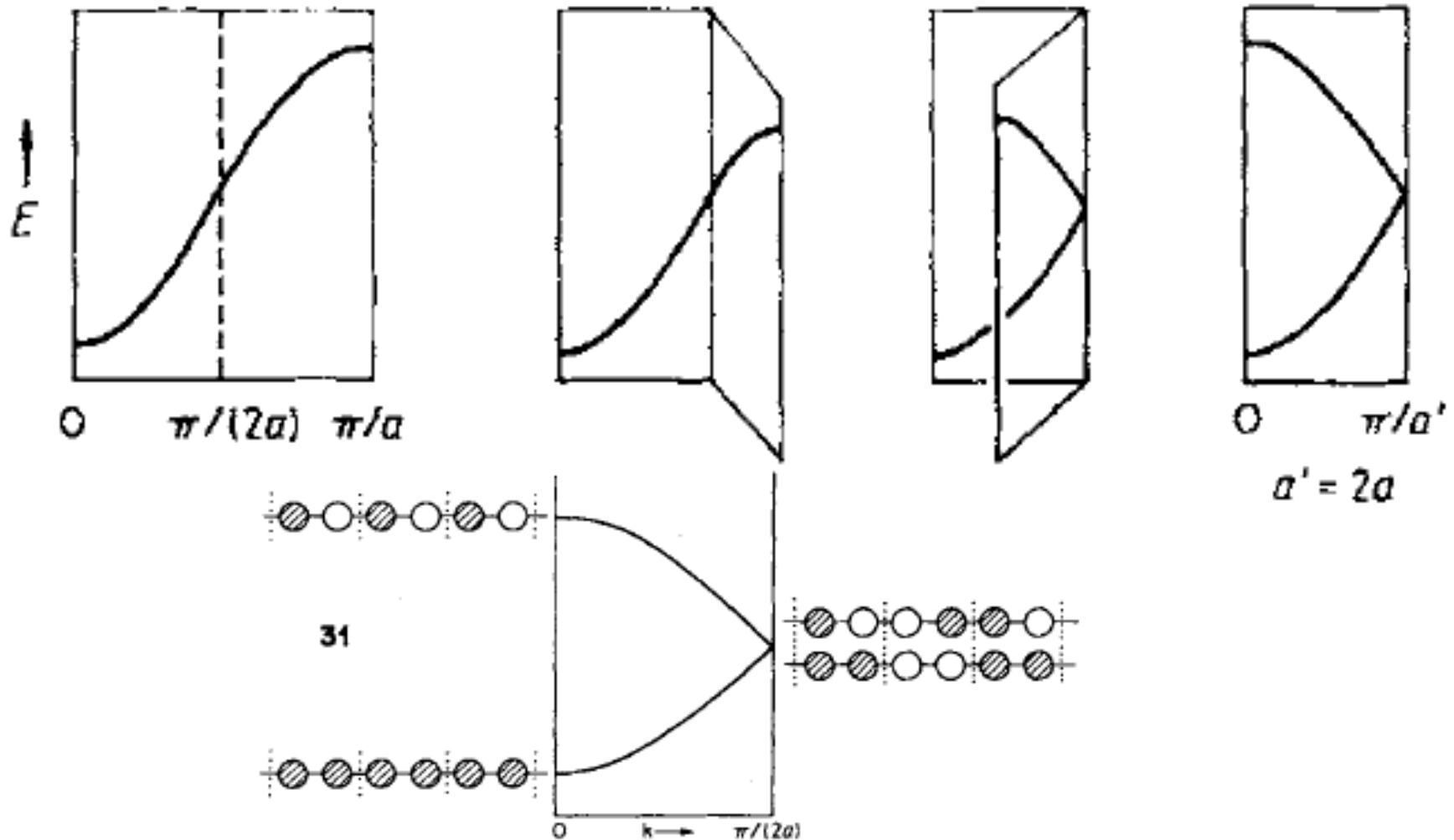




Dirac and Weyl

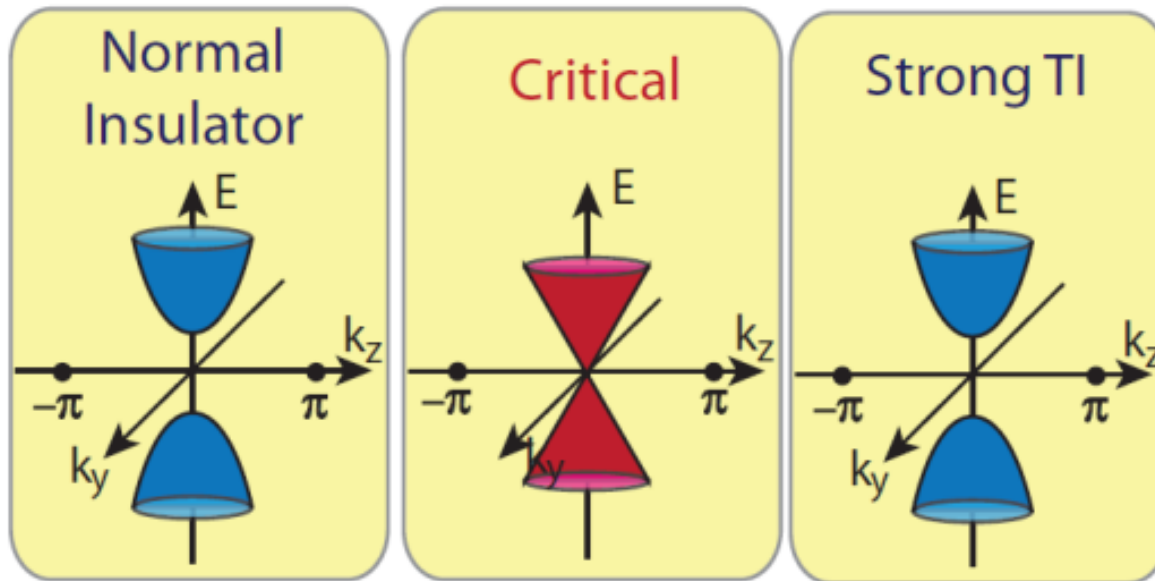
How Chemistry and Physics Meet in the Solid State

By Roald Hoffmann*

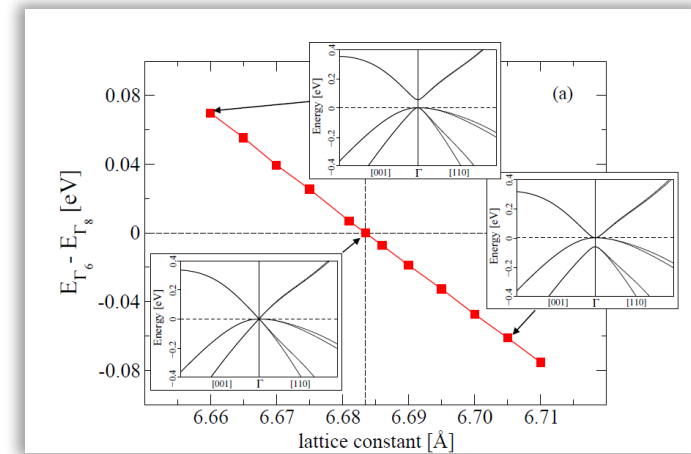




Dirac semimetals



Bohm-Jung Yang and Naoto Nagaosa, arXiv:1404.0754



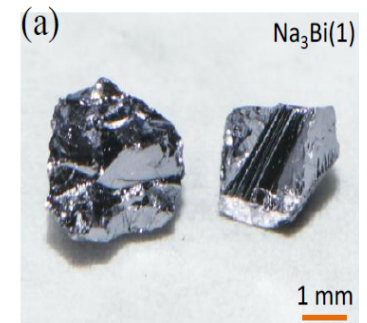
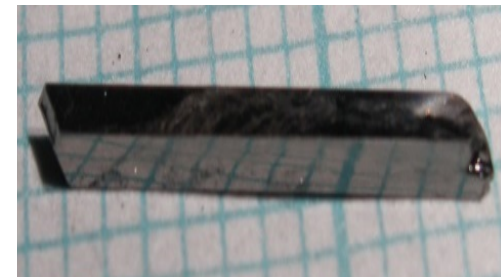
ARTICLE

Received 2 Dec 2013 | Accepted 2 Apr 2014 | Published 7 May 2014

DOI: 10.1038/ncomms4786

Observation of a three-dimensional topological Dirac semimetal phase in high-mobility Cd₃As₂

Madhab Neupane^{1*}, Su-Yang Xu^{1*,}, Raman Sankar^{2,*}, Nasser Alidoust¹, Guang Bian¹, Chang Liu¹, Ilya Belopolski¹, Tay-Rong Chang³, Horng-Tay Jeng^{3,4}, Hsin Lin⁵, Arun Bansil⁶, Fangcheng Chou² & M. Zahid Hasan^{1,7}



Observation of Fermi arc surface states in a topological metal
 Su-Yang Xu *et al.*
Science **347**, 294 (2015);
 DOI: 10.1126/science.1256742



3D Dirac Cd_3As_2

Cd_3As_2 —A Noncubic Semiconductor with Unusually High Electron Mobility*

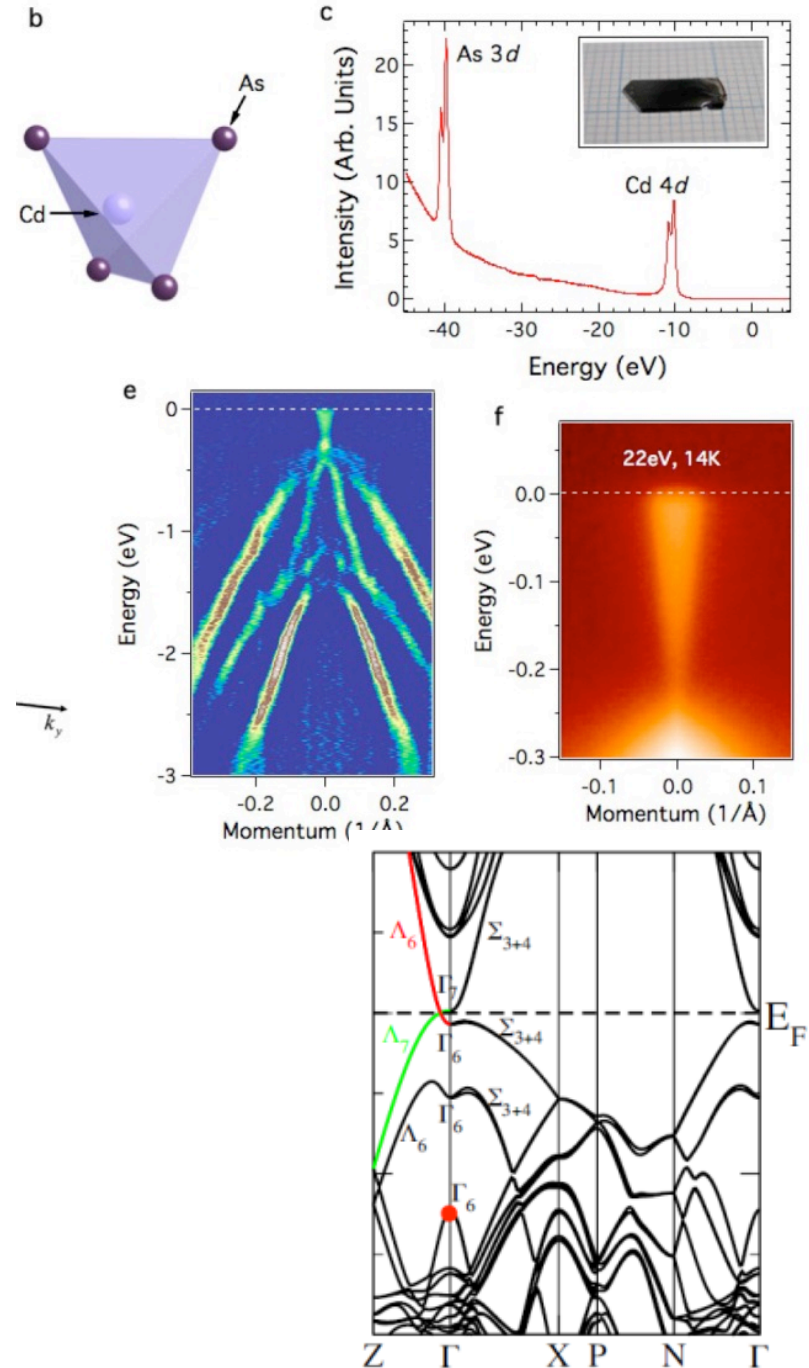
ARTHUR J. ROSENBERG AND THEODORE C. HARMAN
 Lincoln Laboratory, Massachusetts Institute of Technology,
 Lexington, Massachusetts

(Received June 17, 1959)

IN all reported studies of electron transport in solids, the electron mobility at room temperature determined by galvanomagnetic or drift experiments has been found to exceed 10 000 $\text{cm}^2/\text{volt}\text{-sec}$ in but four materials, namely, the compounds InSb, InAs, HgSe, and HgTe at accessible purities [Table I(A)]. Each

TABLE I. Electron Hall mobility at 300°K.^a

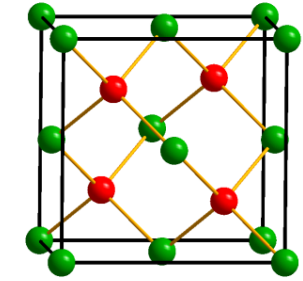
Material	Carrier concentration, cm^{-3}	Hall mobility, $\text{cm}^2/\text{volt}\text{-sec}$
A. Highest measured values		
InSb	2×10^{16}	63 000 ^b
InAs	1.7×10^{16}	30 000 ^c
HgSe	4×10^{17}	18 000 ^d
HgTe	2.6×10^{17}	19 000 ^e
B. Measured values at 4×10^{18} carriers/cm^3		
InSb		8000 ^f
InAs		7000 ^g
HgSe		6000 ^d
Cd_3As_2		10 000



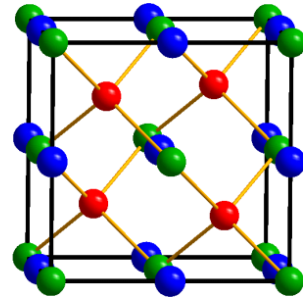
Arthur J. Rosenberg and Theodore C. Harman *Journal of Applied Physics* 30, 1621 (1959)
 Wang, Z. J., Weng, H. M., Wu, Q. S., Dai, X. & Fang, Z., *Phys. Rev. B* 88, 125427 (2013).
 Liu, Z. K. *et al. Nature Mater.* 13, 677-681 (2014).



Electronic structure

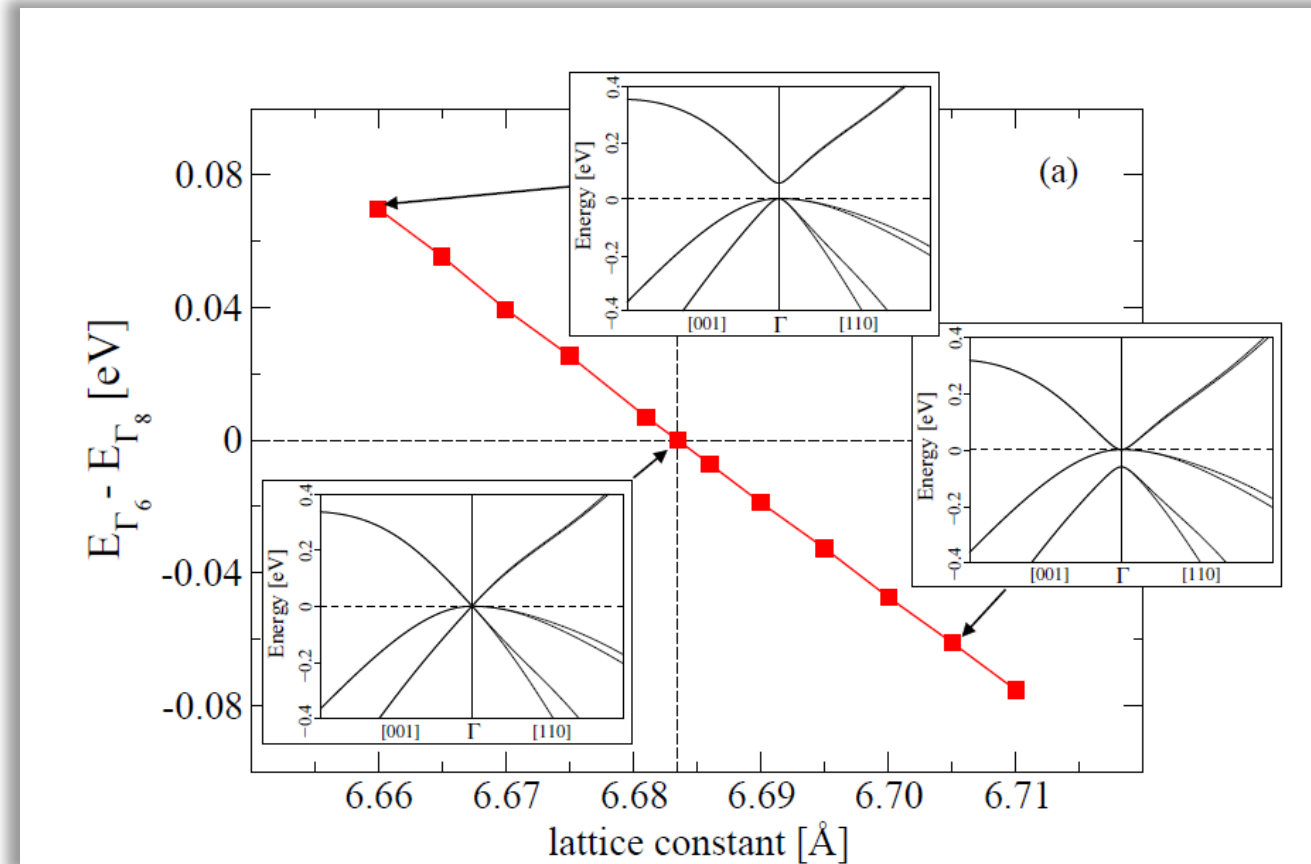


CdTe



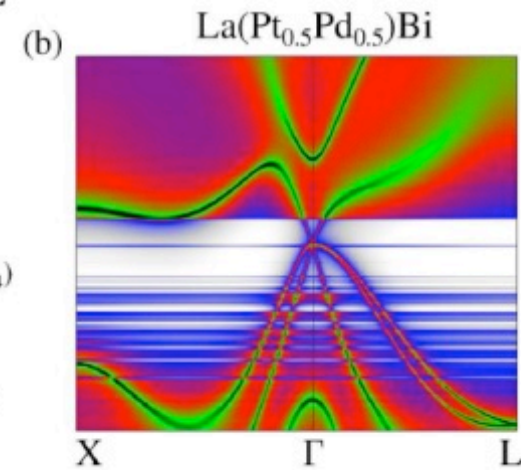
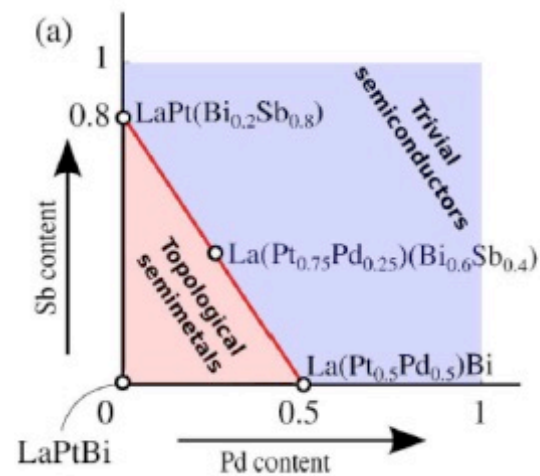
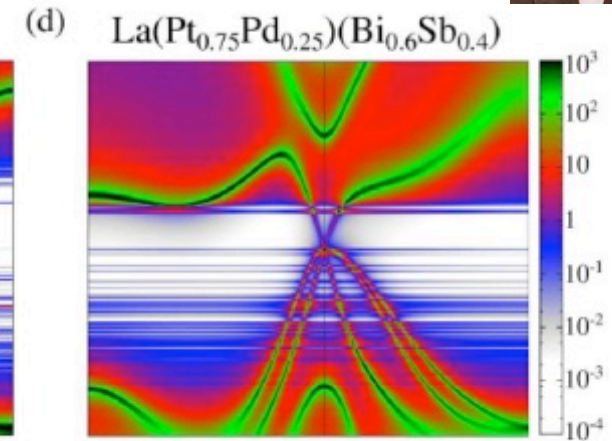
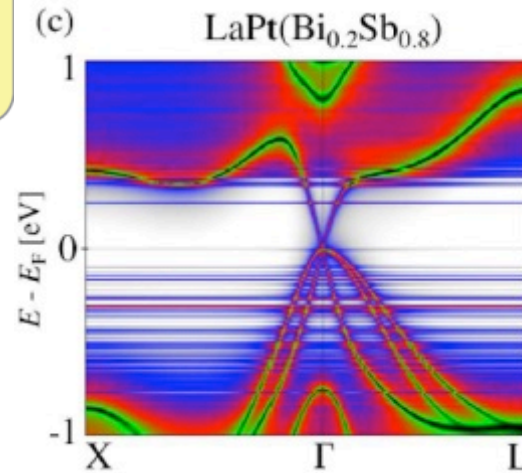
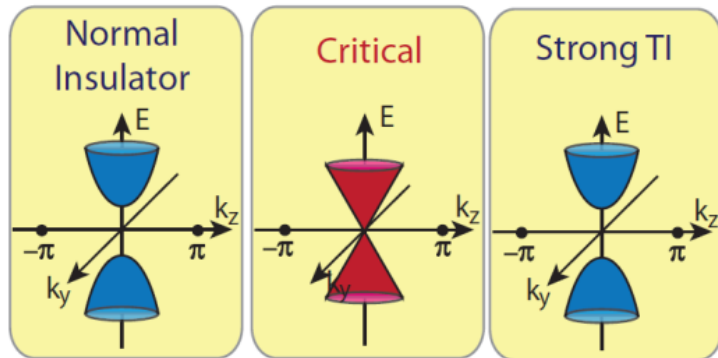
ScPtSb

ScPtBi



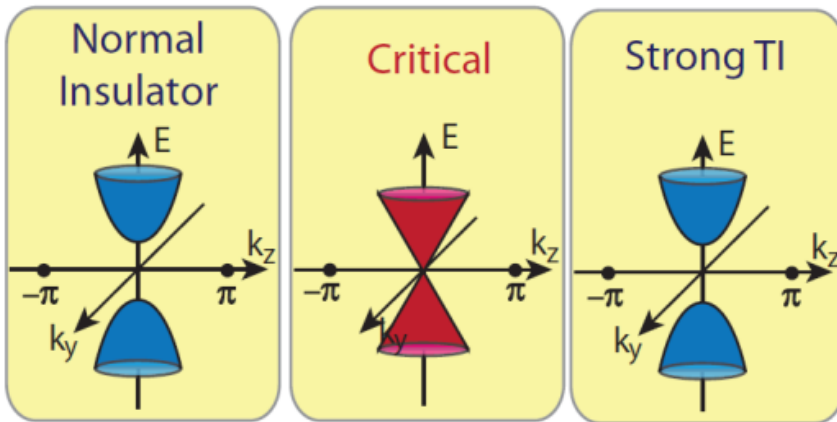


Application Spin Hall Effect

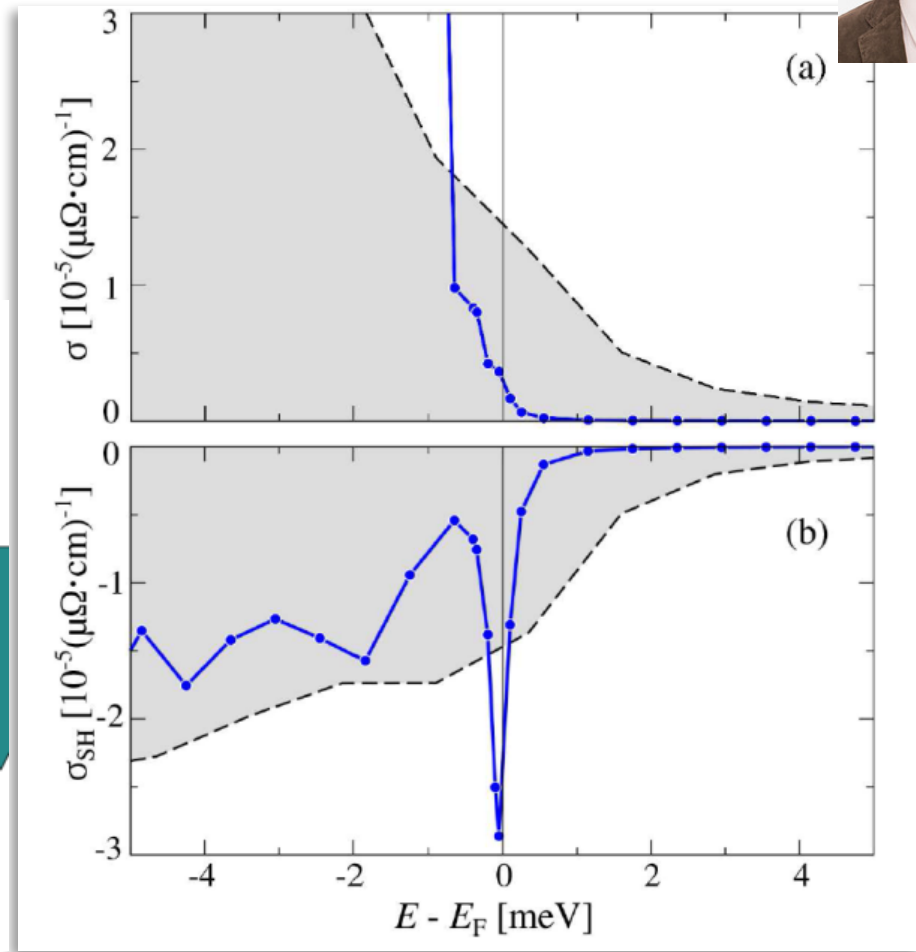
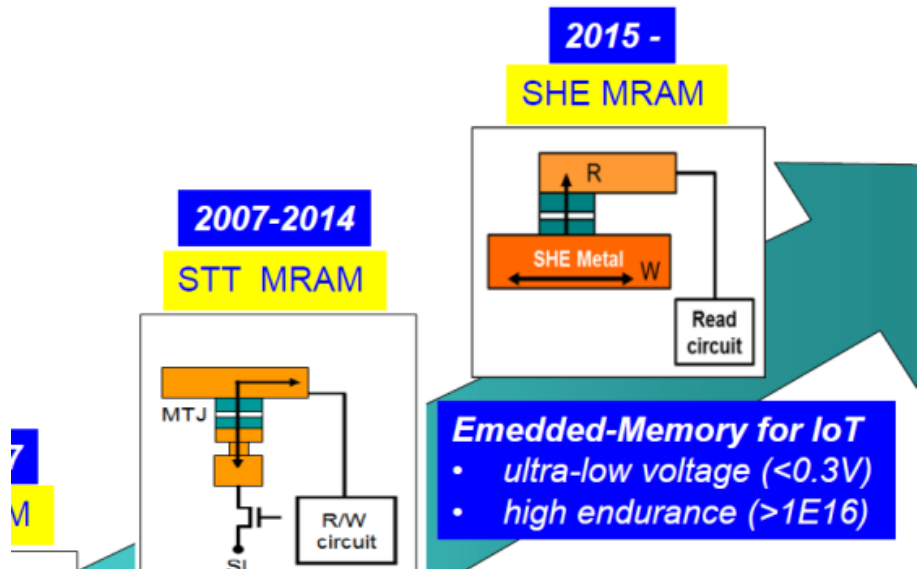




Application Spin Hall Effect



ITRI's MRAM Roadmap

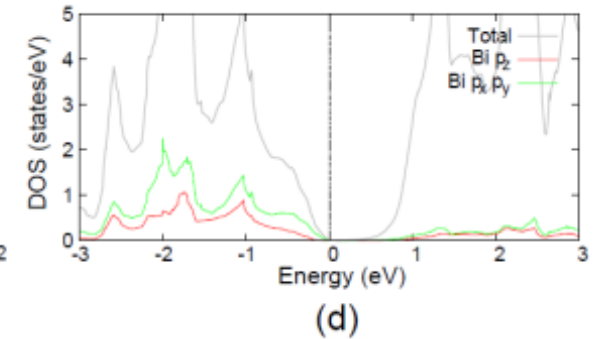
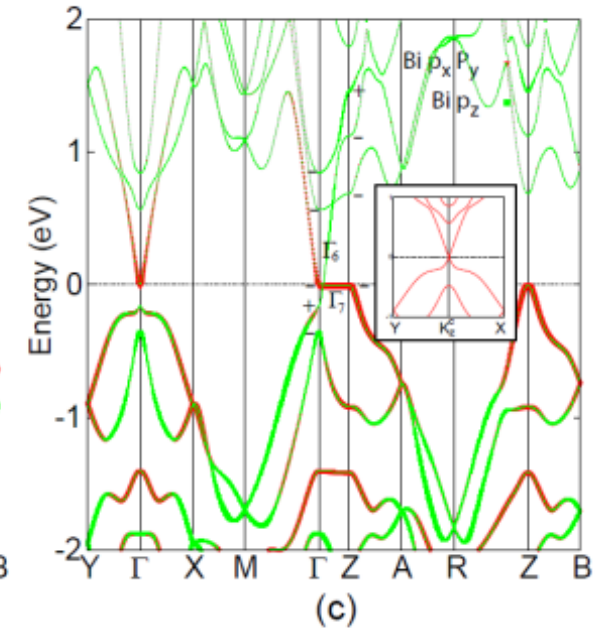
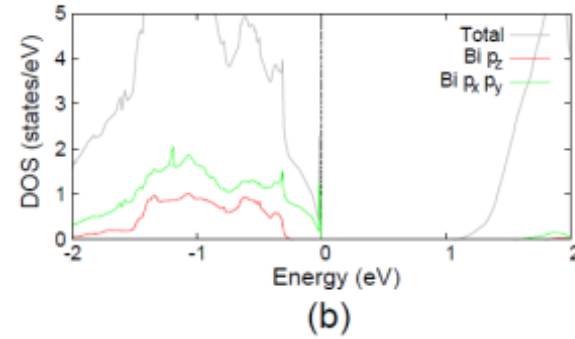
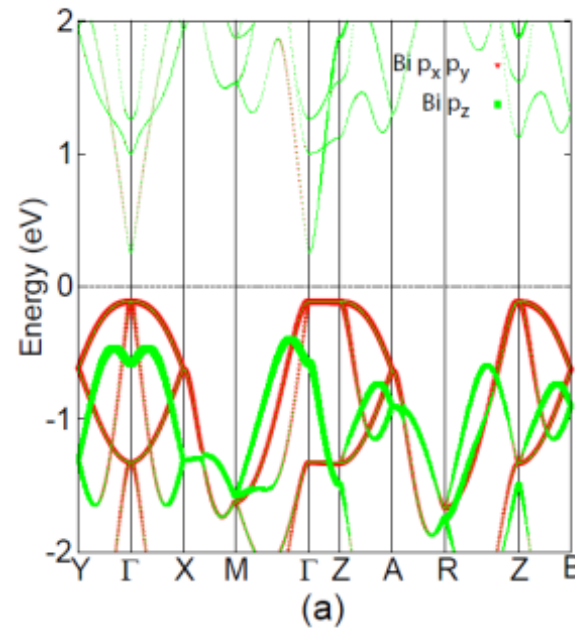
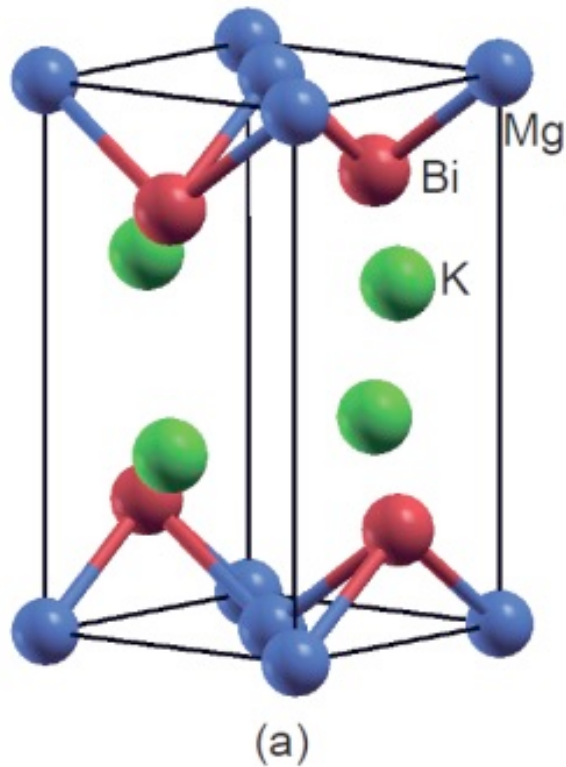




The layered “Heusler”

Three-dimensional Critical Dirac semimetal in KMgBi

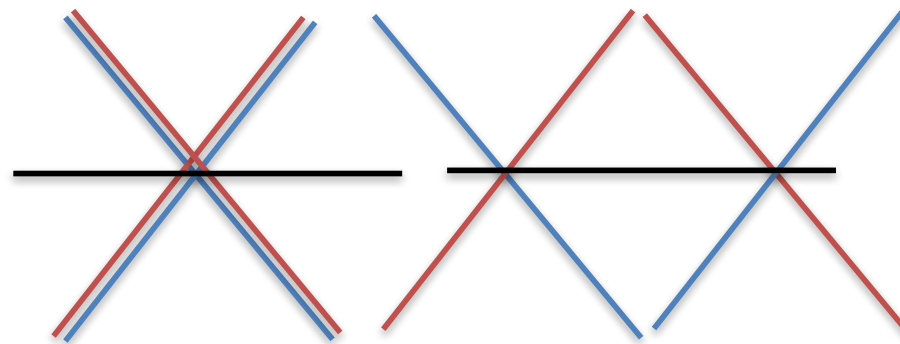
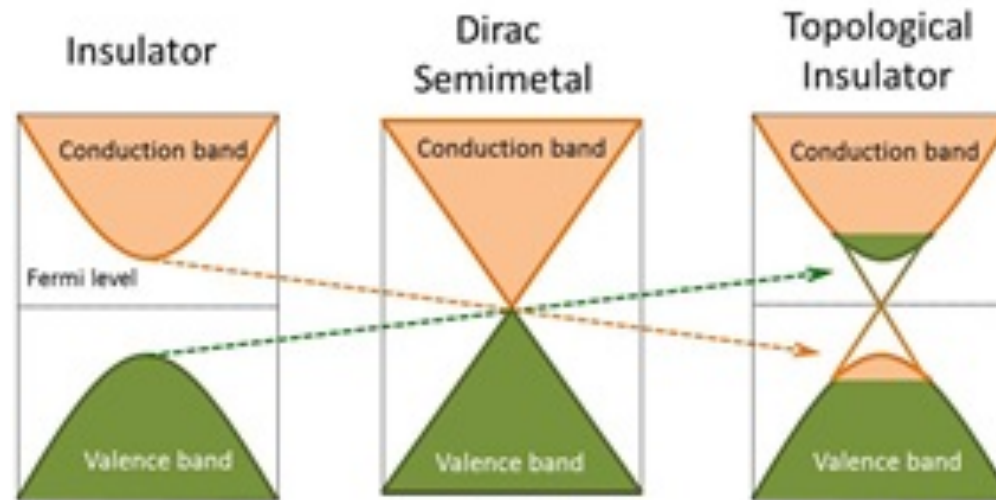
Congcong Le,^{1,*} Shengshan Qin,^{1,*} Xianxin Wu,¹ Xia Dai,¹ Peiyuan Fu,¹ and Jiangping Hu^{1,2,†}





Insulator – semiconductor – metal

Topological Insulator/Semiconductor – Dirac/Weyl Semimetal –



Dirac 4 folded

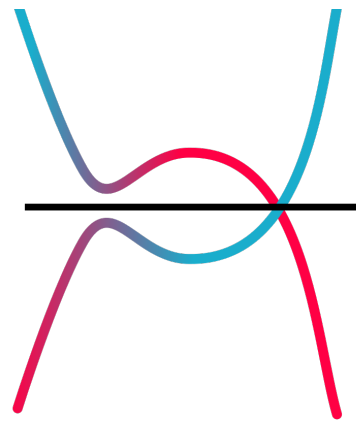
Weyl 4 folded

degenerated



Weyl Semimetals

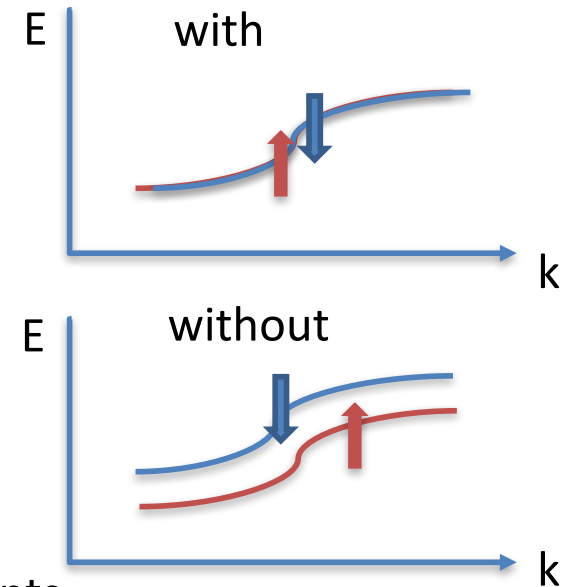
Breaking symmetry – NbP





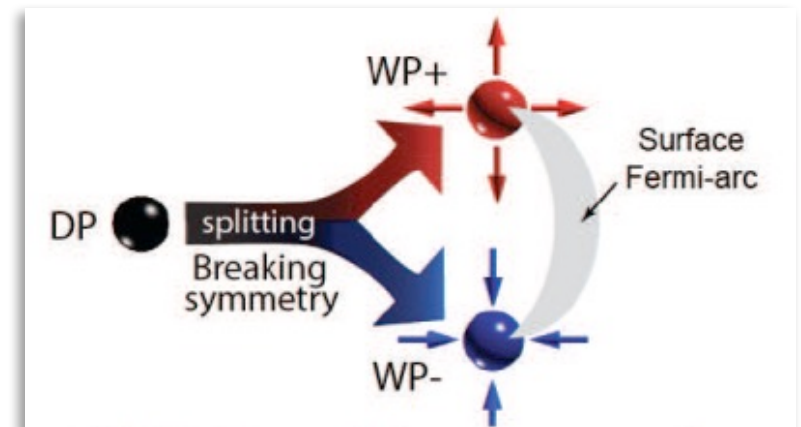
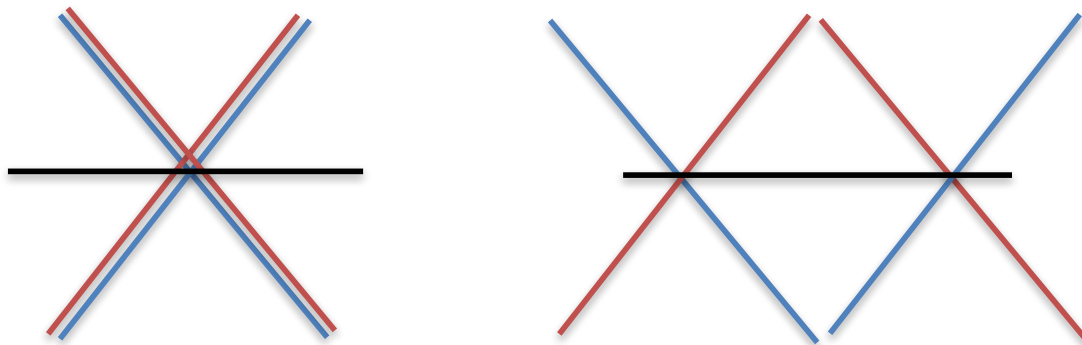
Weyl Semimetal

- Breaking symmetry
 - Inversion symmetry (Structural distortion)
- Breaking time reversal symmetry
 - Magnetic field



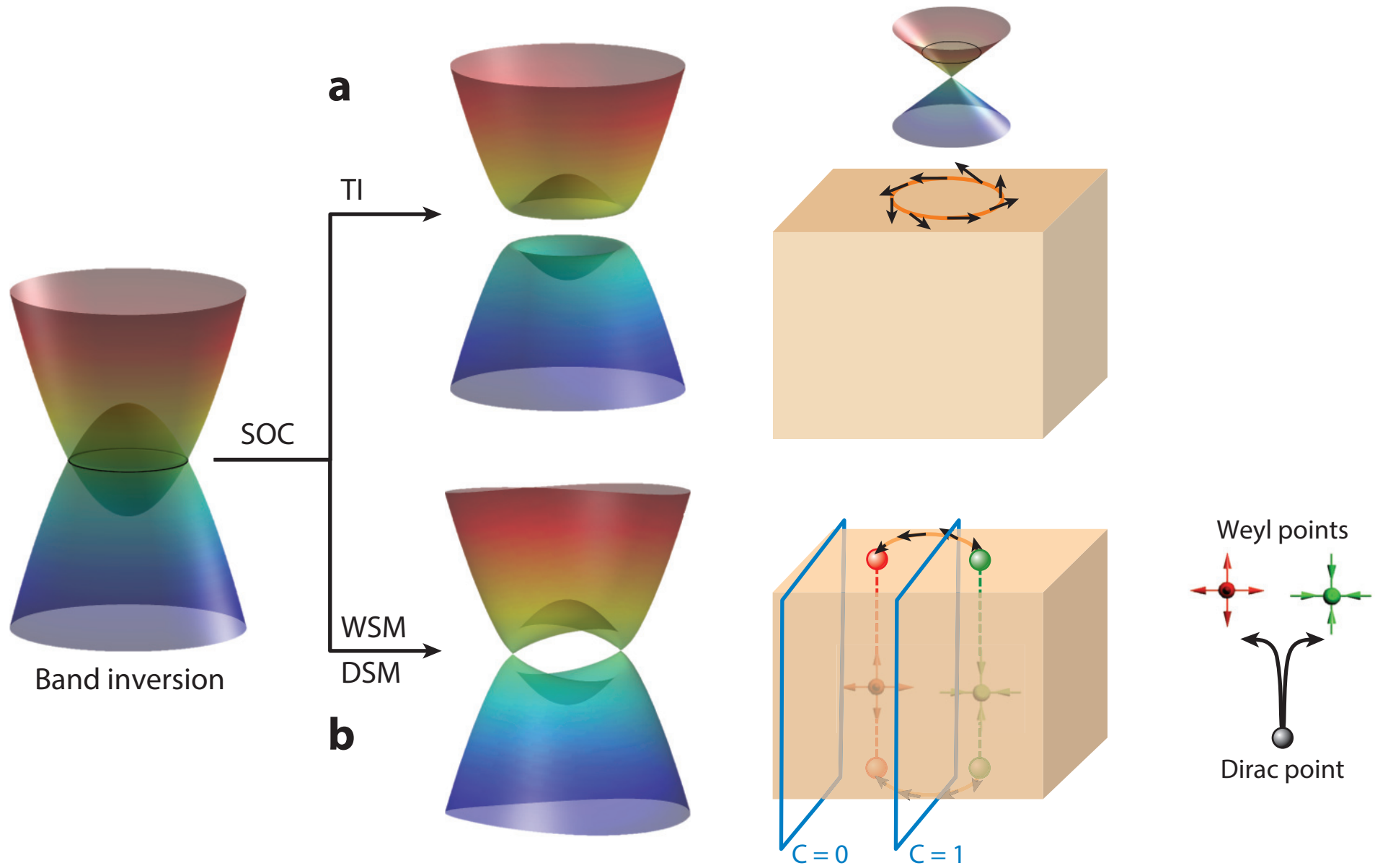
Dirac points are at high symmetry points

Weyl points are not at high symmetry points



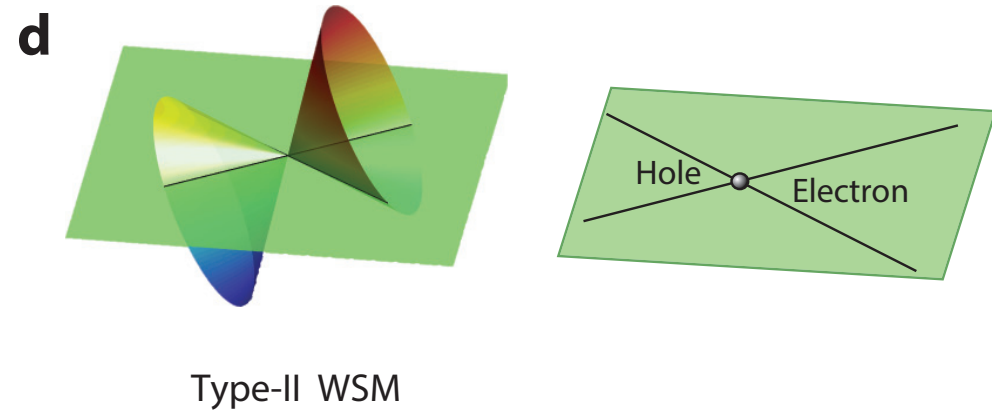
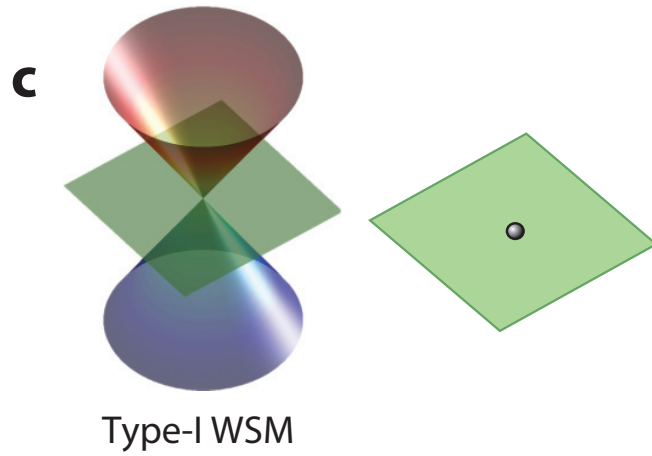


Weyl semimetals

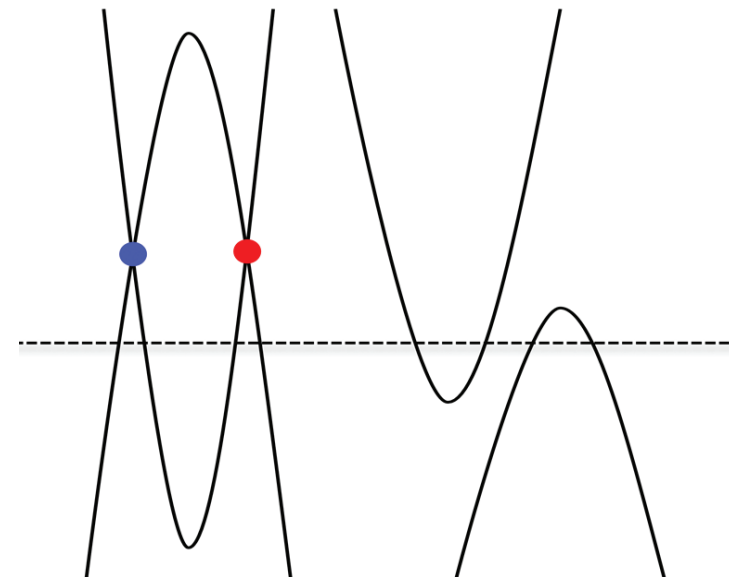
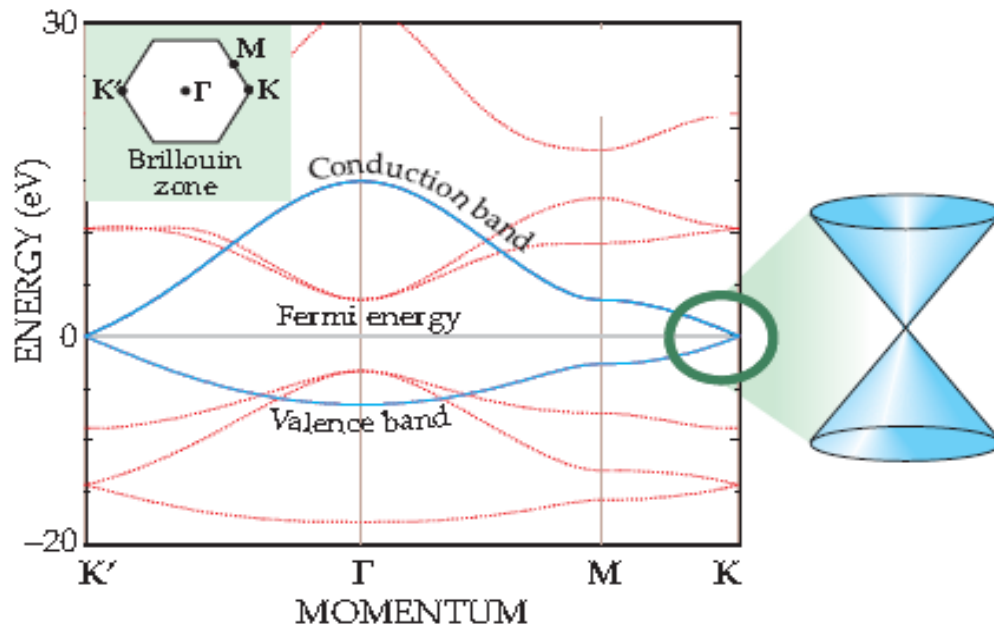




Type I or II



Graphene





Weyl semimetals

3D topological Weyl semimetals - breaking time reversal symmetry – in transport measurement we should see:

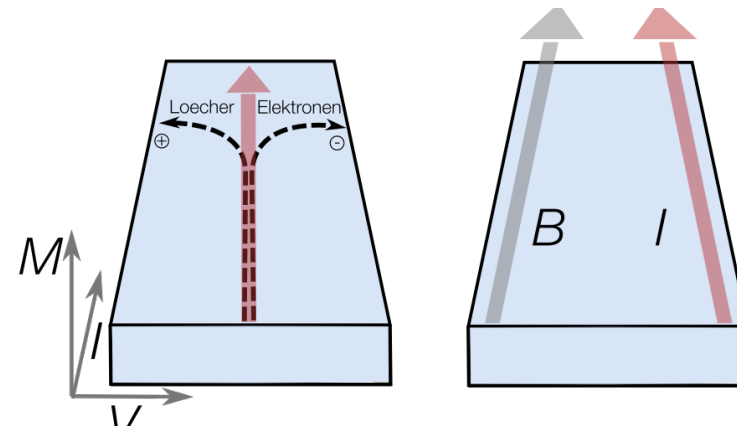
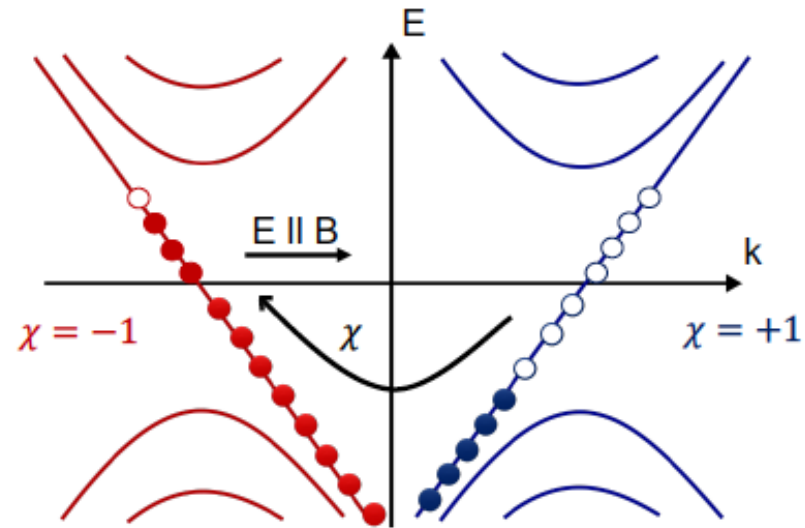
1. Fermi arc



2. Chiral anomaly

$$\partial_\mu j_\chi^\mu = -\chi \frac{e^3}{4\pi^2 \hbar^2} \mathbf{E} \cdot \mathbf{B}$$

$$\sigma_a = \frac{e^3 v_f^3}{4\pi^2 \hbar \mu^2 c} B^2,$$



S. L. Adler, Phys. Rev. 177, 2426 (1969)
J. S. Bell and R. Jackiw, Nuovo Cim. A60, 47 (1969)
AA Zyuzin, AA Burkov - Physical Review B (2012)
AA Burkov, L Balents, PRL 107 12720 (2012)

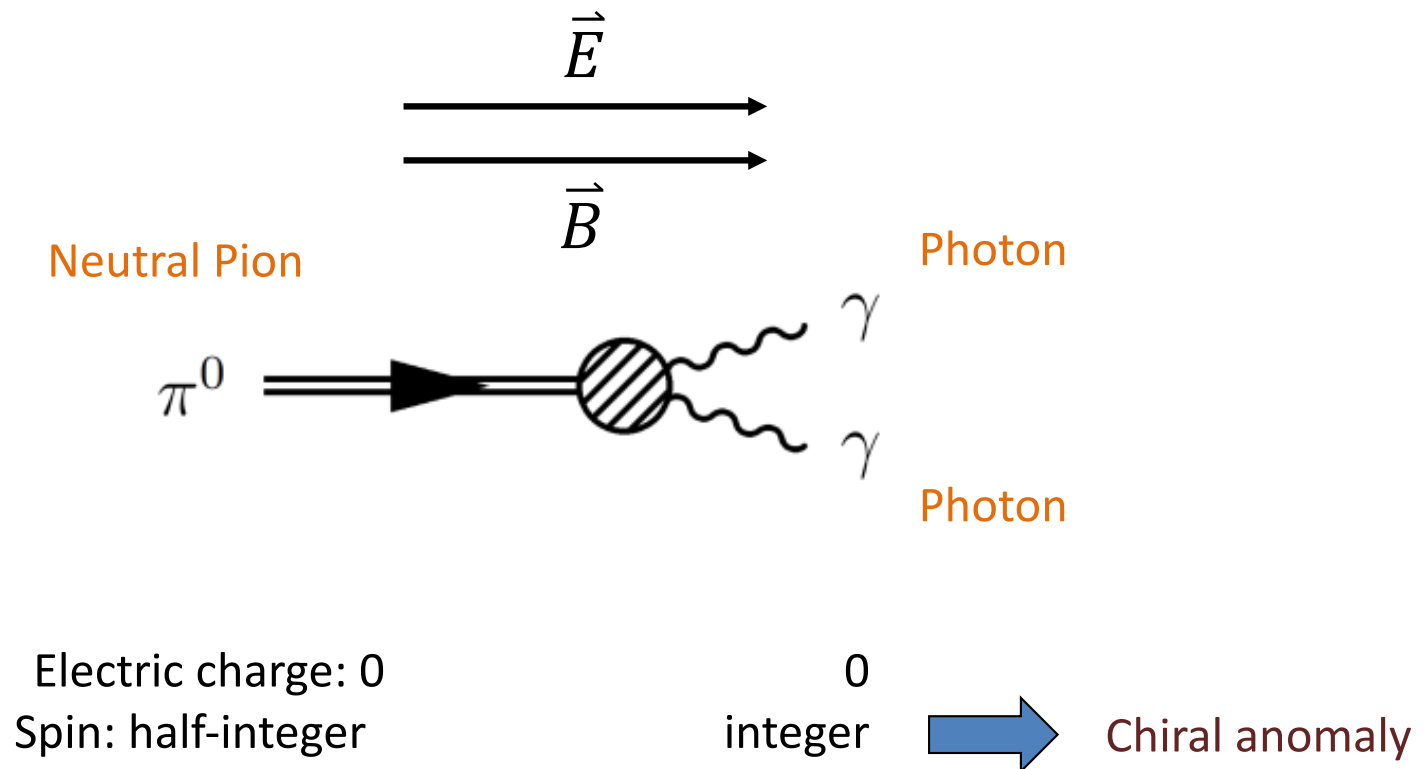


Quantum anomaly in QED

Violation of chiral symmetry.

In Quantum Electro Dynamics (relativistic quantum field theory) chiral charge conservation can be violated for massless fermions!

Pion decay:



Adler, S. L. *Phys. Rev.* **177**, 5 (1969).

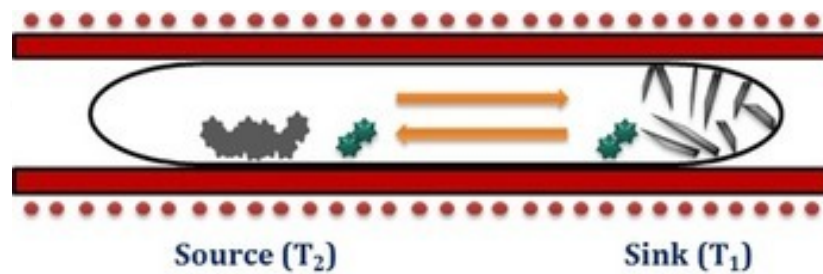
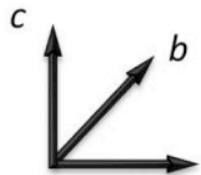
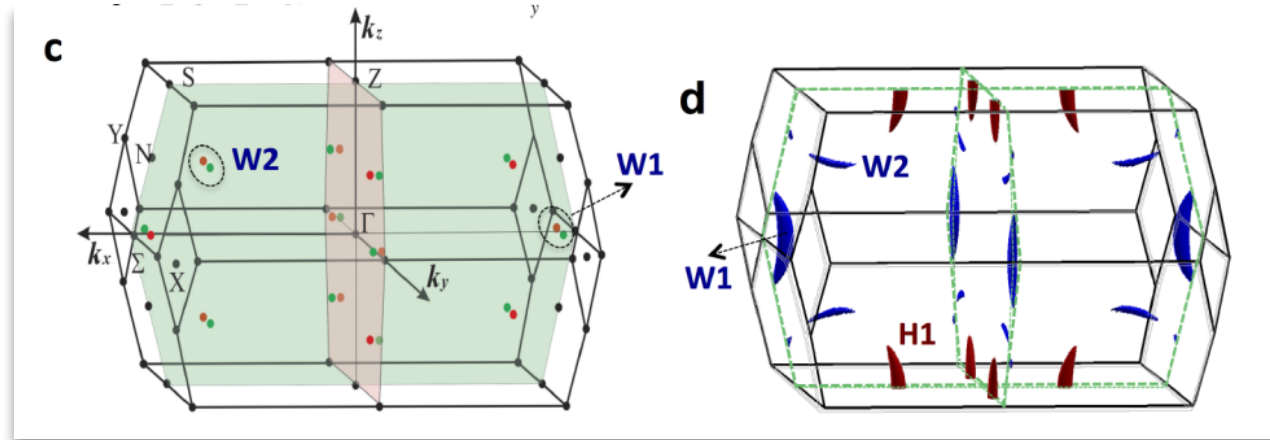
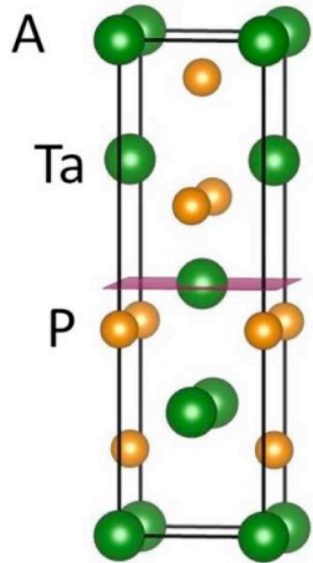
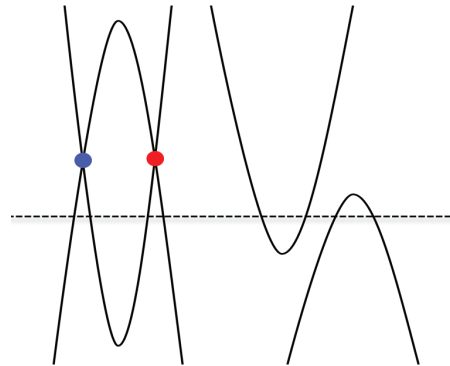
Bell, J. S. & Jackiw, R. *Nuovo Cim.* **A60**, 4 (1969)



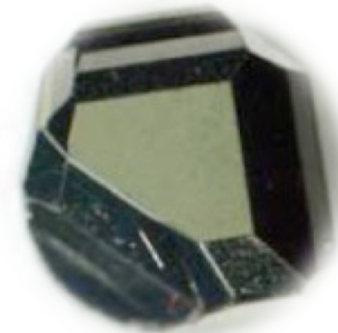
Weyl semimetals in non-centro NbP



NbP, NbAs,
TaP, TaAs

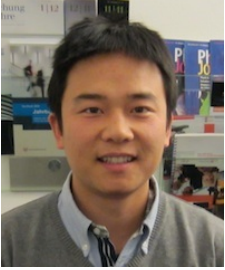


- Transport agent
- Precursor
- Single crystals

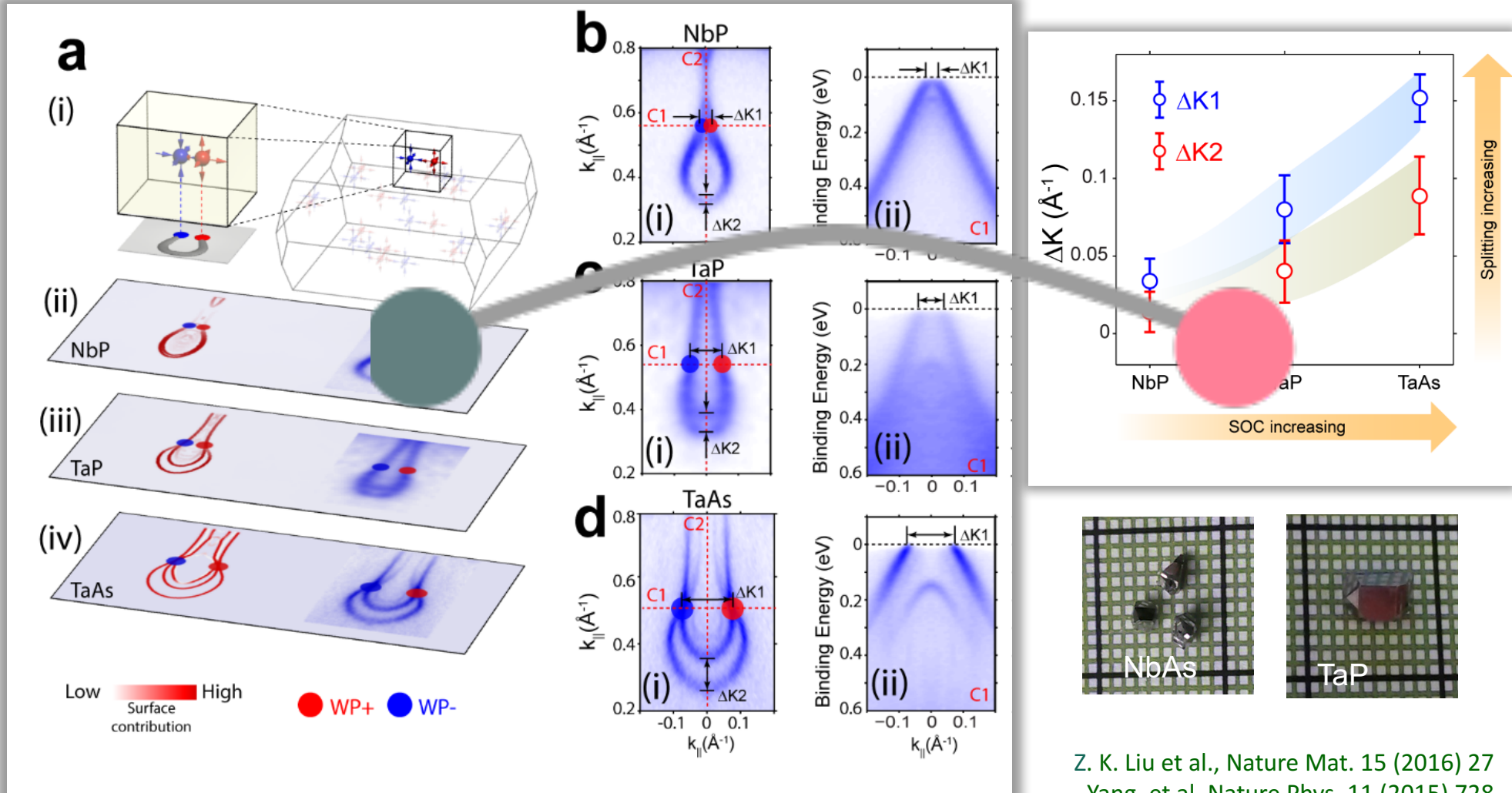




NbP, TaP, TaAs



Increasing spin orbit coupling increases –
heavier elements
Distance between the Weyl points increases

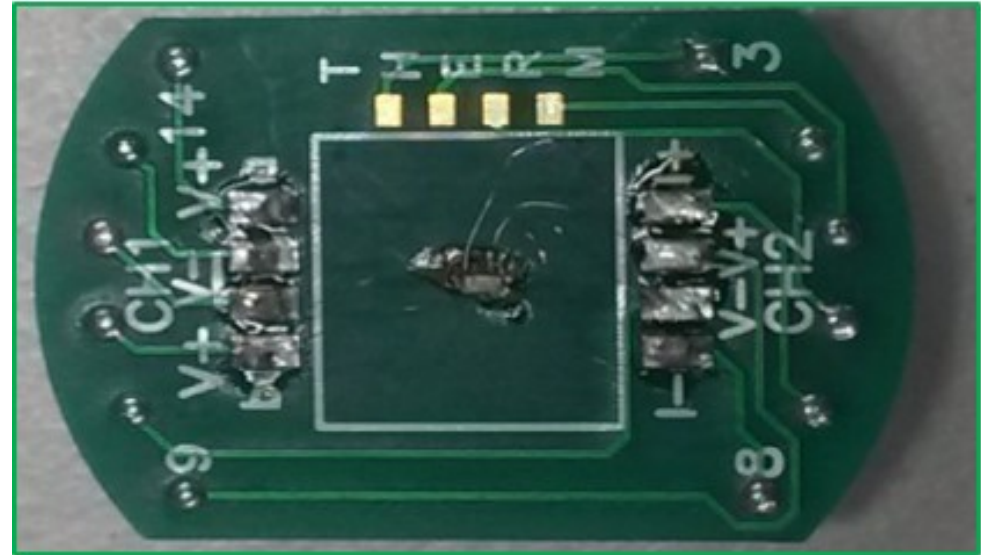
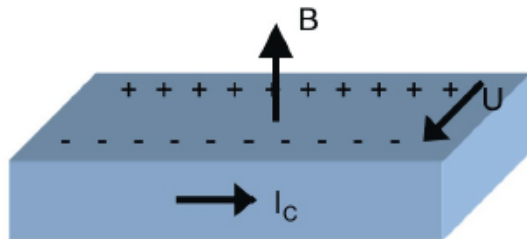


Z. K. Liu et al., Nature Mat. 15 (2016) 27
Yang, et al. Nature Phys. 11 (2015) 728



Resistance Measurement

Hall effect
1879

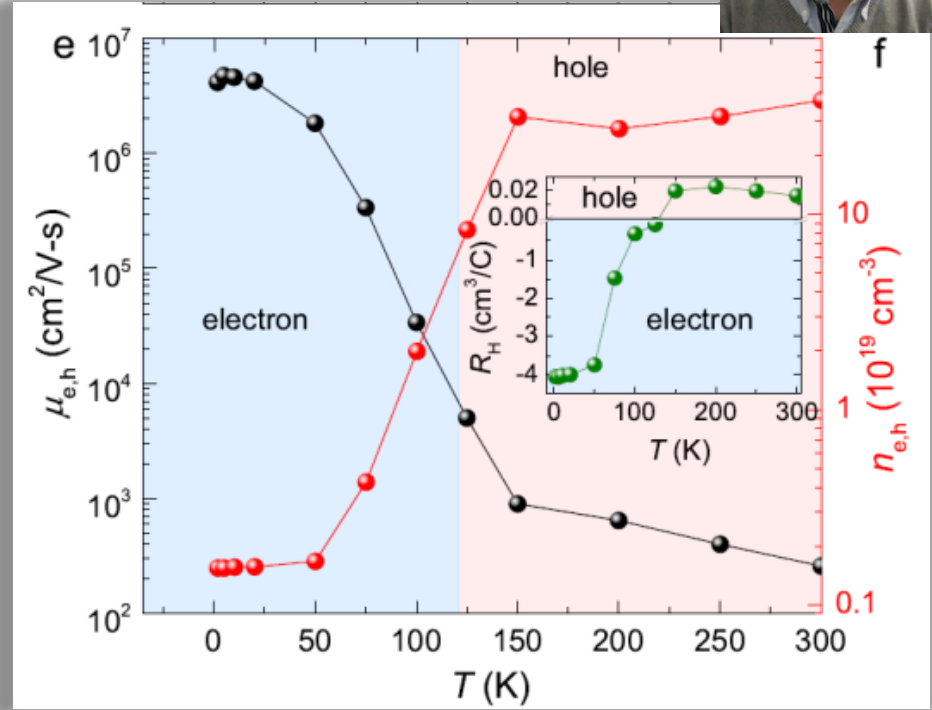
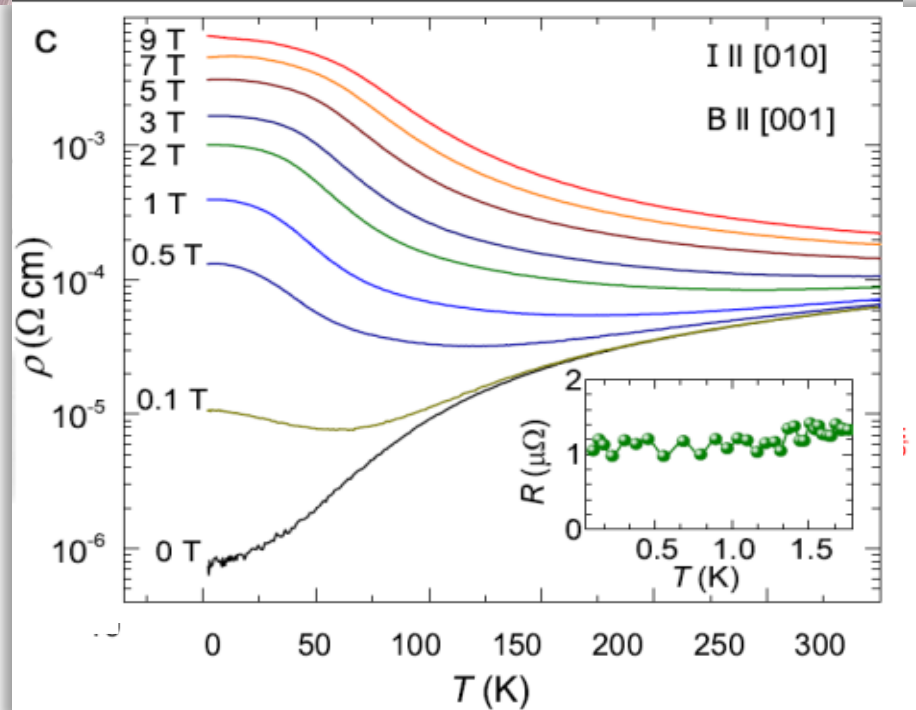


We measure the resistance without and with a magnetic field

- Metal, semiconductor, or insulator
- Electron or hole conductivity
- Resistance in a magnetic field: Magnetoresistance



Weyl Points in non-centro NbP



NbP is a topological Weyl semimetal

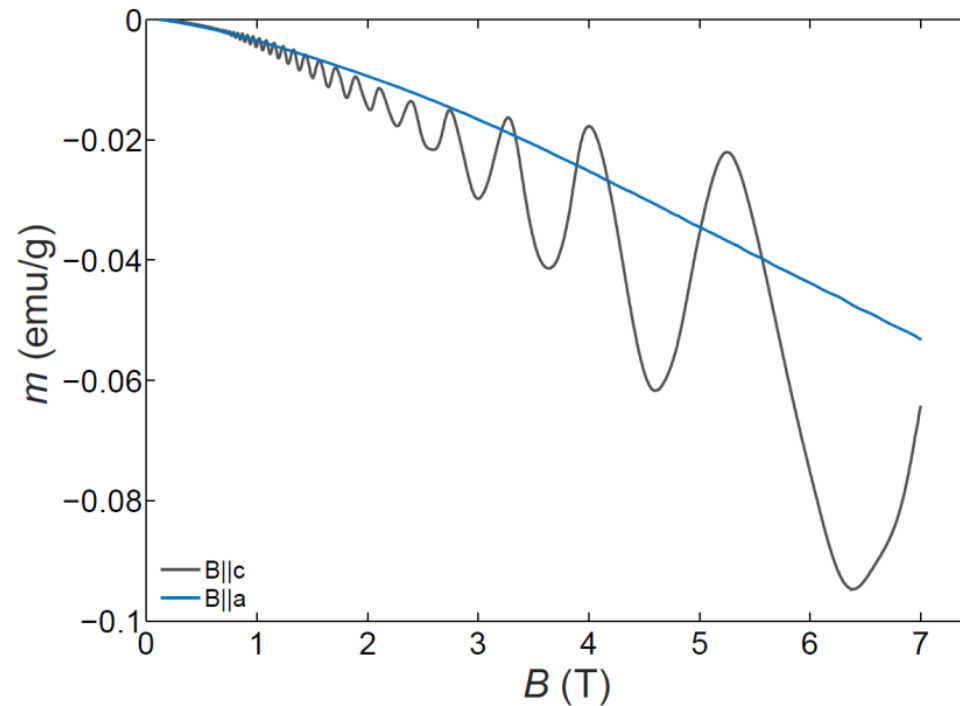
- with massless relativistic electrons
- extremely large magnetoresistance of **850,000%** at 1.85 K, 9T (250% at room temperature)
- an ultrahigh carrier mobility of **$5 \cdot 10^6 \text{ cm}^2 / \text{V s}$**

Shekhar, et al. , Nature Physics 11 (2015) 645,
Frank Arnold, et al. Nature Communication 7 (2016) 11615

Weng, et al. Phys. Rev. X 5, 11029 (2015)
Huang . et al. preprint arXiv:1501.00755



TaP Quantum Oscillations

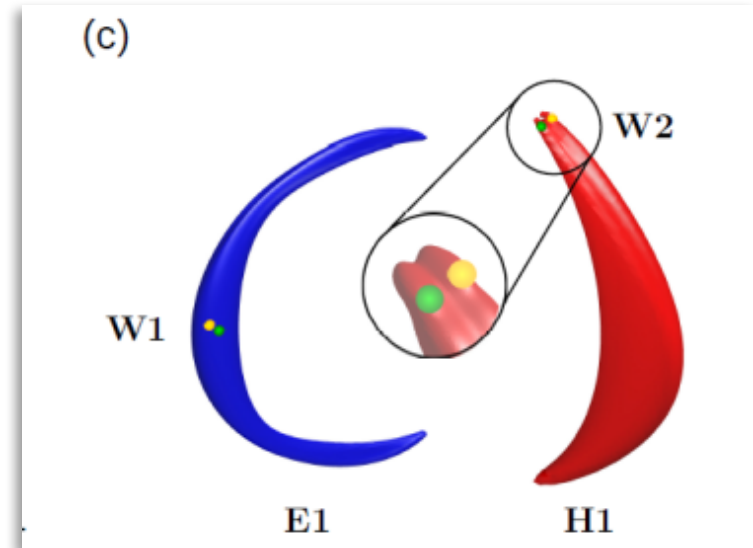
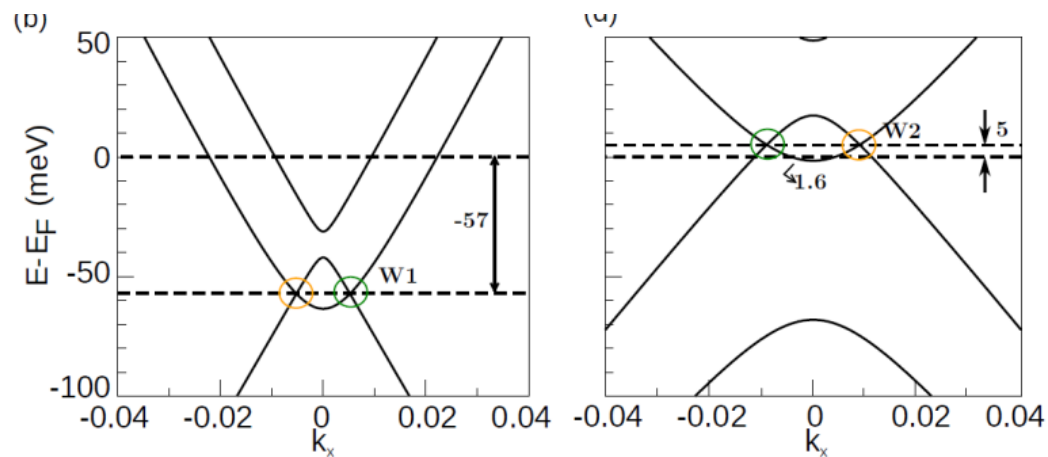
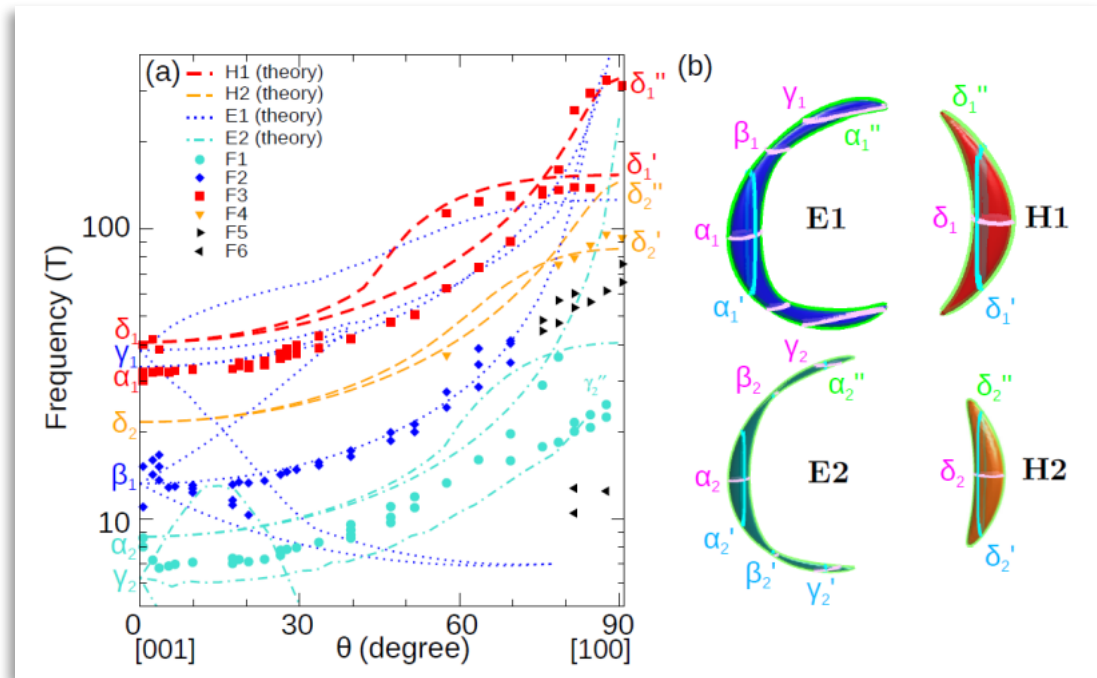
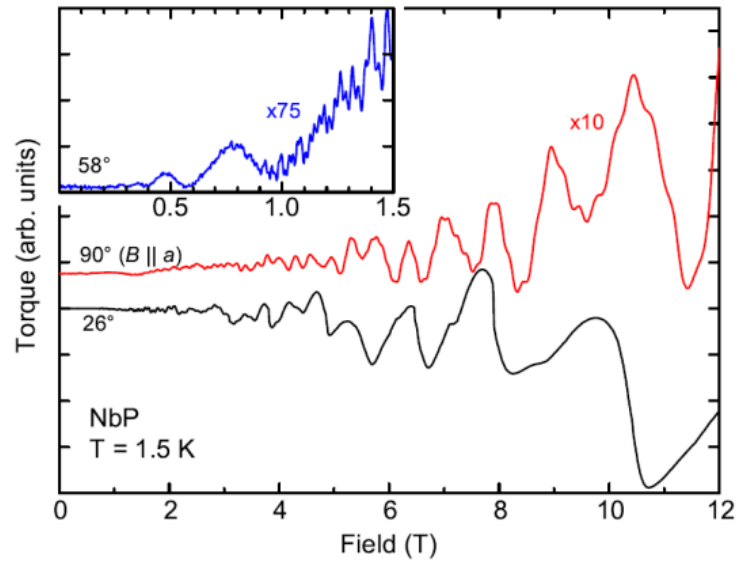


SQUID-VSM magnetization

- In c-direction the diamagnetic magnetization is superimposed by quantum oscillations starting at 0.6 T
- In a-direction only weak quantum oscillations are visible
- The frequency proportional to the extremal Fermi surface perpendicular to \mathbf{B}

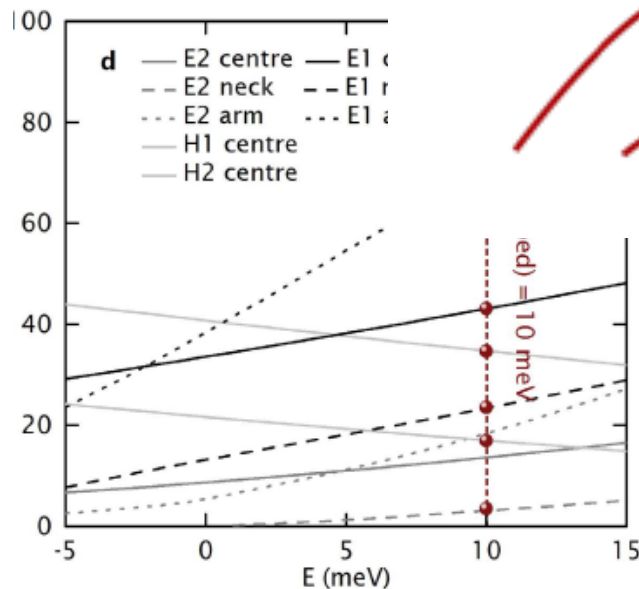
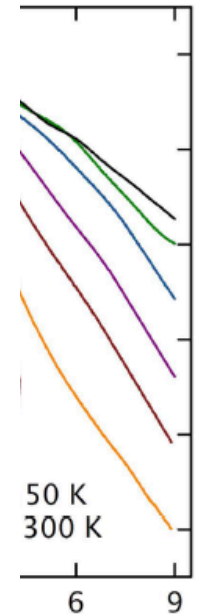
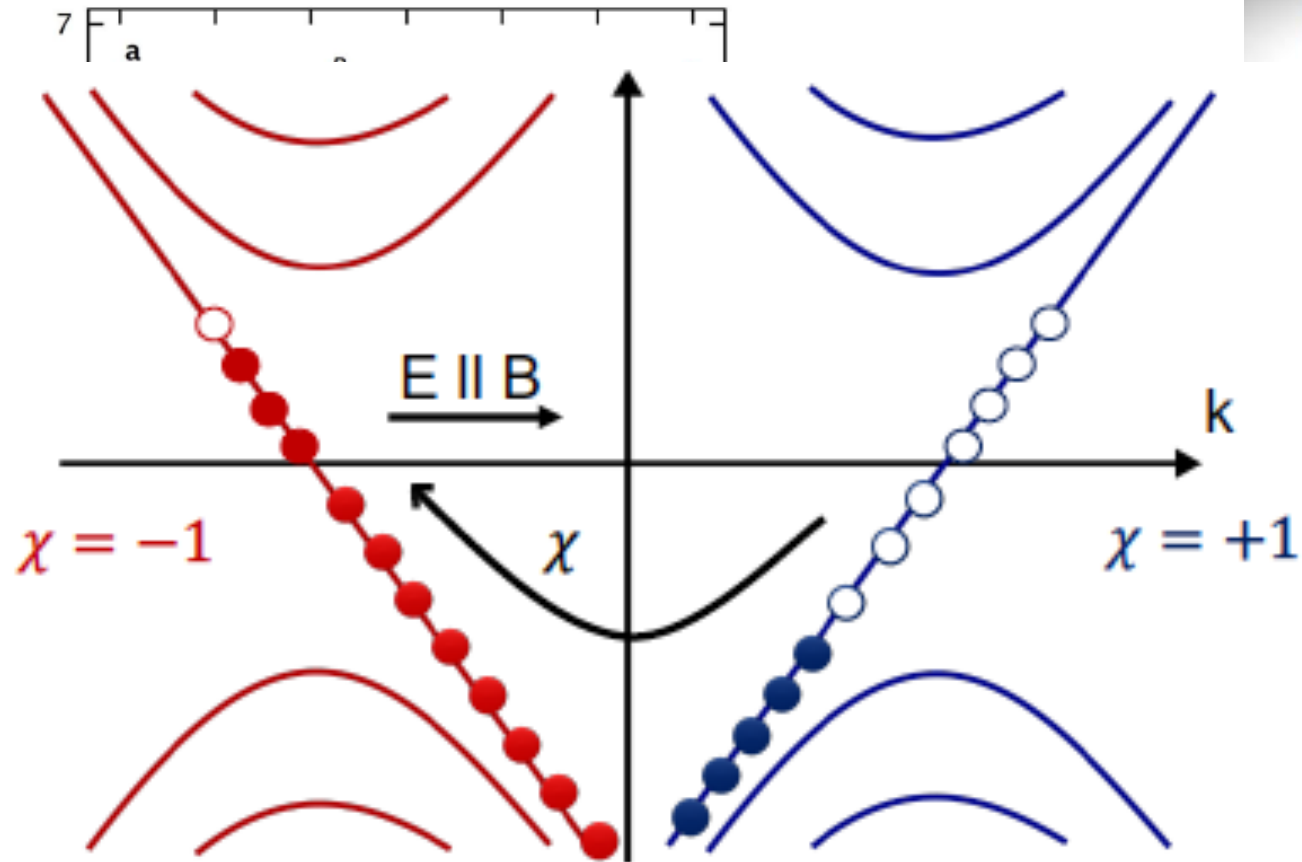
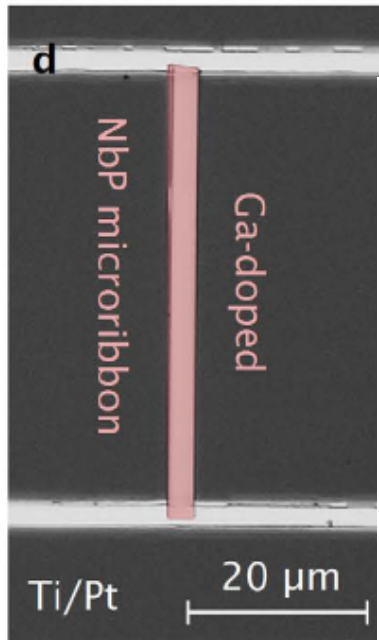


NbP and the Fermi surface





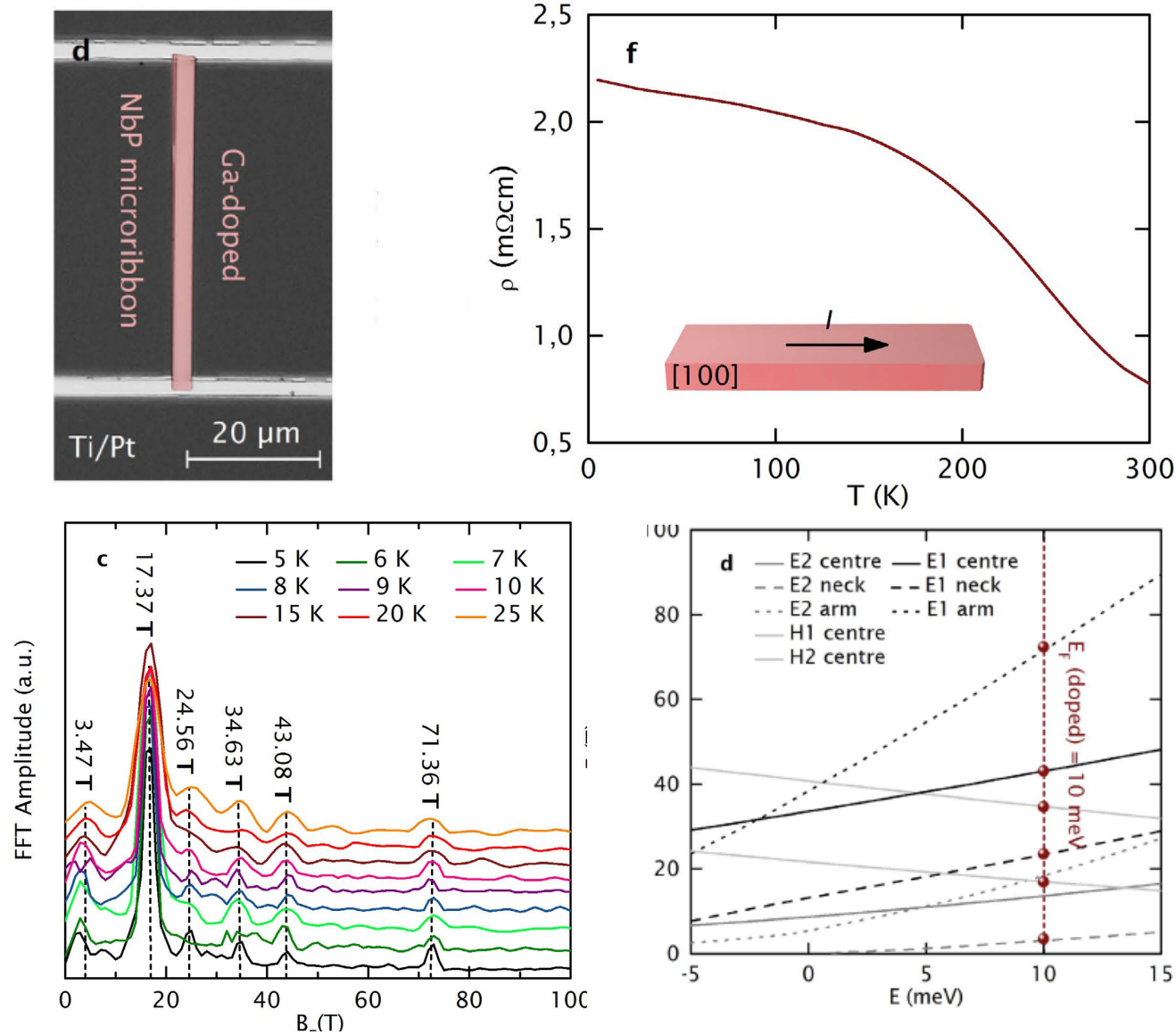
Chiral Anomaly



Ga-doping relocate the Fermi energy in NbP close to the W2 Weyl points
Therefore we observe a negative MR as a signature of the chiral anomaly the, NMR survives up to room temperature



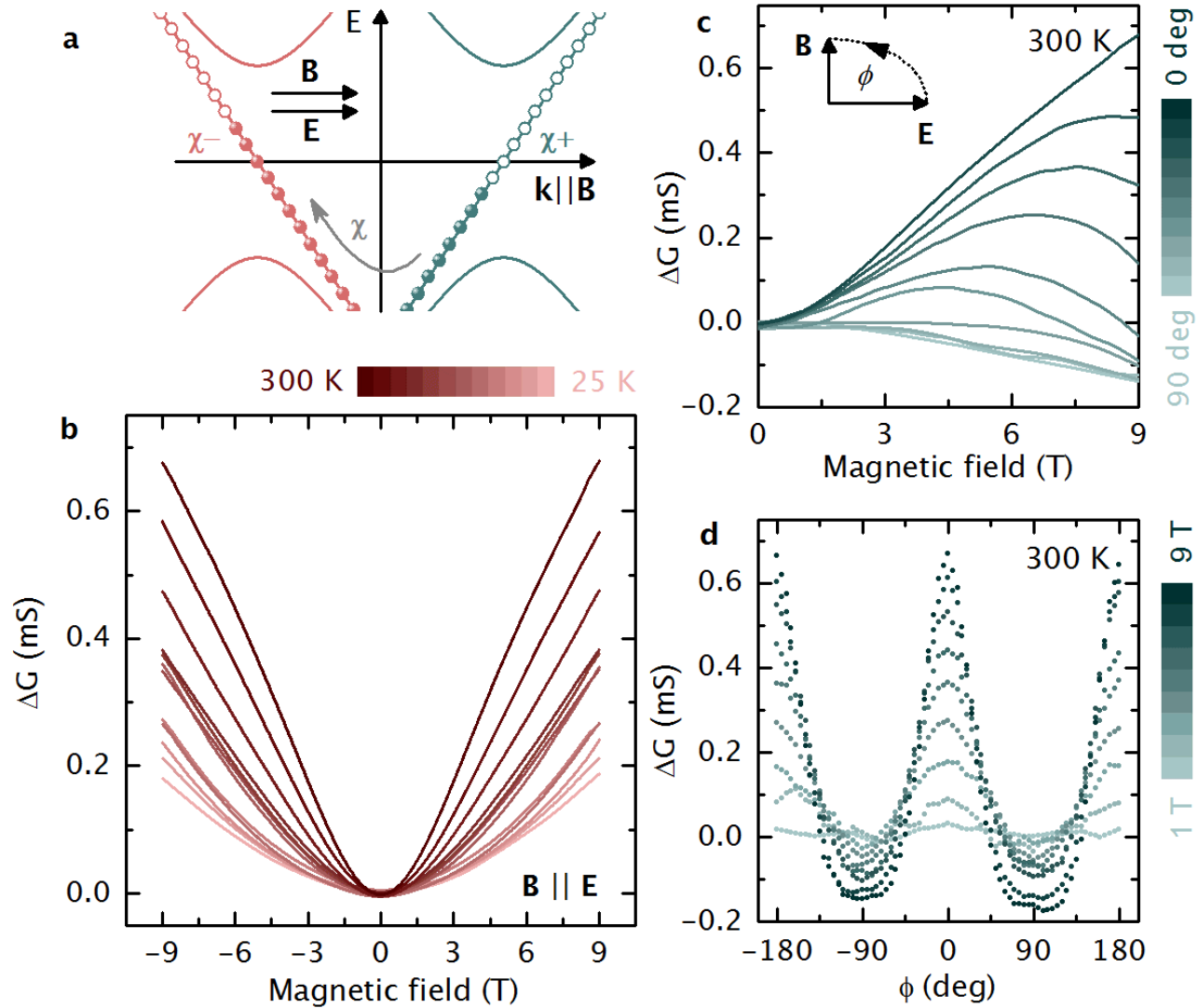
Chiral Anomaly



Ga-doping relocate the Fermi energy in NbP close to the W2 Weyl points



Longitudinal magneto-transport – $E \parallel B$



The PMC is locked to $E \parallel B$, as expected for Chiral anomaly.



Chiral Anomaly

Experimental signatures for the mixed axial-gravitational anomaly in Weyl semimetals

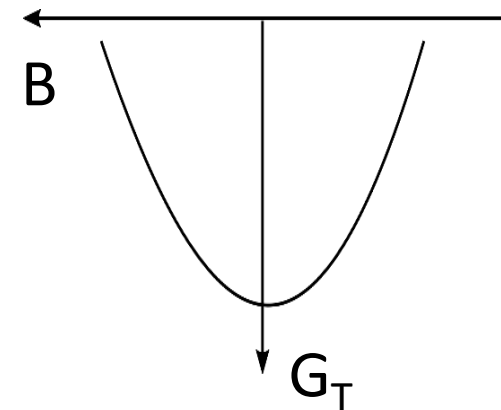
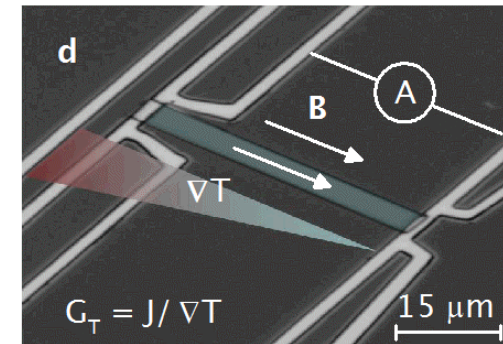
- In solid state physics, mixed axial-gravitational anomaly can be identified by a positive magneto-thermoelectric conductance (PMTG) for $\Delta T \parallel B$.

- Low fields: **quadratic**

$$G_T = d_{\text{th}} + c_2 a_\chi a_g B_{\parallel}^2$$

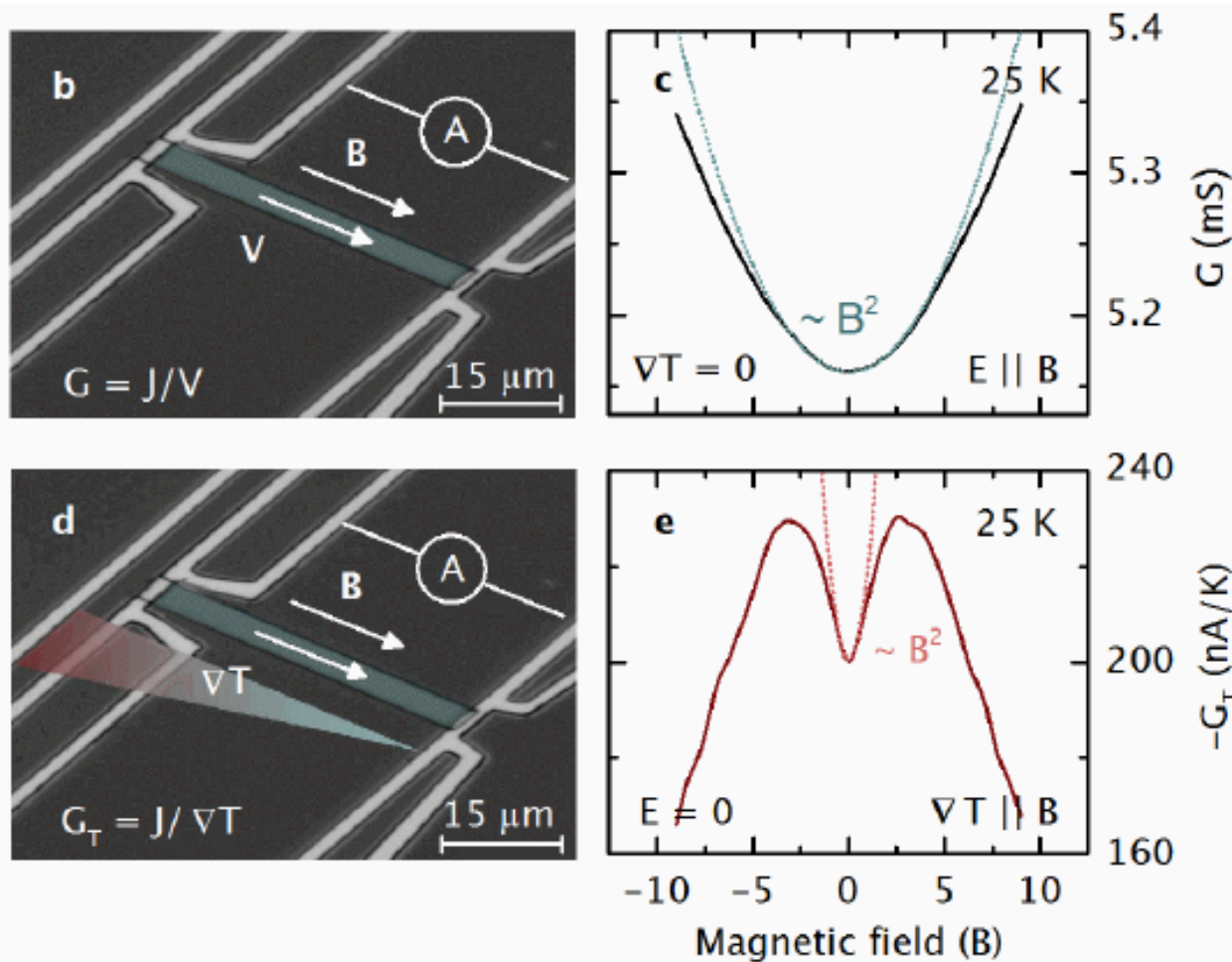
- High fields: **deminishes**

- $\Delta T \parallel B$ dictates sensitivity on alignment of B and ΔT .





Gravitational Anomaly

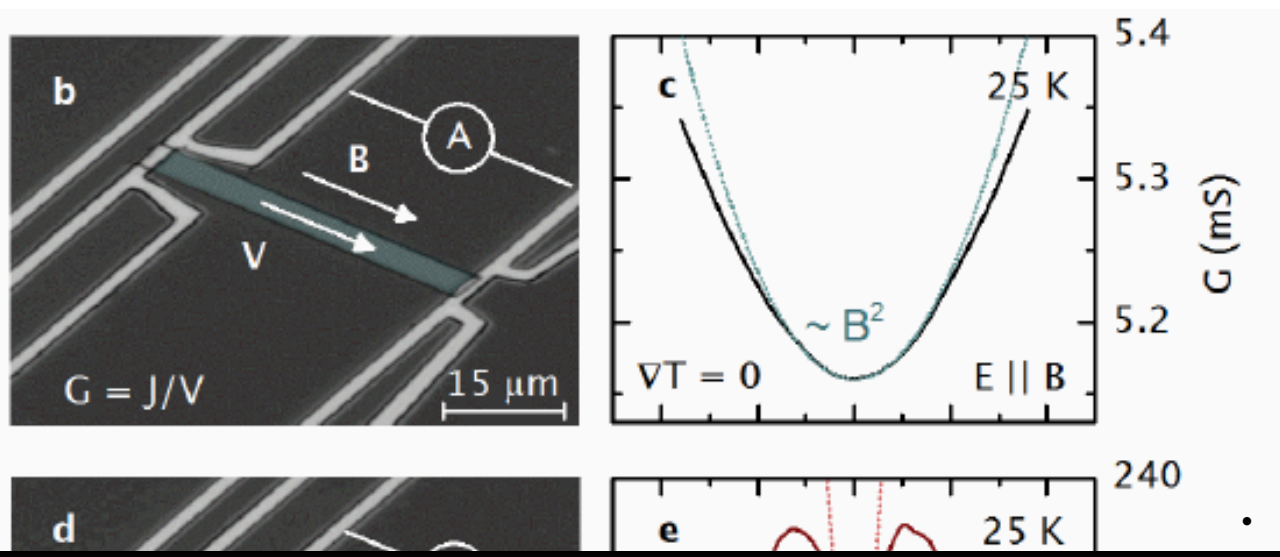


- Landsteiner, et al. Gravitational anomaly and transport phenomena. Phys. Rev. Lett. 107, 021601 (2011). URL
- Jensen, et al. Thermodynamics, gravitational anomalies and cones. Journal of High Energy Physics 2013, 88 (2013).
- Lucas, A., Davison, R. A. & Sachdev, S. Hydrodynamic theory of thermoelectric transport and negative magnetoresistance in weyl semimetals. PNAS 113, 9463–9468 (2016).

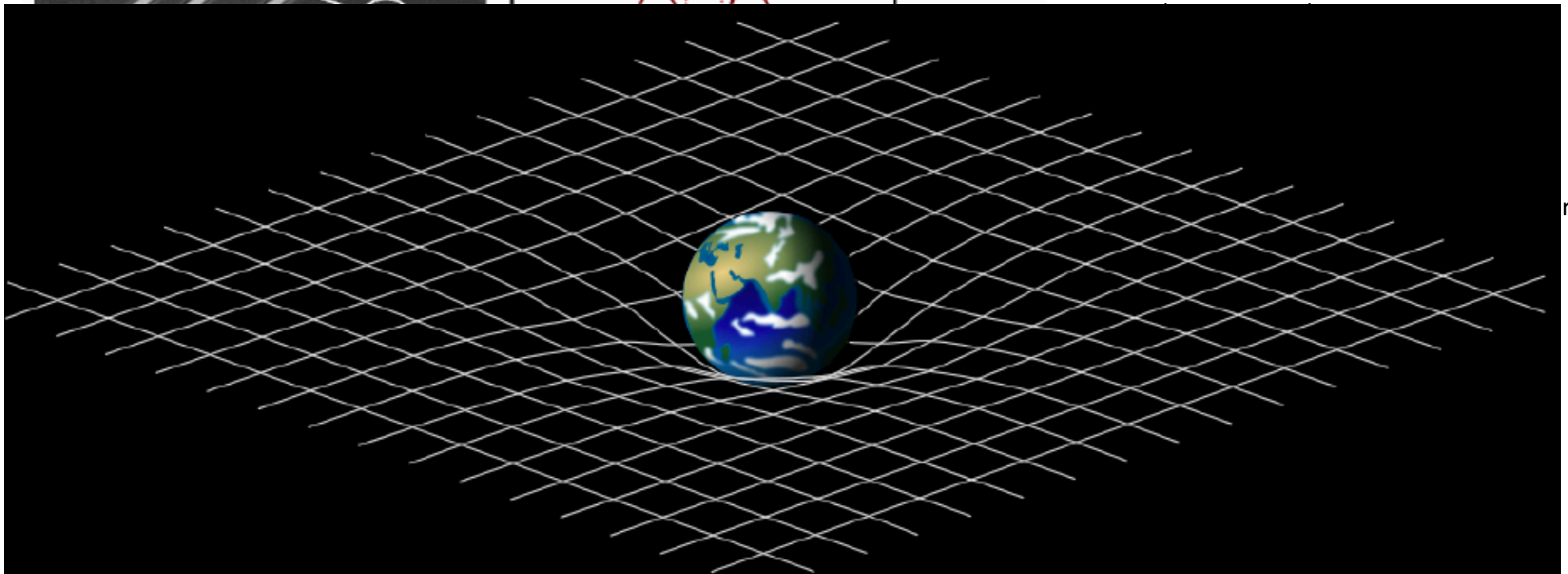
A positive longitudinal magneto-thermoelectric conductance (PMTTC) in the Weyl semimetal NbP for collinear temperature gradients and magnetic fields that vanishes in the ultra quantum limit.



Gravitational Anomaly



• Landsteiner, et al. Gravitational anomaly and



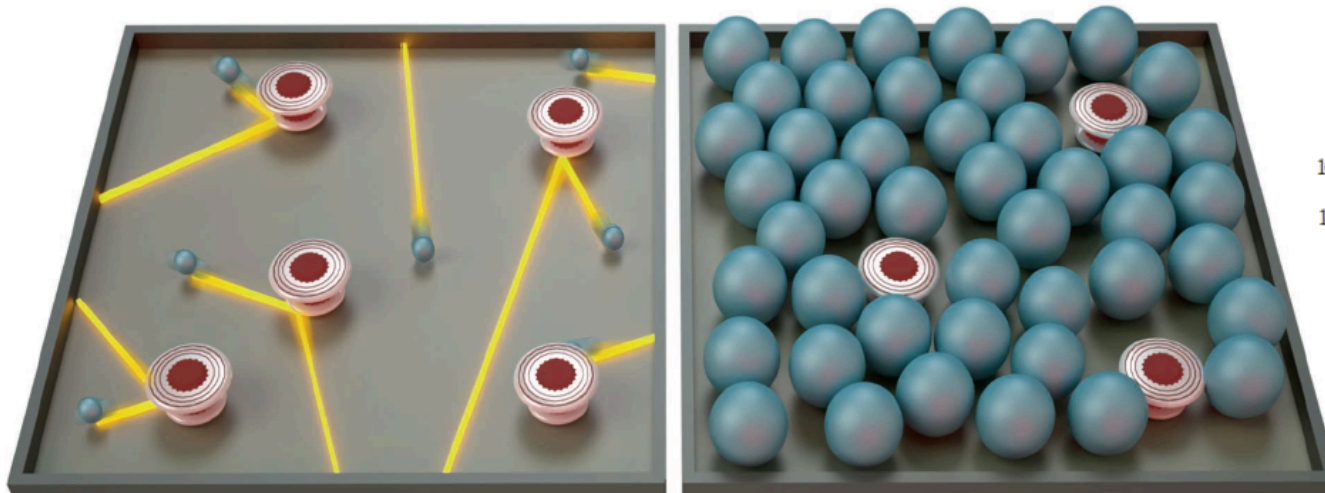
rt



PHYSICS

Electrons go with the flow in exotic material systems

Electronic hydrodynamic flow—making electrons flow like a fluid—has been observed



REFERENCES

1. J. Crossno, J. K. Shi, K. Wang, X. Liu, A. Harzheim, A. Lucas, S. Sachdev, P. Kim, T. Taniguchi, K. Watanabe, T. A. Ohki, K. C. Fong, *Science* **351**, 1058 (2016).
2. D. A. Bandurin, I. Torre, R. Krishna Kumar, M. Ben Shalom, A. Tomadin, A. Principi, G. H. Auton, E. Khestanova, K. S. Novoselov, I. V. Grigorieva, L. A. Ponomarenko, A. K. Geim, M. Polini, *Science* **351**, 1055 (2016).
3. P. J. W. Moll *et al.*, *Science* **351**, 1061 (2016).
4. J. Zaanen, Y.-W. Sun, Y. Liu, K. Schalm, *Holographic Duality in Condensed Matter Physics* (Cambridge Univ. Press, 2015).
5. S. A. Hartnoll, P. K. Kovtun, M. Mueller, S. Sachdev, *Phys. Rev. B* **76**, 144502 (2007).
6. A. H. Castro Neto *et al.*, *Rev. Mod. Phys.* **81**, 109 (2009).
7. M. Mueller, J. Schmalian, L. Fritz, *Phys. Rev. Lett.* **103**, 025301 (2009).
8. M. S. Foster, I. L. Aleiner, *Phys. Rev. B* **79**, 085415 (2009).
9. A. Lucas, J. Crossno, K. C. Fong, P. Kim, S. Sachdev, <http://arxiv.org/abs/1510.01738> (2015).
10. L. Levitov, G. Falkovich, <http://arxiv.org/abs/1508.00836> (2015).
11. M. J. M. de Jong, L. W. Molenkamp, *Phys. Rev. B* **51**, 13389 (1995).

- Hydrodynamic electron fluid is defined by momentum-conserving electron-electron scattering
- Violation of Wiedeman-Franz law
- Viscosity-induced shear forces making the electrical resistivity a function of the channel width



Evidence for hydrodynamic electron flow in PdCoO₂

Philip J. W. Moll,^{1,2,3} Pallavi Kushwaha,³ Nabhanila Nandi,³ Burkhard Schmidt,³ Andrew P. Mackenzie^{3,4*}

Experimental evidence that the resistance of restricted channels of the ultra-pure two-dimensional metal PdCoO₂ has a large viscous contribution

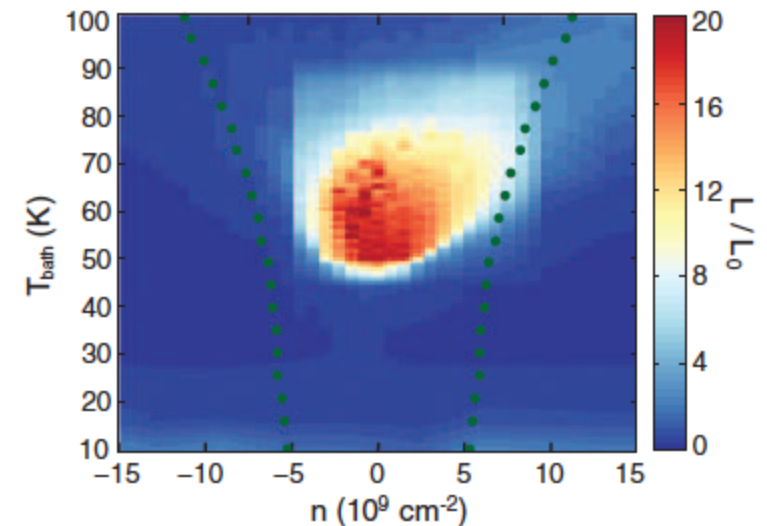
Negative local resistance caused by viscous electron backflow in graphene

D. A. Bandurin,¹ I. Torre,² R. Krishna Kumar,^{1,3} M. Ben Shalom,^{1,4} A. Tomadin,⁵ A. Principi,⁶ G. H. Auton,⁴ E. Khestanova,^{1,4} K. S. Novoselov,⁴ I. V. Grigorieva,¹ L. A. Ponomarenko,^{1,3} A. K. Geim,^{1*} M. Polini^{7*}

ELECTRON TRANSPORT

Observation of the Dirac fluid and the breakdown of the Wiedemann-Franz law in graphene

Jesse Crossno,^{1,2} Jing K. Shi,¹ Ke Wang,¹ Xiaomeng Liu,¹ Achim Harzheim,¹ Andrew Lucas,¹ Subir Sachdev,^{1,3} Philip Kim,^{1,2*} Takashi Taniguchi,⁴ Kenji Watanabe,⁴ Thomas A. Ohki,⁵ Kin Chung Fong^{5*}





High mobility wires

PHYSICAL REVIEW B

VOLUME 51, NUMBER 19

15 MAY 1995-I

Hydrodynamic electron flow in high-mobility wires

M. J. M. de Jong* and L. W. Molenkamp[†]

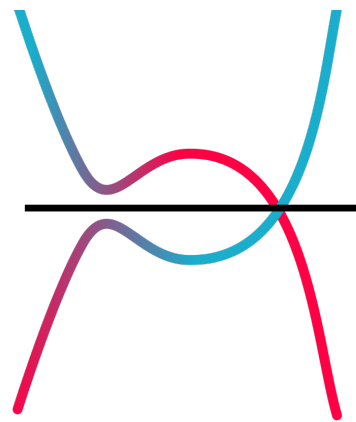
Philips Research Laboratories, 5656 AA Eindhoven, The Netherlands

(Received 24 October 1994)

Hydrodynamic electron flow is experimentally observed in the differential resistance of electrostatically defined wires in the two-dimensional electron gas in (Al,Ga)As heterostructures. In these experiments current heating is used to induce a controlled increase in the number of electron-electron collisions in the wire. The interplay between the partly diffusive wire-boundary scattering and the electron-electron scattering leads first to an increase and then to a decrease of the resistance of the wire with increasing current. These effects are the electronic analog of Knudsen and Poiseuille flow in gas transport, respectively. The electron flow is studied theoretically through a Boltzmann transport equation, which includes impurity, electron-electron, and boundary scattering. A solution is obtained for arbitrary scattering parameters. By calculation of flow profiles inside the wire it is demonstrated how normal flow evolves into Poiseuille flow. The boundary-scattering parameters for the gate-defined wires can be deduced from the magnitude of the Knudsen effect. Good agreement between experiment and theory is obtained.



A Better Weyl Semimetals





WP₂ protected Weyl

PRL 117, 066402 (2016)

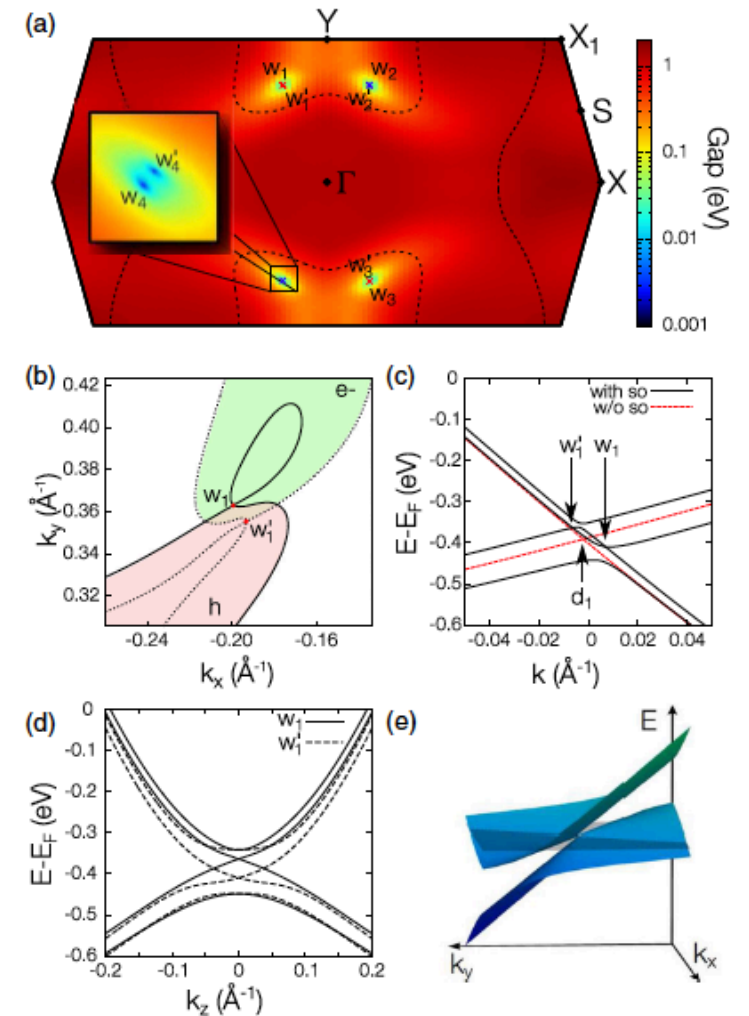
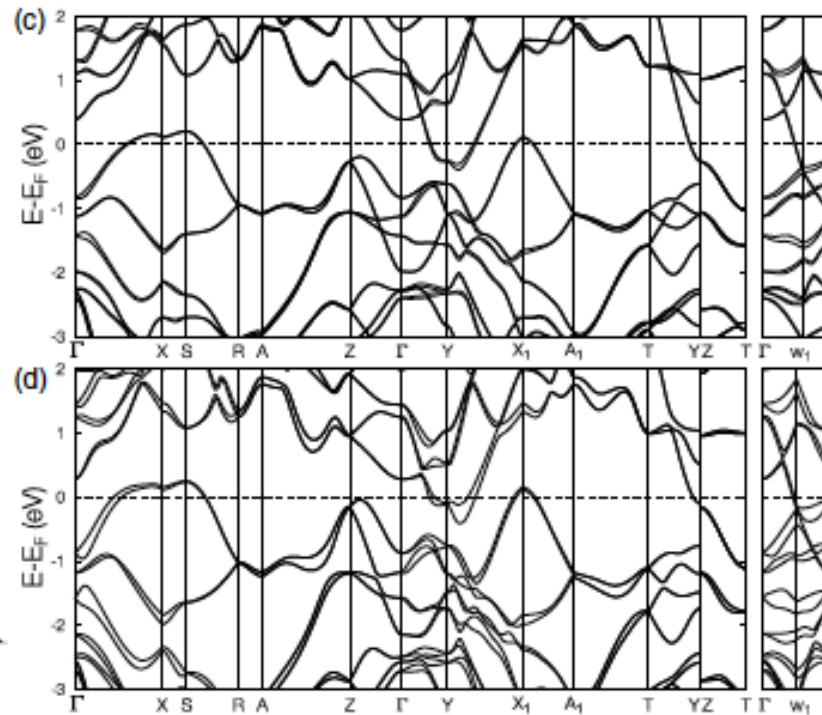
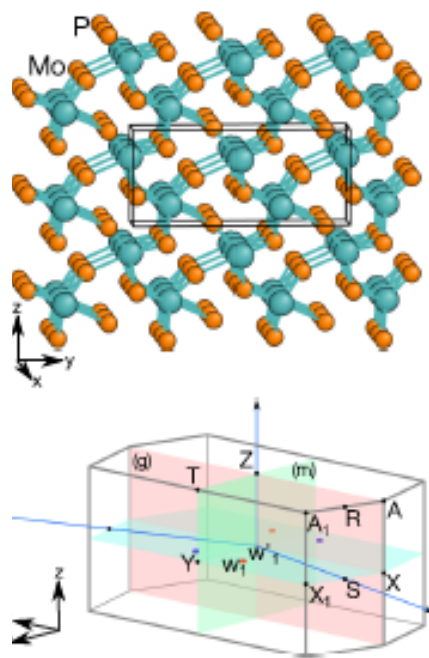
PHYSICAL REVIEW LETTERS

week ending
5 AUGUST 2016



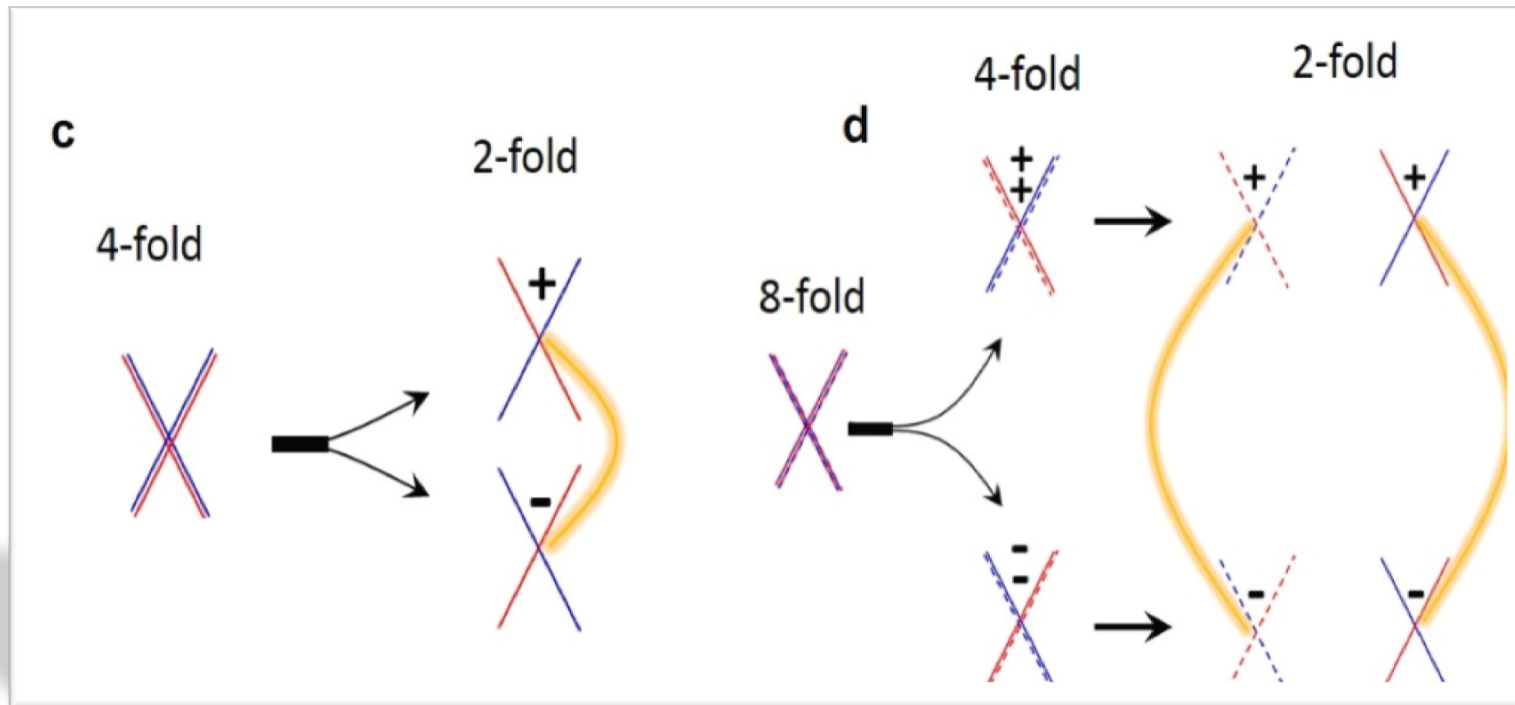
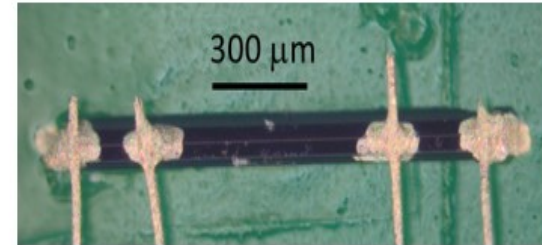
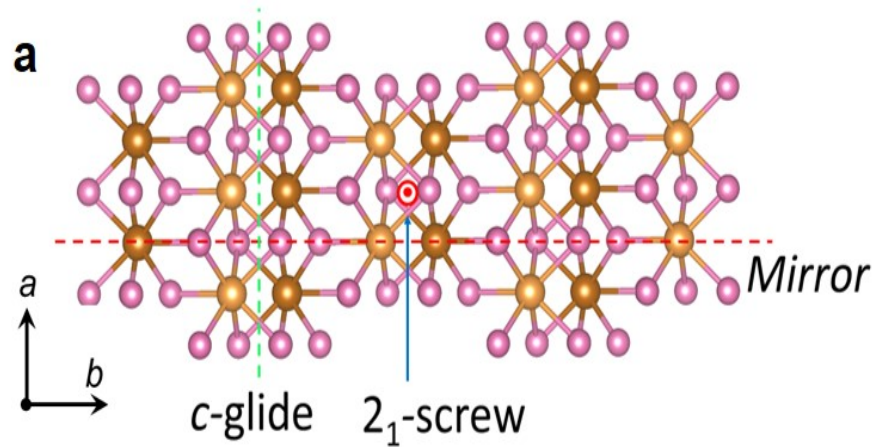
Robust Type-II Weyl Semimetal Phase in Transition Metal Diphosphides XP_2 ($X = \text{Mo}, \text{W}$)

G. Autès,^{1,2} D. Gresch,³ M. Troyer,³ A. A. Soluyanov,^{3,4} and O. V. Yazyev^{1,2}



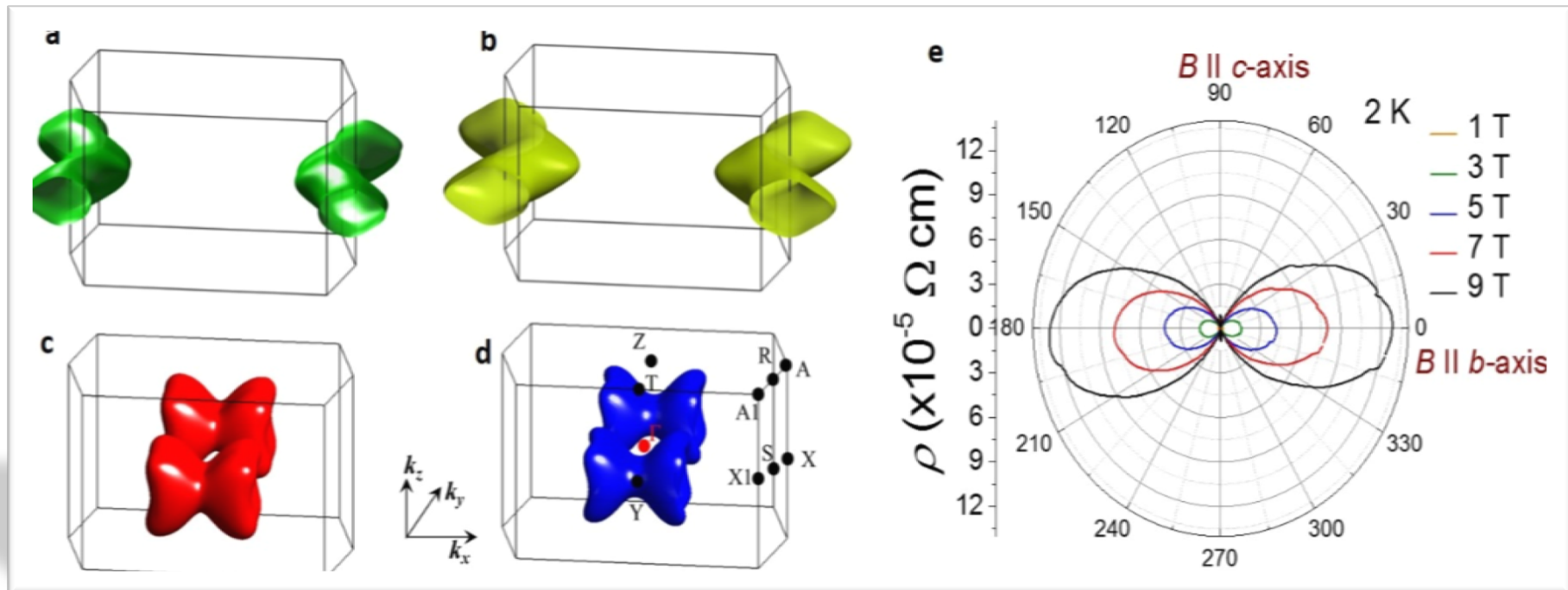
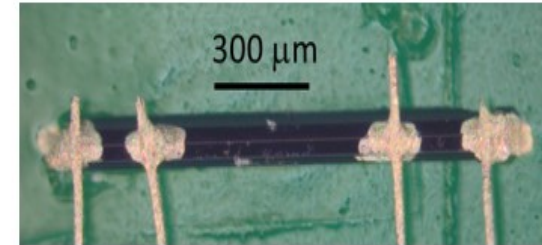
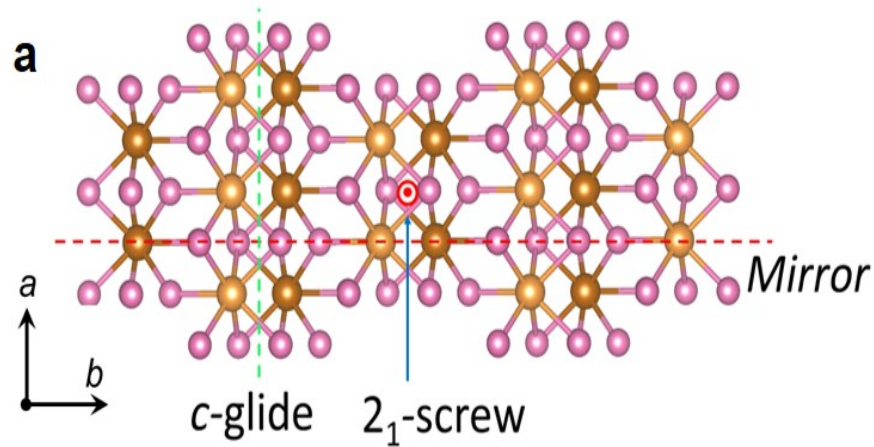


WP₂ protected Weyl



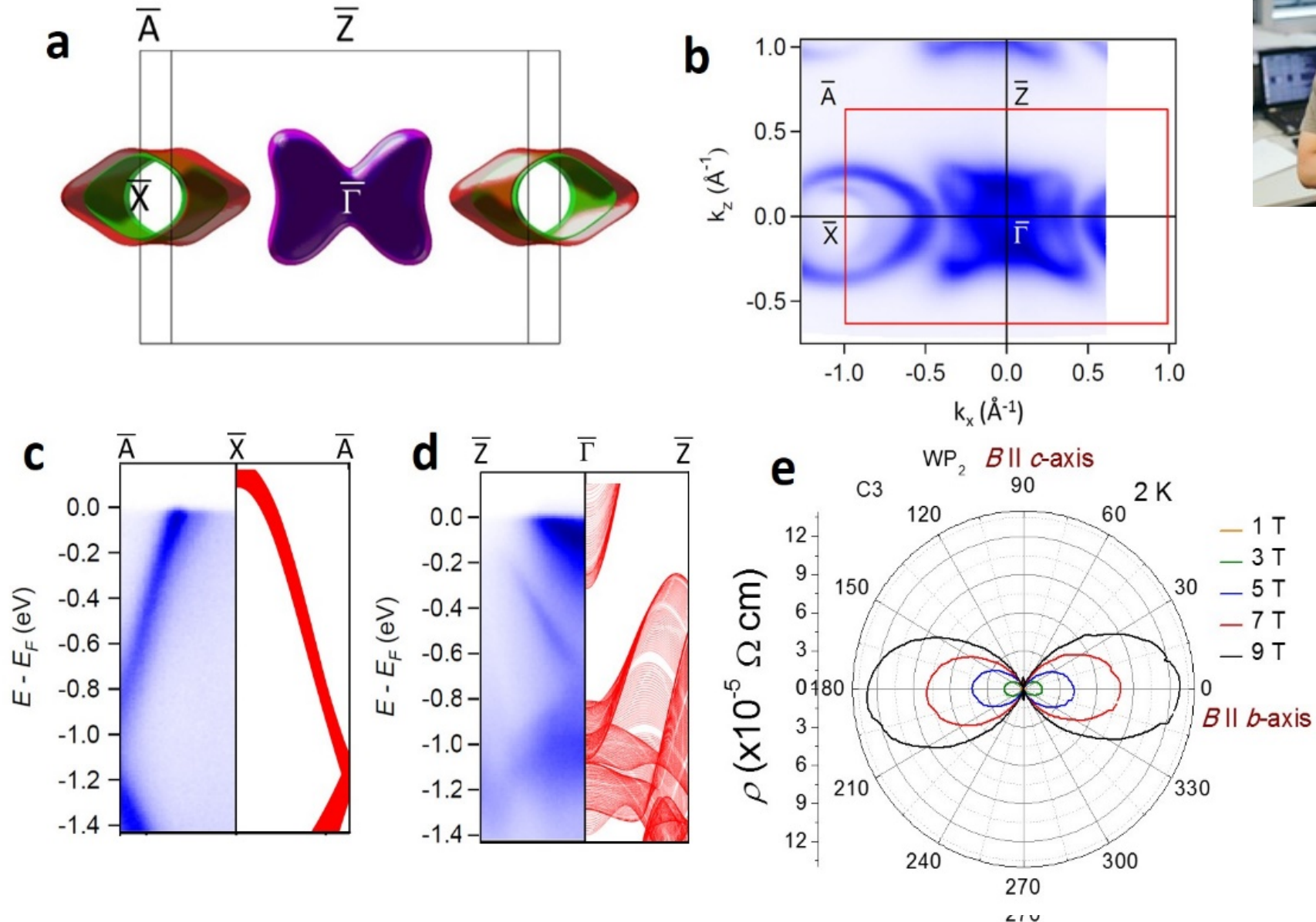


WP₂ protected Weyl





ARPES and the Band Structure



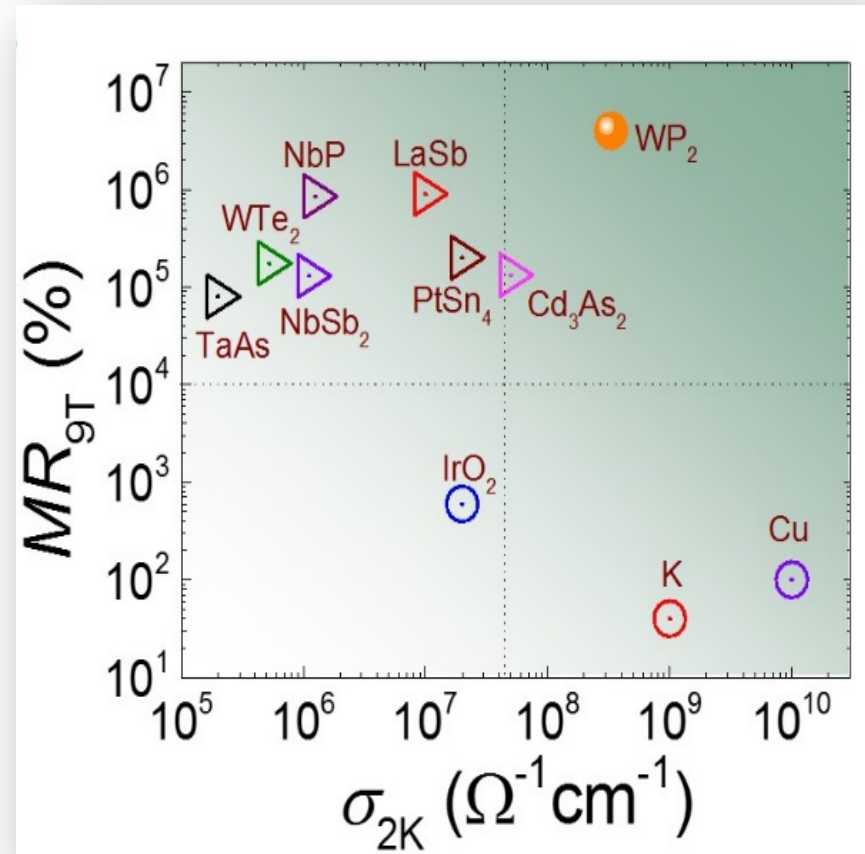
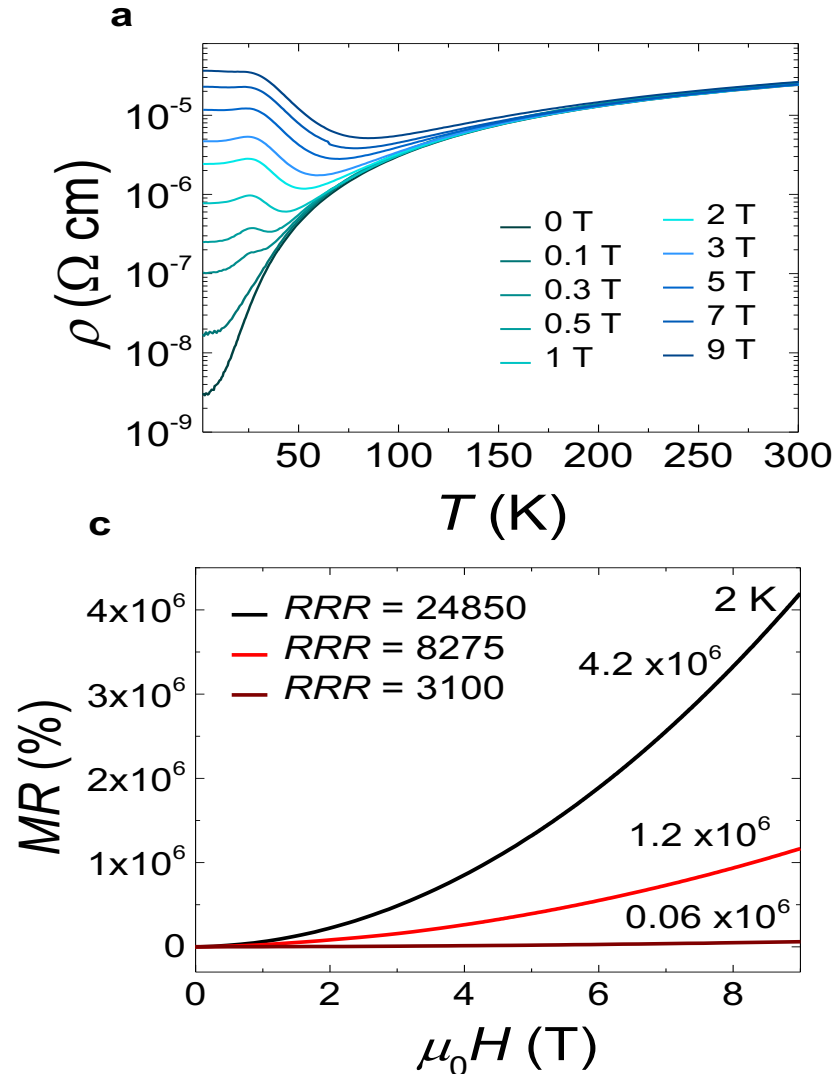
Photoemission, Nan Xu, Ming Shi, Paul Scherrer Institute, Swiss Light Source, CH-5232 Villigen PSI, Switzerland.

Extremely high magnetoresistance and conductivity in the type-II Weyl semimetal WP2, Nitesh, et al.; arXiv:1703.04527



WP₂ protected Weyl

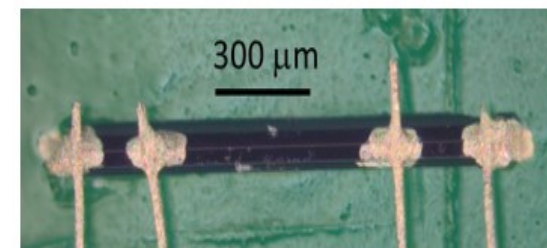
Magnetotransport in a novel Weyl WP₂





Macroscopic Mean Free Path

Compound	ρ (Ωcm)	l (μm)	μ ($\text{cm}^2\text{V}^{-1}\text{s}^{-1}$)	n (cm^{-3})
MoP	6×10^{-9}	11	2.4×10^4	2.9×10^{22}
WP ₂	3×10^{-9}	530	4×10^6	5×10^{20}
WC	0.35×10^{-6}		$\sim 1 \times 10^4$	4×10^{20}
PtCoO ₂	40×10^{-9}	5	0.7×10^4	2.2×10^{22}
PdCoO ₂	9×10^{-9}	20	2.8×10^4	2.4×10^{22}



WC J. B. He et al. arXiv:1703.03211
Pallavi Kushwaha, et al. Sci. Adv.1 (2015) e150069
P. Moll Science 351, (2016) 1061

Chandra Shekhar et al. arXiv:1703.03736
Nitesh, et al.; arXiv:1703.04527



Hydrodynamic Electron Flow and Hall Viscosity

Thomas Scaffidi,¹ Nabhanila Nandi,² Burkhard Schmidt,² Andrew P. Mackenzie,^{2,3} and Joel E. Moore^{1,4}

In the ballistic regime ($w \ll l_{\text{er}}, l_{\text{mr}}$): $\rho \sim w^{-1}$

Hydrodynamic effects become dominant

- electron-electron scattering $l_{\text{er}} \ll w \ll l_{\text{mr}}$
- with electron-electron scattering length $l_{\text{er}} = v_{\text{F}} \tau_{\text{er}}$
- w the sample width,
- $l_{\text{mr}} = v_{\text{F}} \tau_{\text{mr}}$ the mean free path and v_{F} the Fermi velocity

In the Navier-Stokes flow limit: $\rho = m^*/(e^2 n) \cdot 12 \eta w^{-2}$

R. N. Gurzhy, A. N. Kalinenko, A. I. Kopeliovich, Hydrodynamic effects in the electrical conductivity of impure metals. *Sov. Physics-JETP*. **69**, 863–870 (1989).

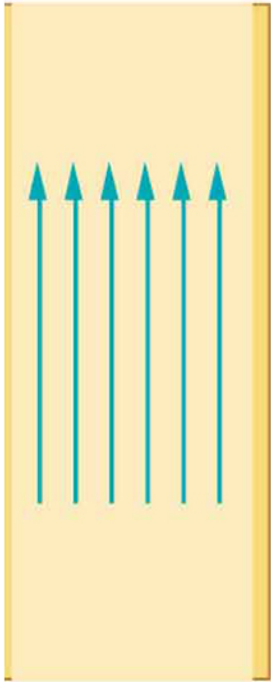
P. S. Alekseev, Negative magnetoresistance in viscous flow of two-dimensional electrons. *Phys. Rev. Lett.* **117** (2016).

T. Scaffidi, N. Nandi, B. Schmidt, A. P. Mackenzie, J. E. Moore, Hydrodynamic Electron Flow and Hall Viscosity. *Phys. Rev. Lett.* **118**, 226601 (2017).

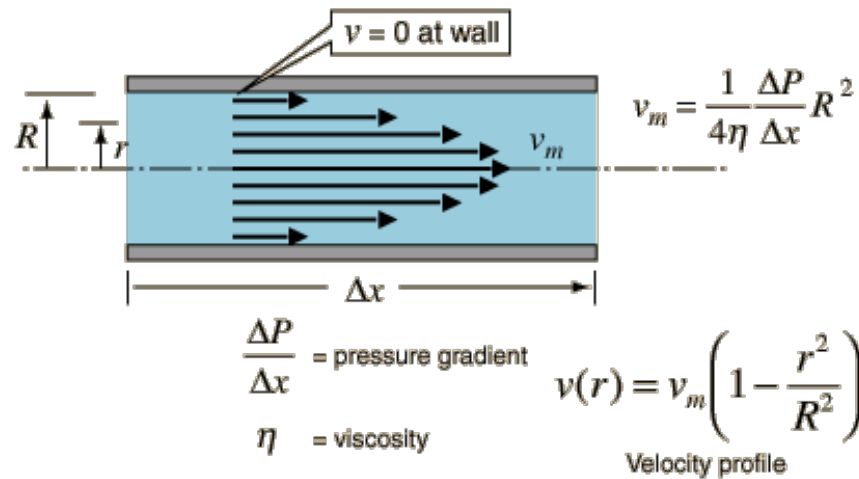
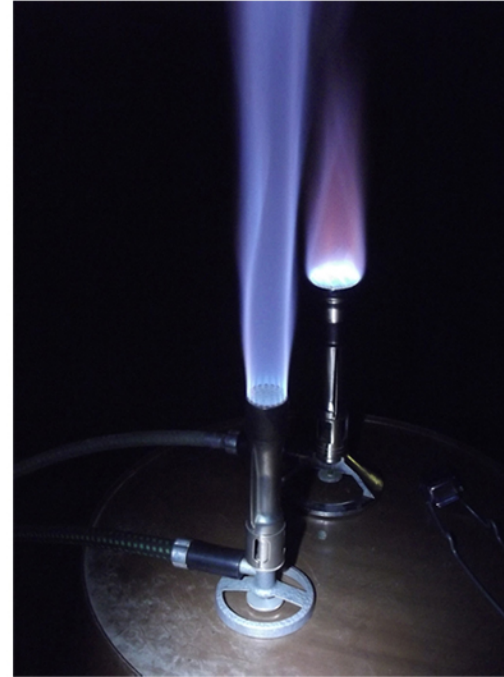
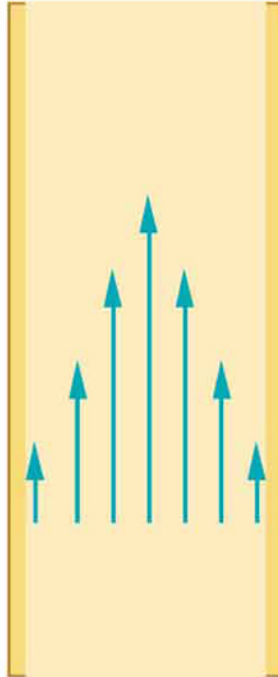


Water, Gas or Electrons

Nonviscous
 $\eta = 0$

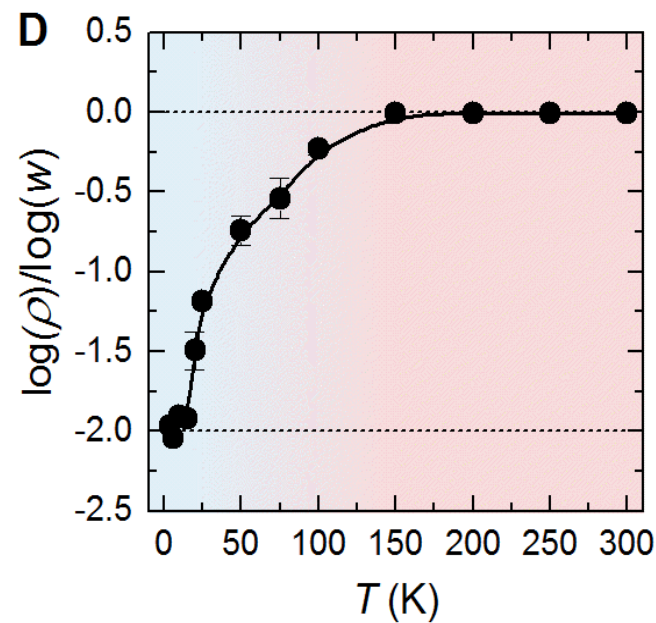
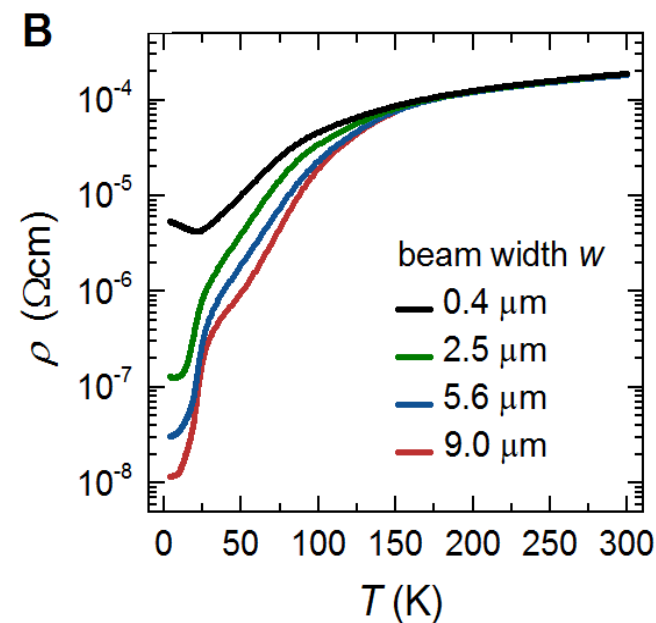
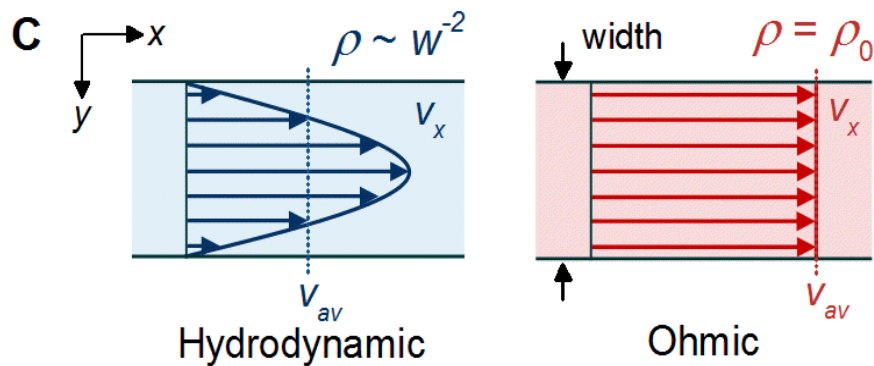
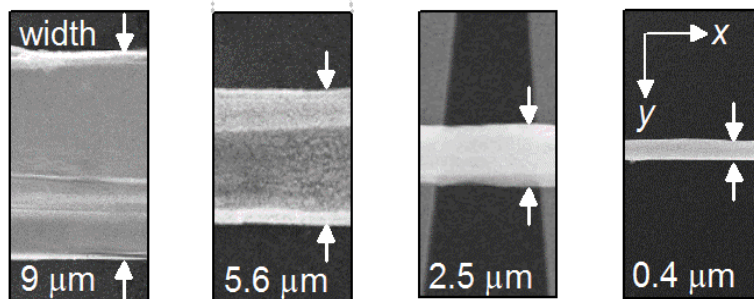
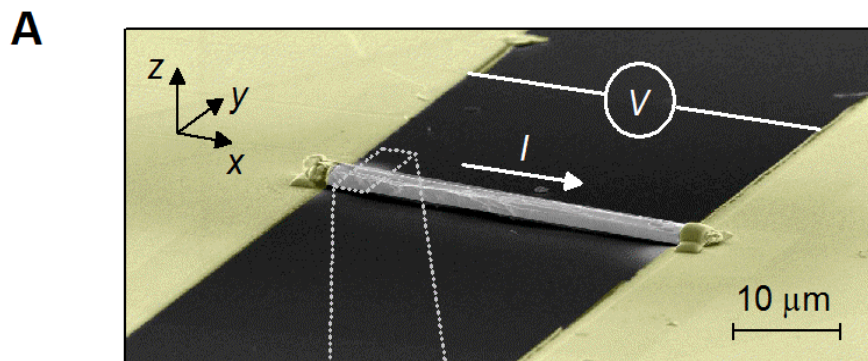


Viscous



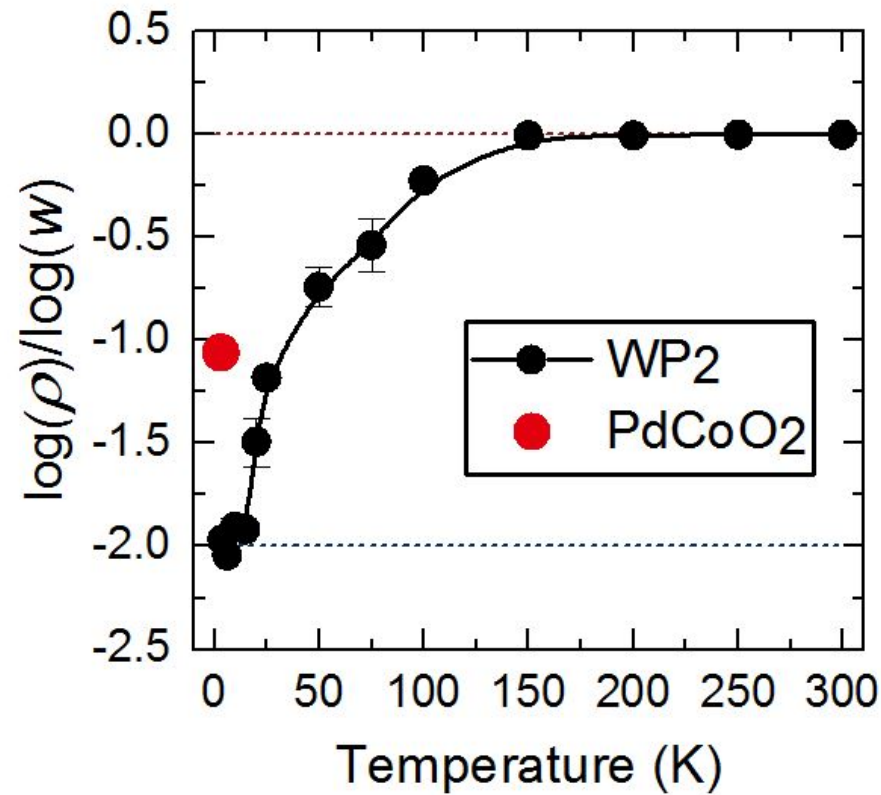
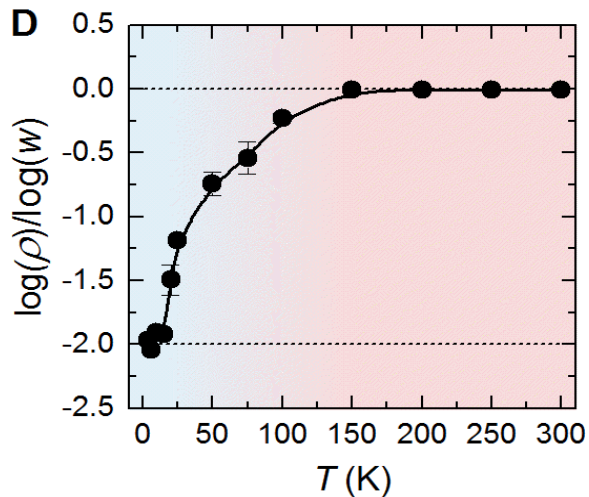
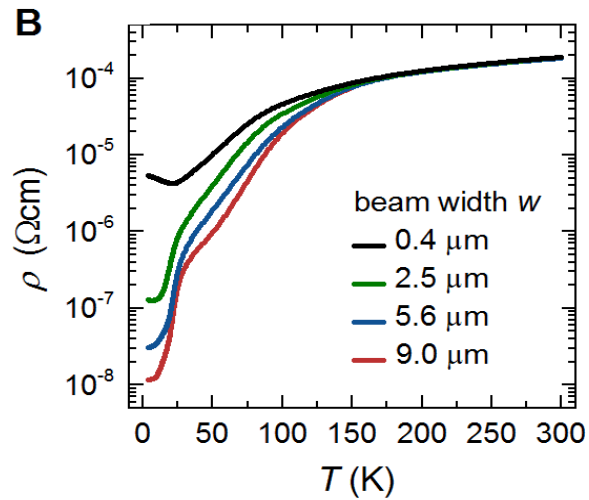
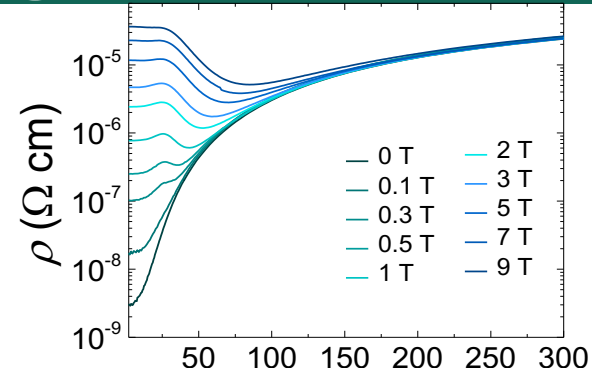


Hydrodynamic flow





Hydrodynamic flow

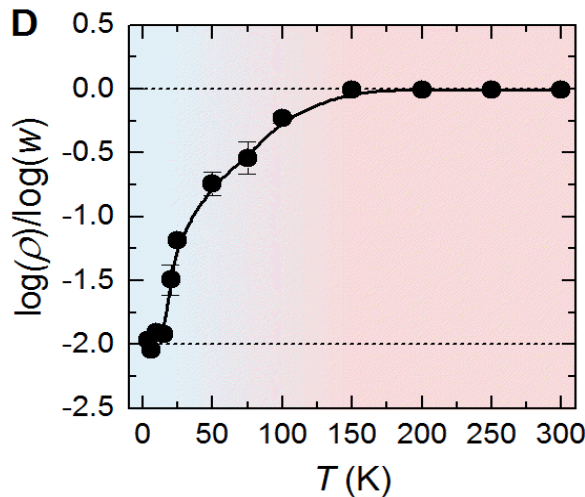
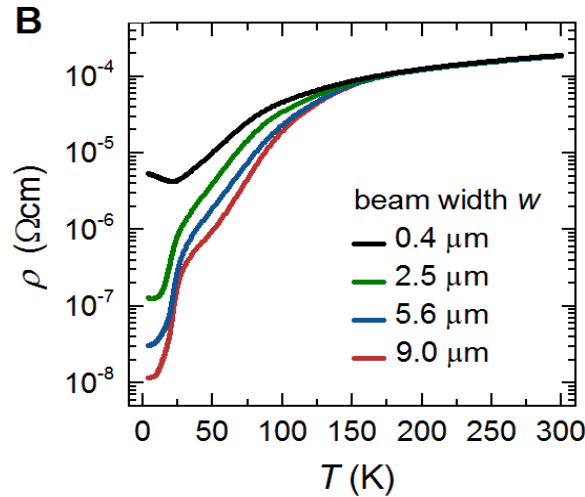
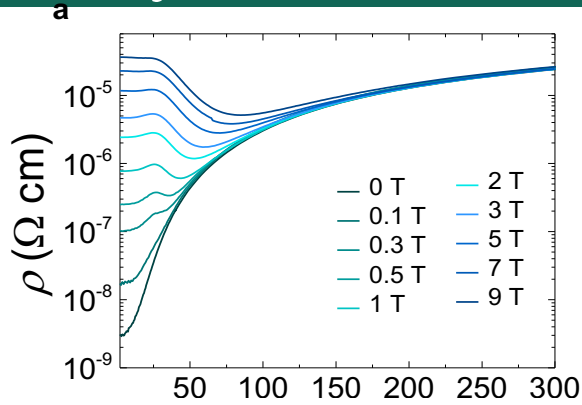
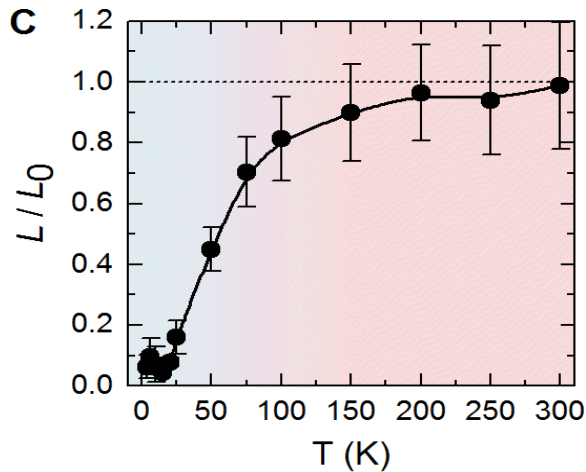
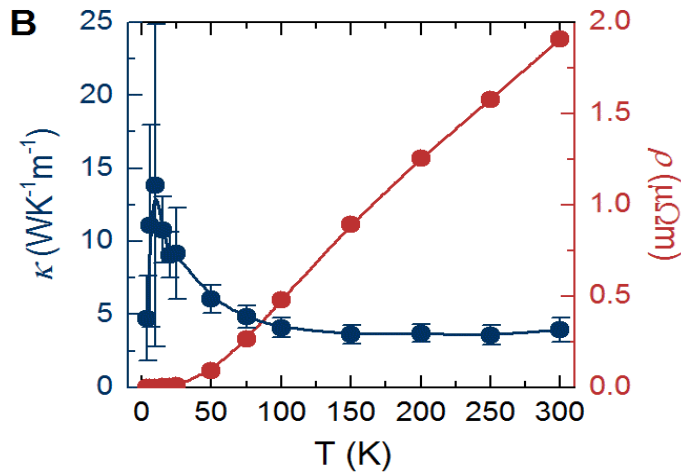
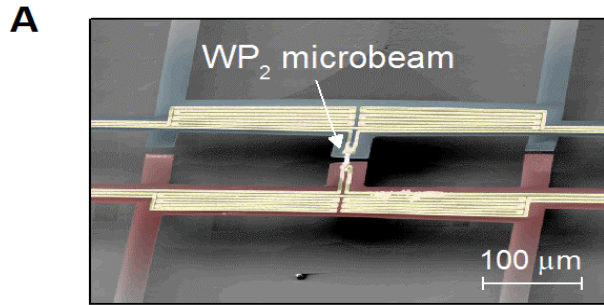


P. J. W. Moll *et al.*, *Science* 10.1126/science.aac8385 (2016).

J. Gooth *et al.* submitted, arXiv:1706.05925



Hydrodynamic flow



- Hydrodynamic electron fluid <15K
- conventional metallic state at T higher 150K

The hydrodynamic regime:

- a viscosity-induced dependence of the electrical resistivity on the square of the channel width

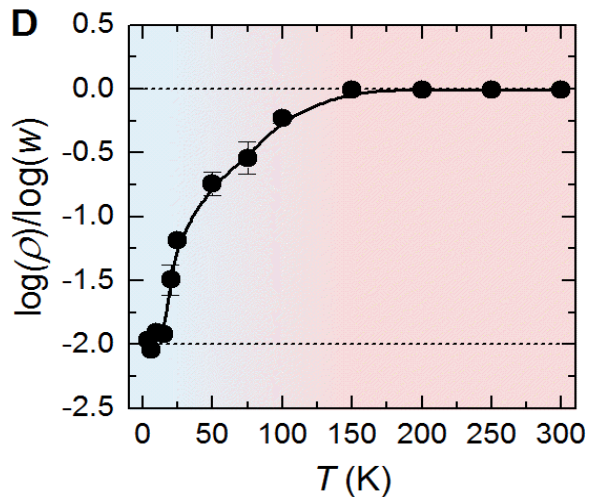
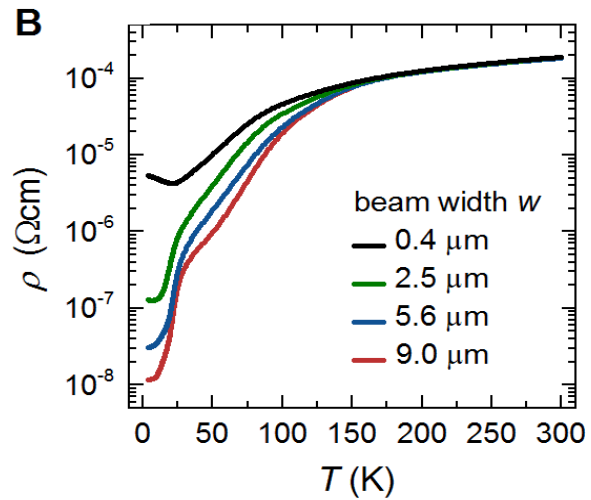
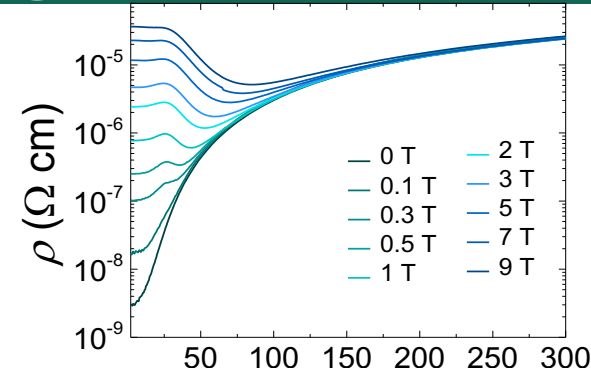
$$\rho = m^*/(e^2 n) \cdot 12 \eta w^{-2}$$

- a strong violation of the

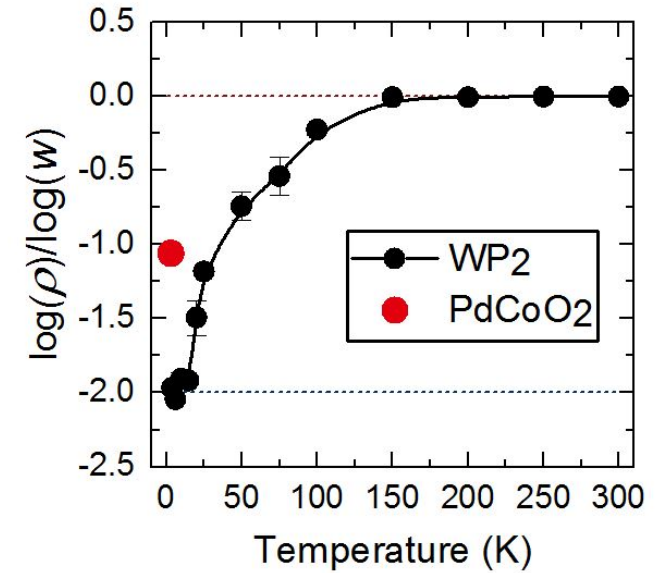
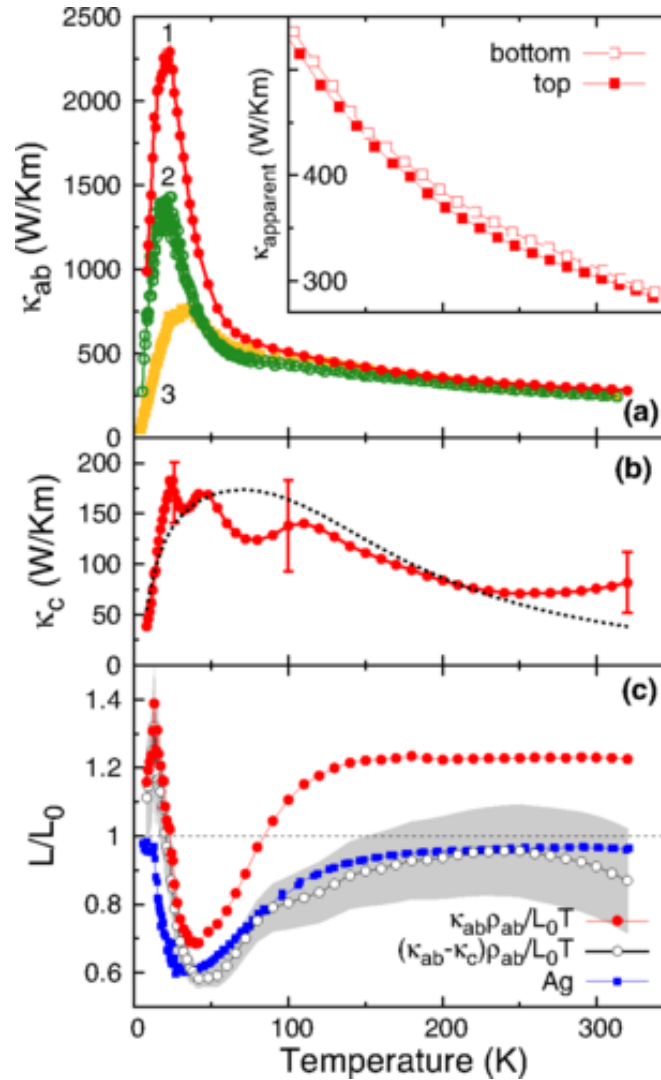
$$L \equiv \frac{\kappa}{\sigma T} = \frac{\pi^2}{3} \equiv L_0$$



Hydrodynamic flow



PdCoO₂





Giant Nernst – Topology - Hydrodynamic

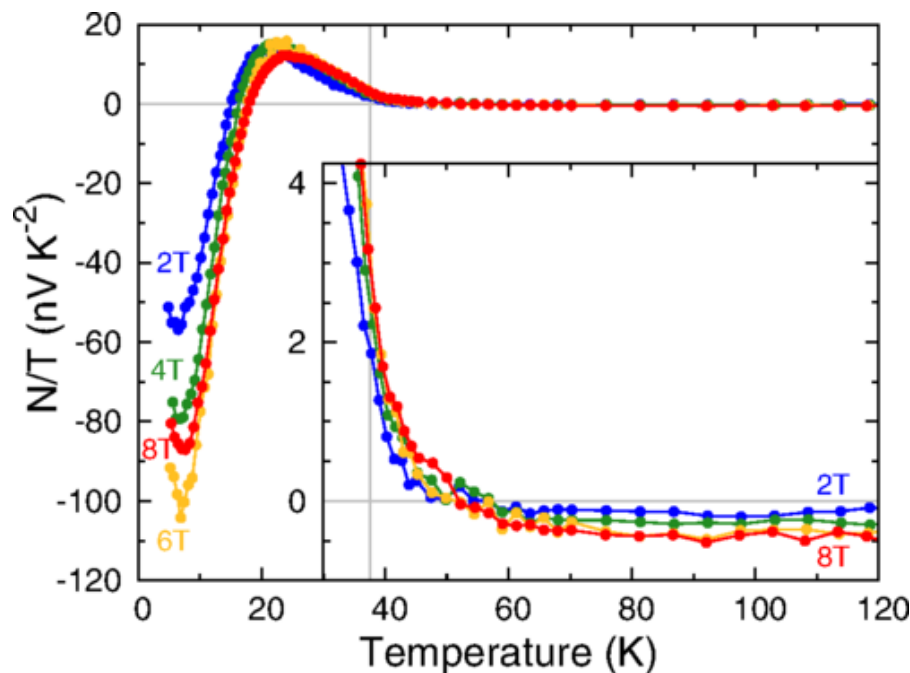
Rep. Prog. Phys. 79 (2016) 046502 (23pp)

doi:10.1088/0034-4885/79/4/046502

Review

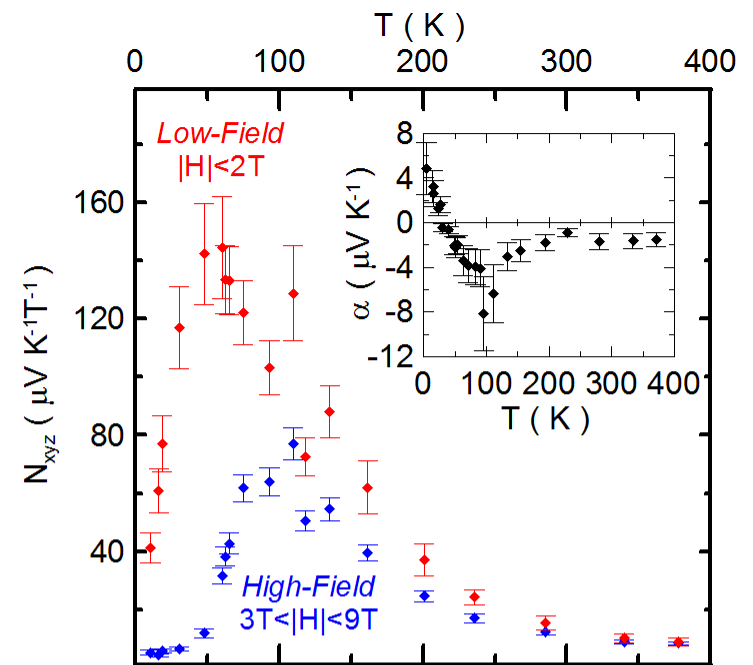
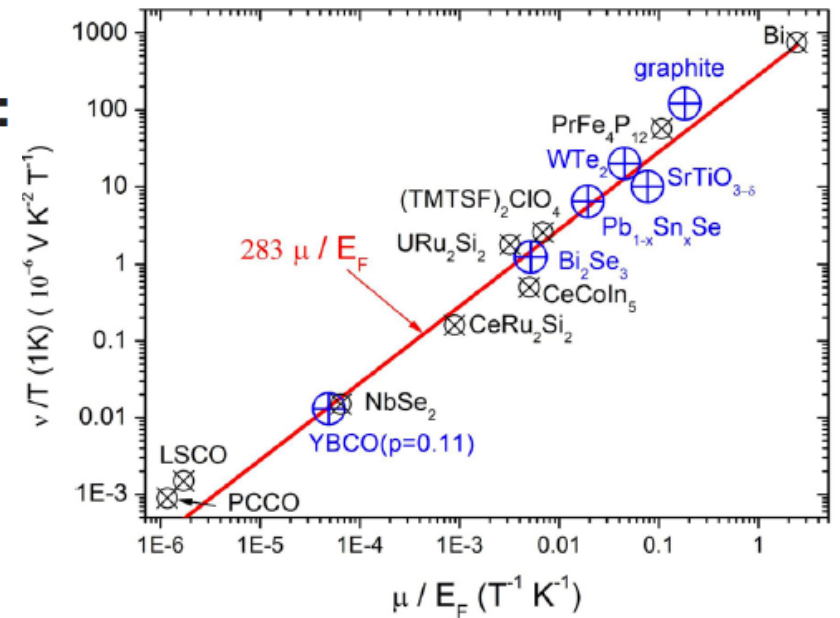
Nernst effect in metals and superconductors: a review of concepts and experiments

Kamran Behnia and Hervé Aubin



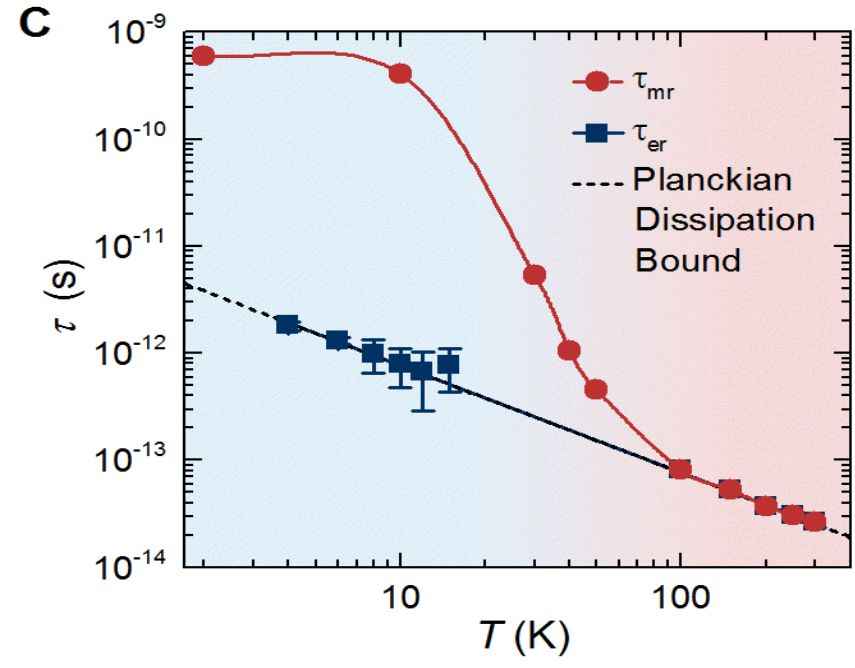
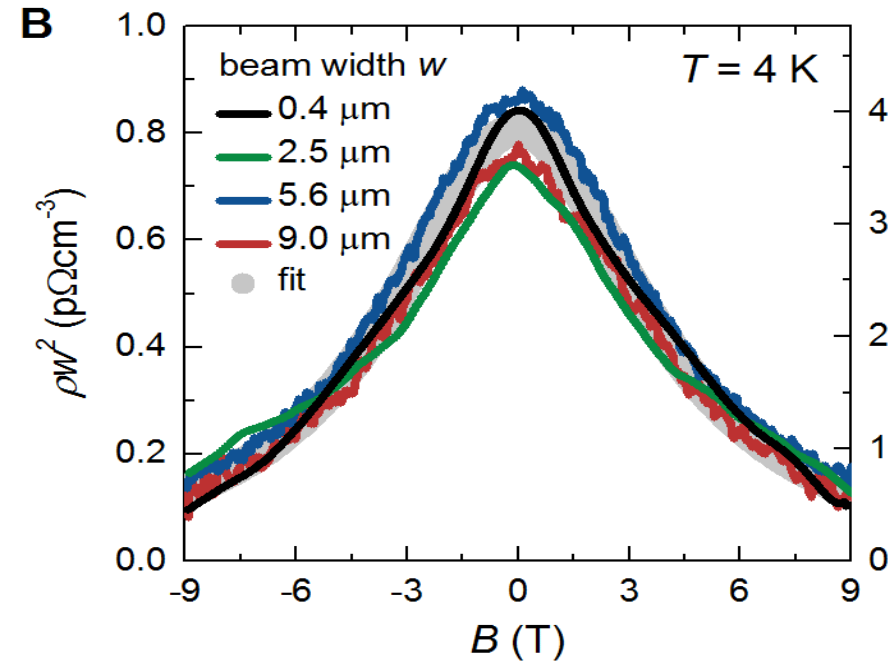
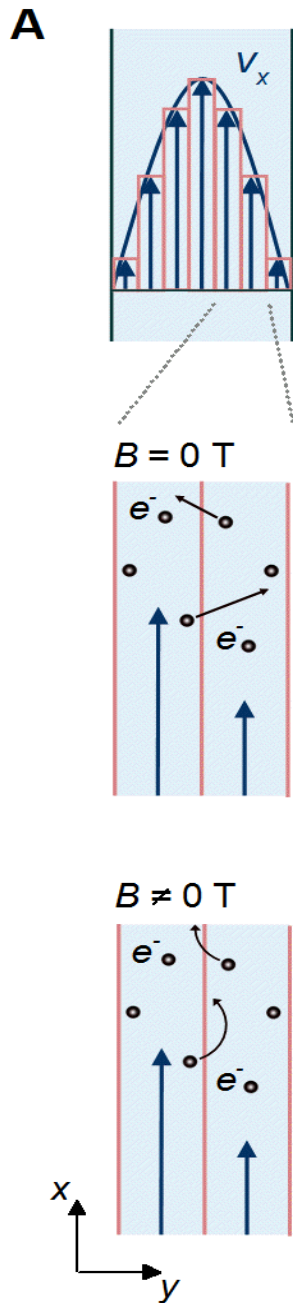
Ramzy Daou, Raymond Frésard, Sylvie Hébert, and Antoine Maignan, Phys. Rev. B 92, 245115 (2015)

Sarah J. Watzman, et al. preprint arXiv:1704.02241





Magnetohydrodynamics, Planckian bound of dissipation



$\eta \text{ (} 10^{-2} \text{ m}^2 \text{s}^{-1}\text{)}$

Grey dots:
the magnetohydrodynamic
model in the Navier-Stokes
flow limit

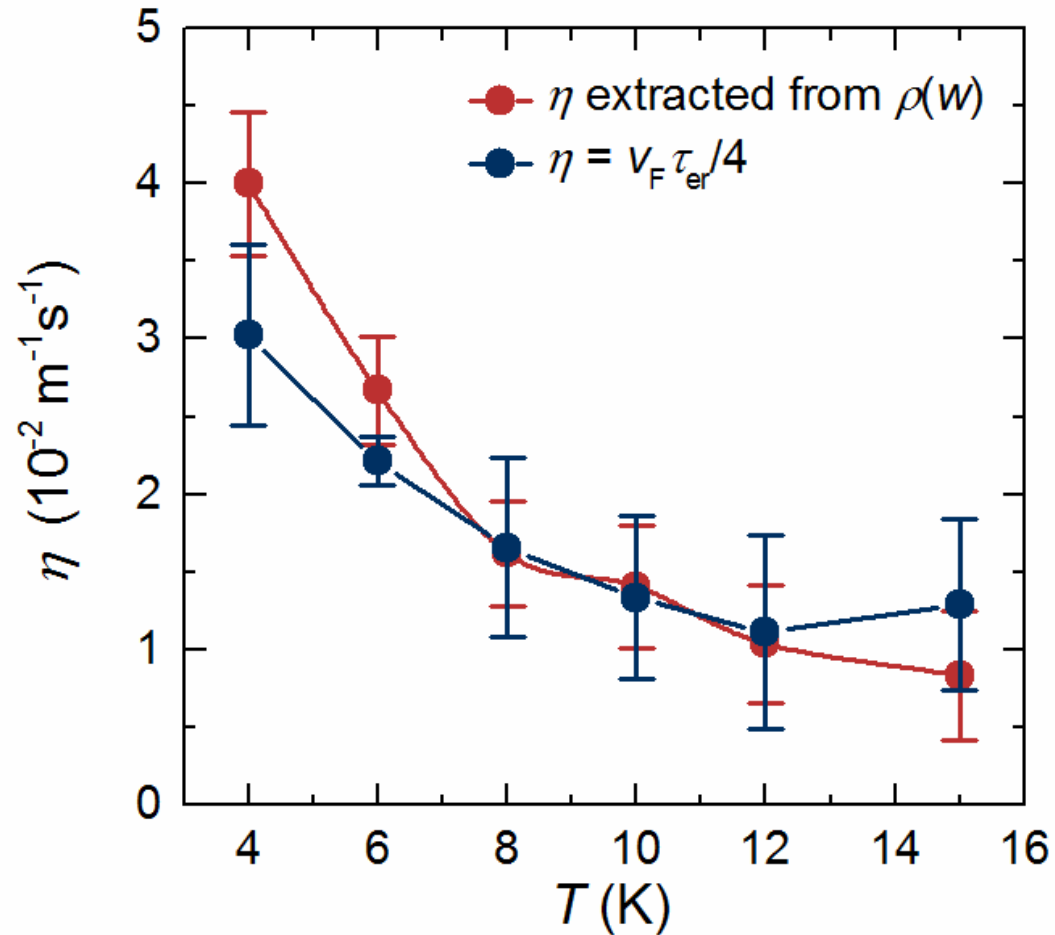
Momentum relaxation
times t_{mr}

thermal energy relaxation
times t_{er}

Dashed line marks the
Planckian bound on the
dissipation time $\tau_h =$
 $\hbar/(k_B T)$.



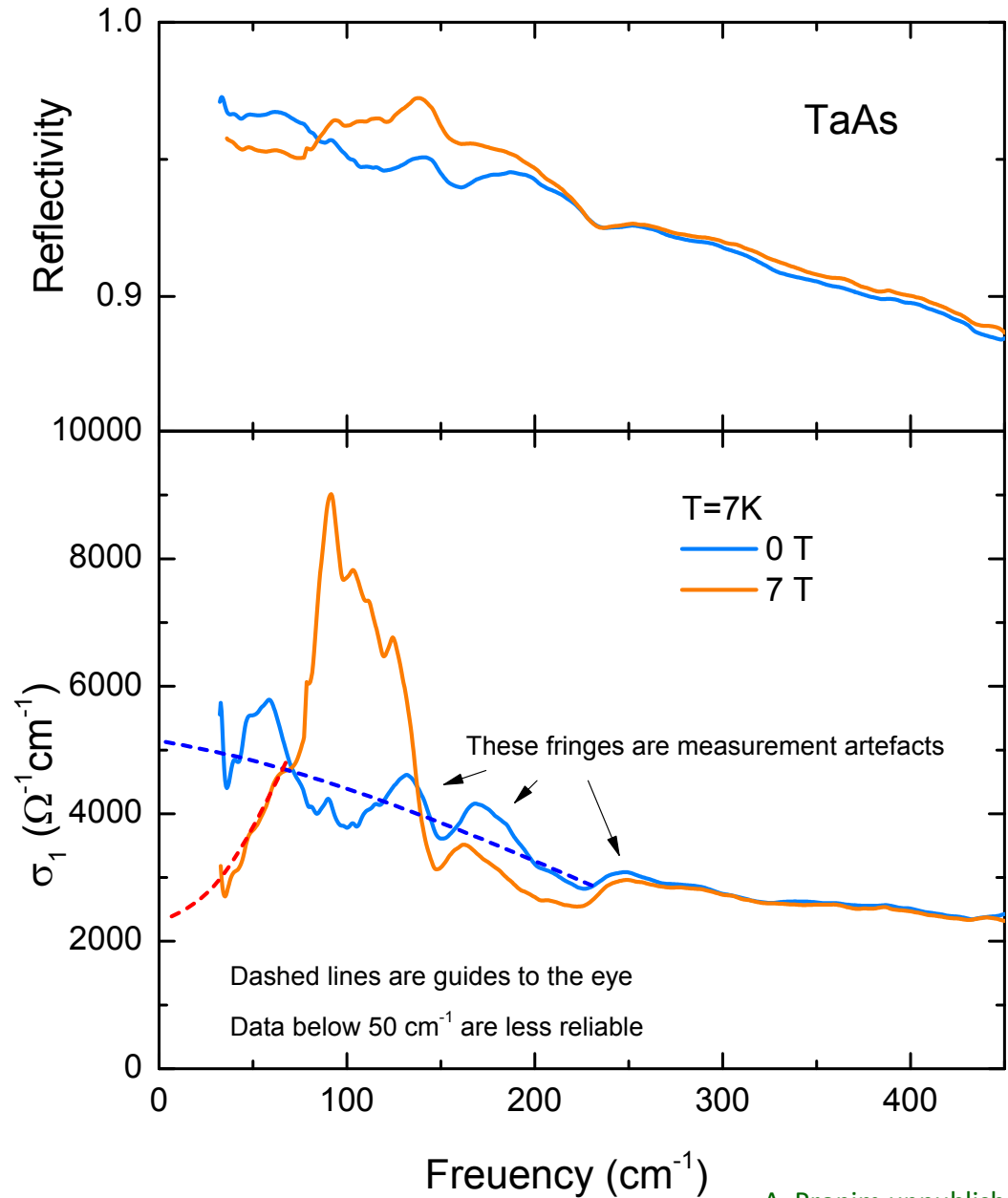
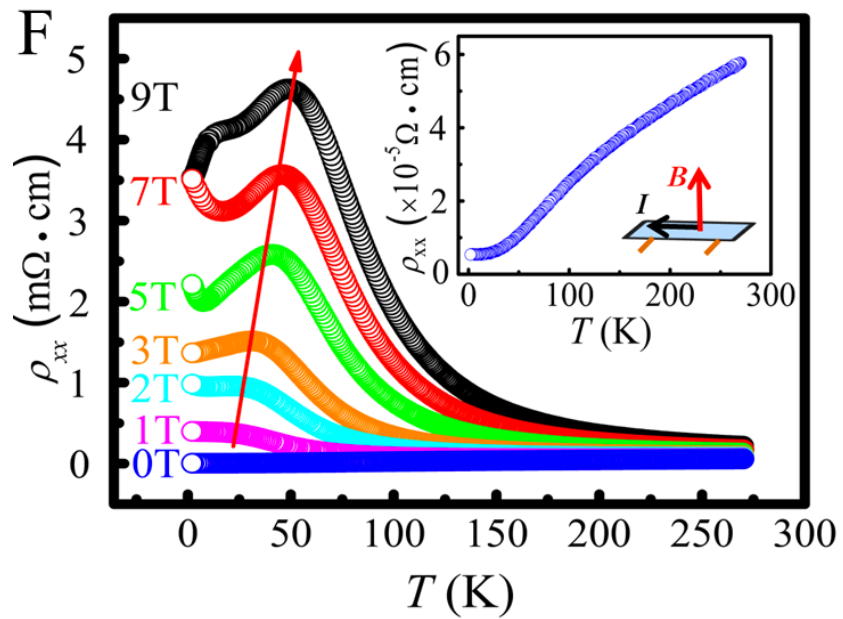
Viscosity of the electron fluid in WP₂



The dynamic viscosity is $\eta_D = 1 \times 10^{-4} \text{ kgm}^{-1} \text{ s}^{-1}$ at 4 K.



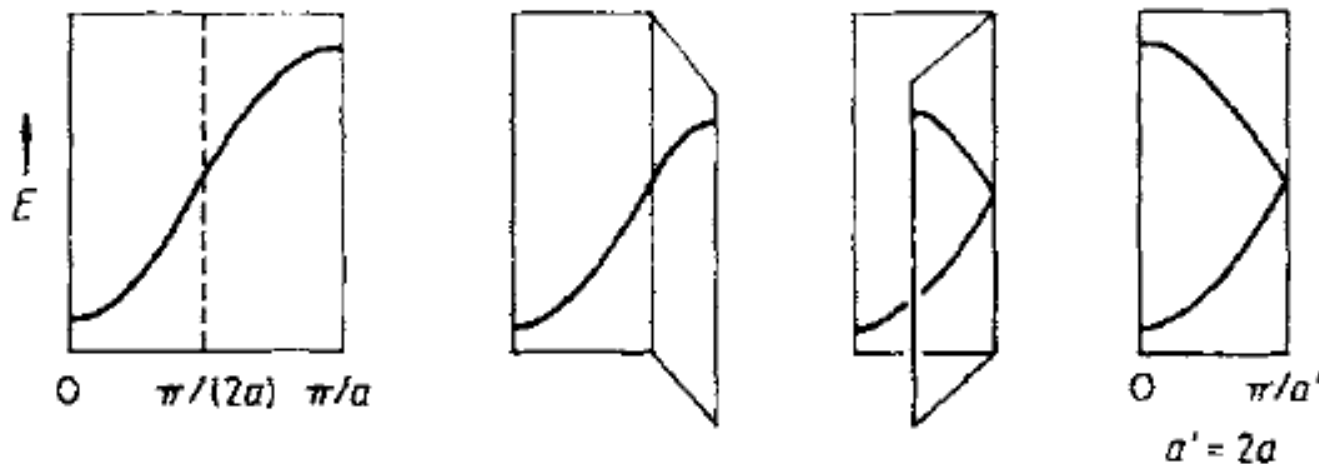
TaAs





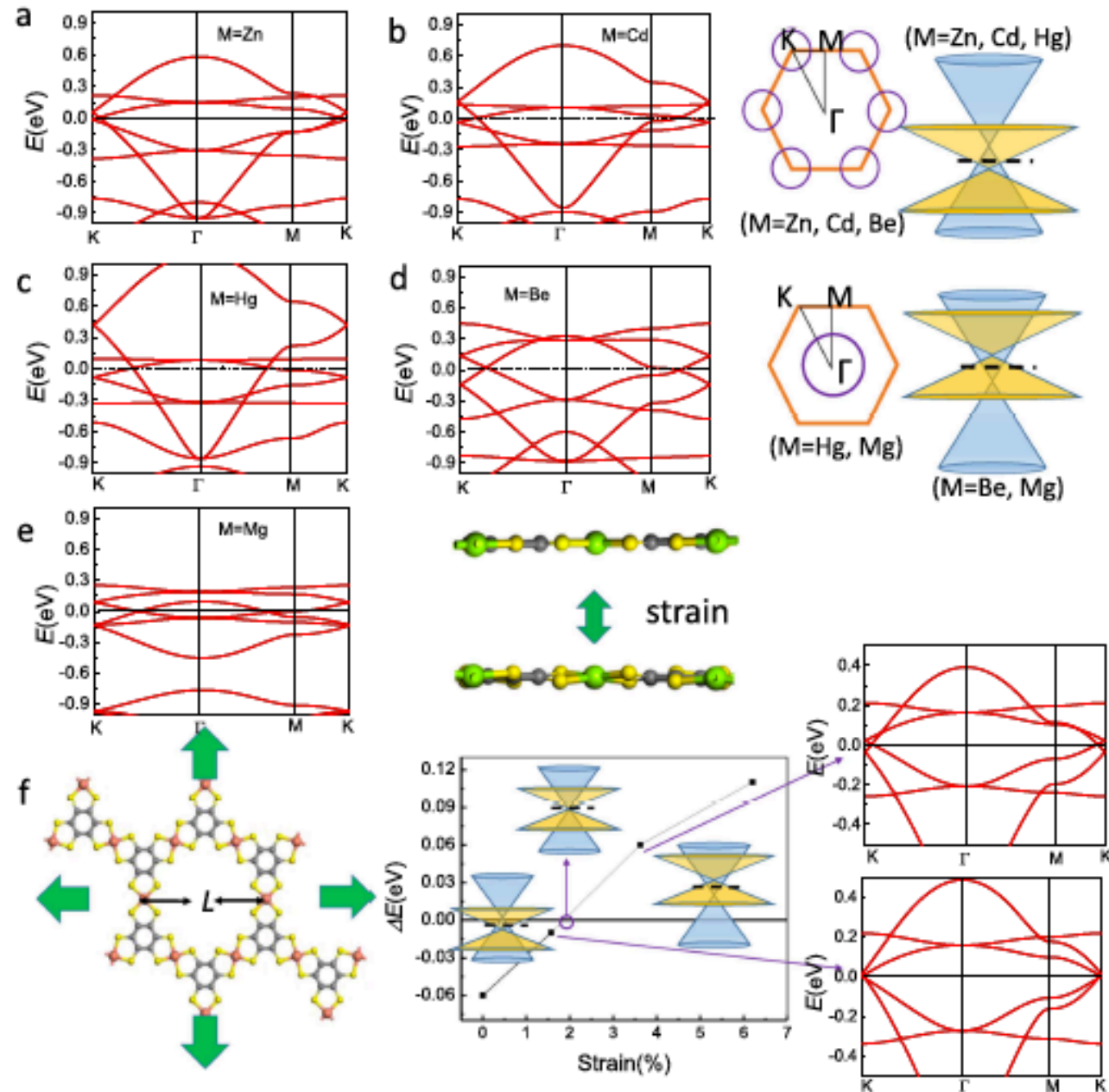
Design scheme: Dirac and Weyl

- Semimetal
- Band inversion – e.g. inert pair effect
- Crossing band due to enforced degeneracy
- New quantum effects – electron liquid





Conetronics in 2D Metal-Organic Frameworks





Topological Metals



Weyl Semimetals

Magnetically induced



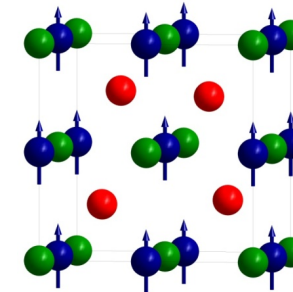
REPtBi... multifunctional topologic insulators

Magnetism and heavy fermion-like behavior in the RBiPt series

P. C. Canfield, J. D. Thompson, W. P. Beyermann, A. Lacerda, M. F. Hundley,
E. Peterson, and Z. Fisk
Los Alamos National Laboratory, Los Alamos, New Mexico 87545

H. R. Ott
ETH, Zurich, Switzerland

J. Appl. Phys. **70** (10), 15 November 1991

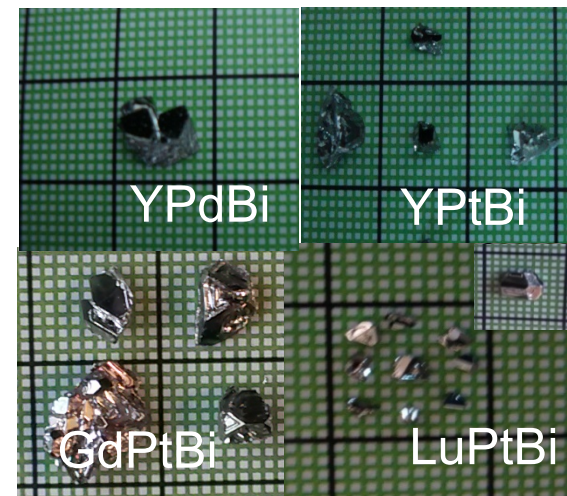


Multifunctional properties

- RE: Gd, Tb, Sm Magnetism and TI
 - Antiferromagnetism with GdPtBi
- RE: Ce
 - complex behaviour of the Fermi surface
- RE: Yb Kondo insulator and TI
 - YbPtBi is a super heavy fermion with the highest γ value



$$10 + 3 (+f^n) + 5 = 18$$

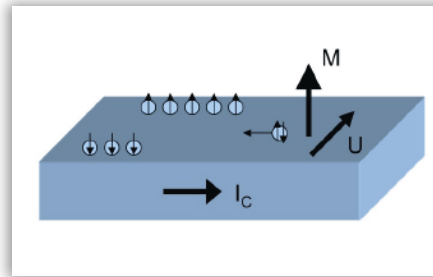




Weyl semimetals

3D topological Weyl semimetals - breaking time reversal symmetry –
in transport measurement we should see

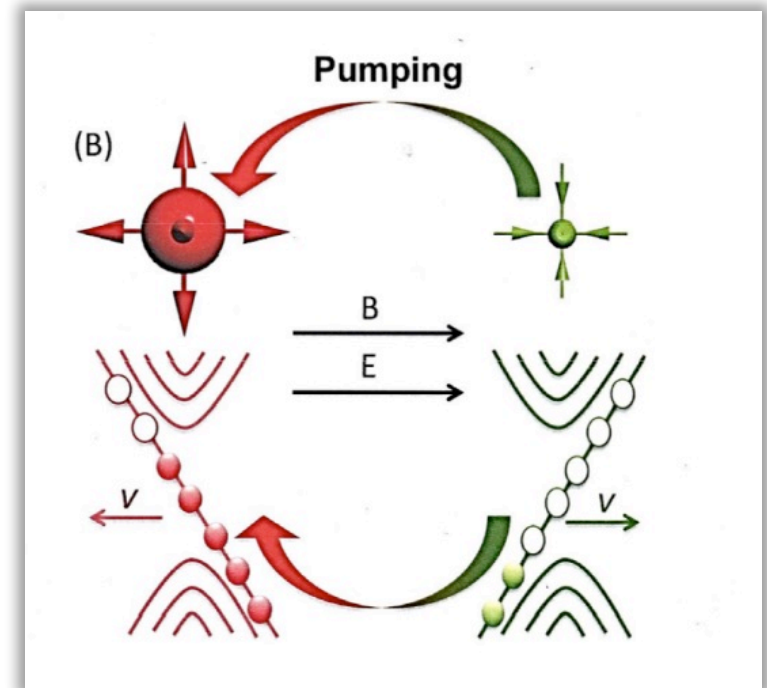
1. Intrinsic anomalous Hall effect



2. Chiral anomaly

$$\partial_\mu j_\chi^\mu = -\chi \frac{e^3}{4\pi^2 \hbar^2} \mathbf{E} \cdot \mathbf{B}$$

$$\sigma_a = \frac{e^3 v_f^3}{4\pi^2 \hbar \mu^2 c} B^2$$



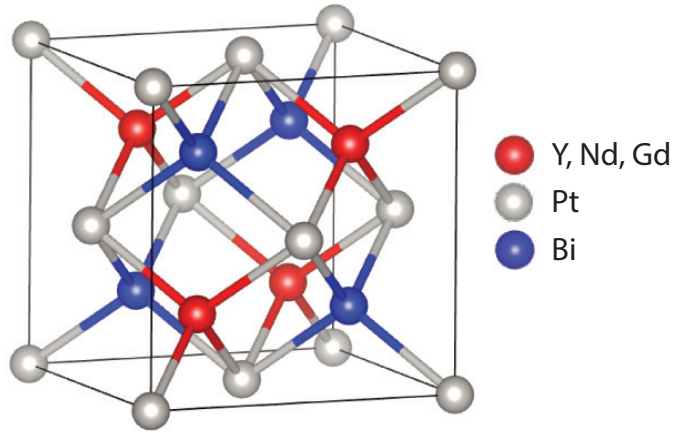
- S. L. Adler, Phys. Rev. 177, 2426 (1969)
- J. S. Bell and R. Jackiw, Nuovo Cim. A60, 47 (1969)
- AA Zyuzin, AA Burkov - Physical Review B (2012)
- AA Burkov, L Balents, PRL 107 12720 (2012)



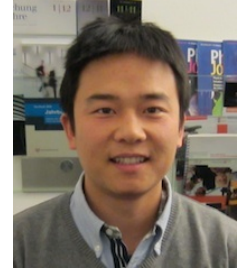
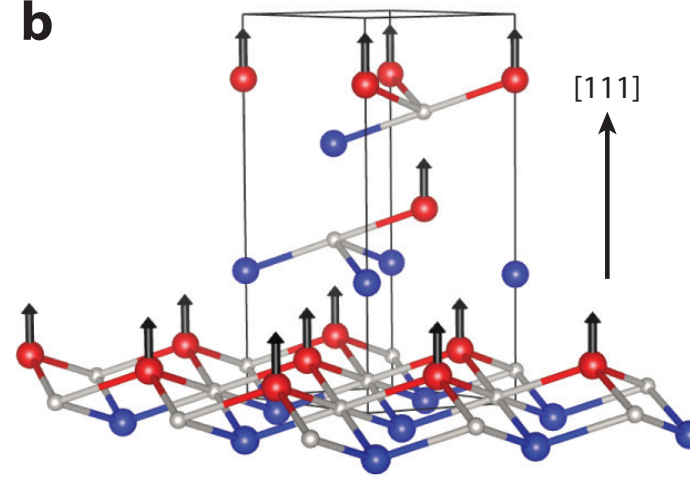
Weyl GdPtBi in a magnetic field



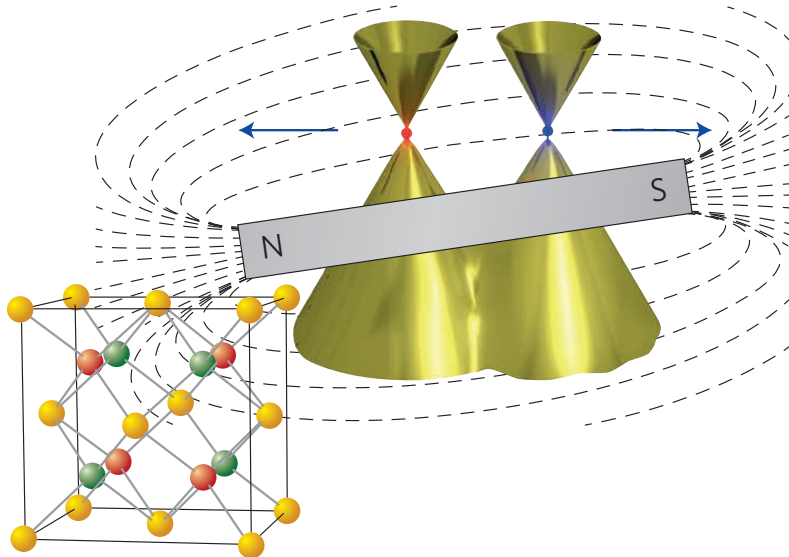
a



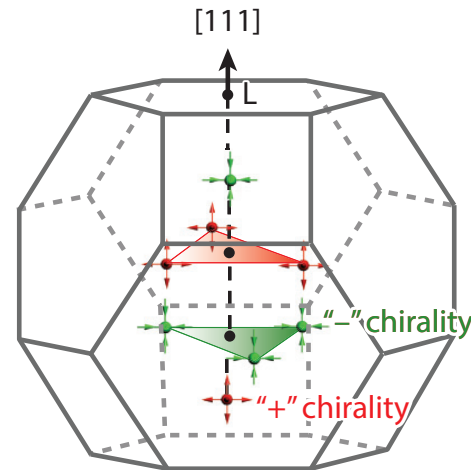
b



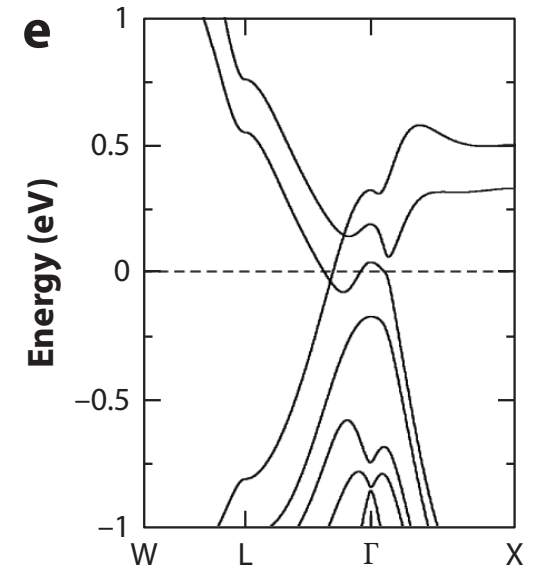
b



d



e

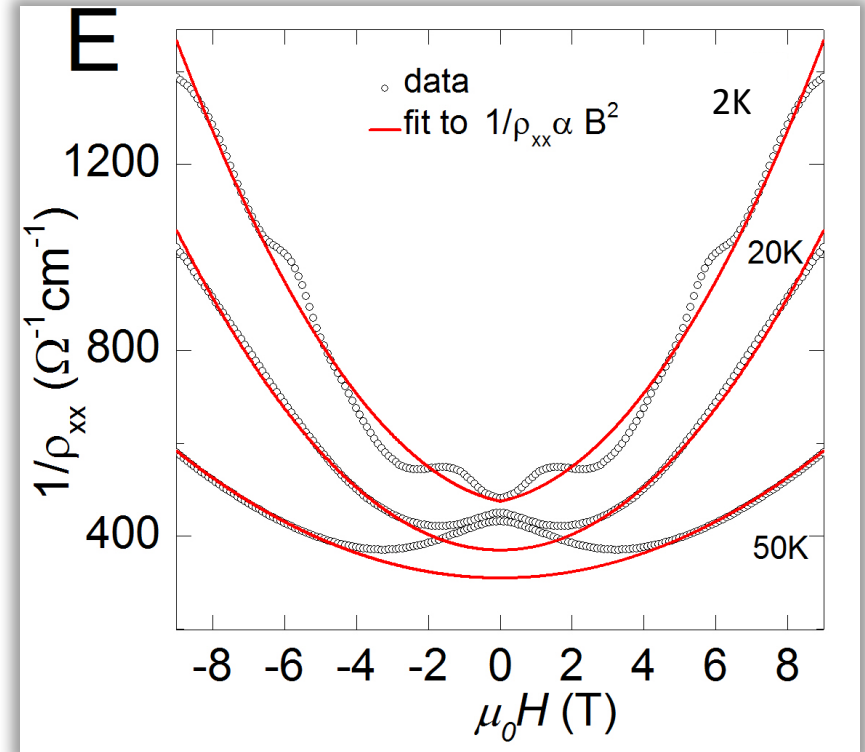
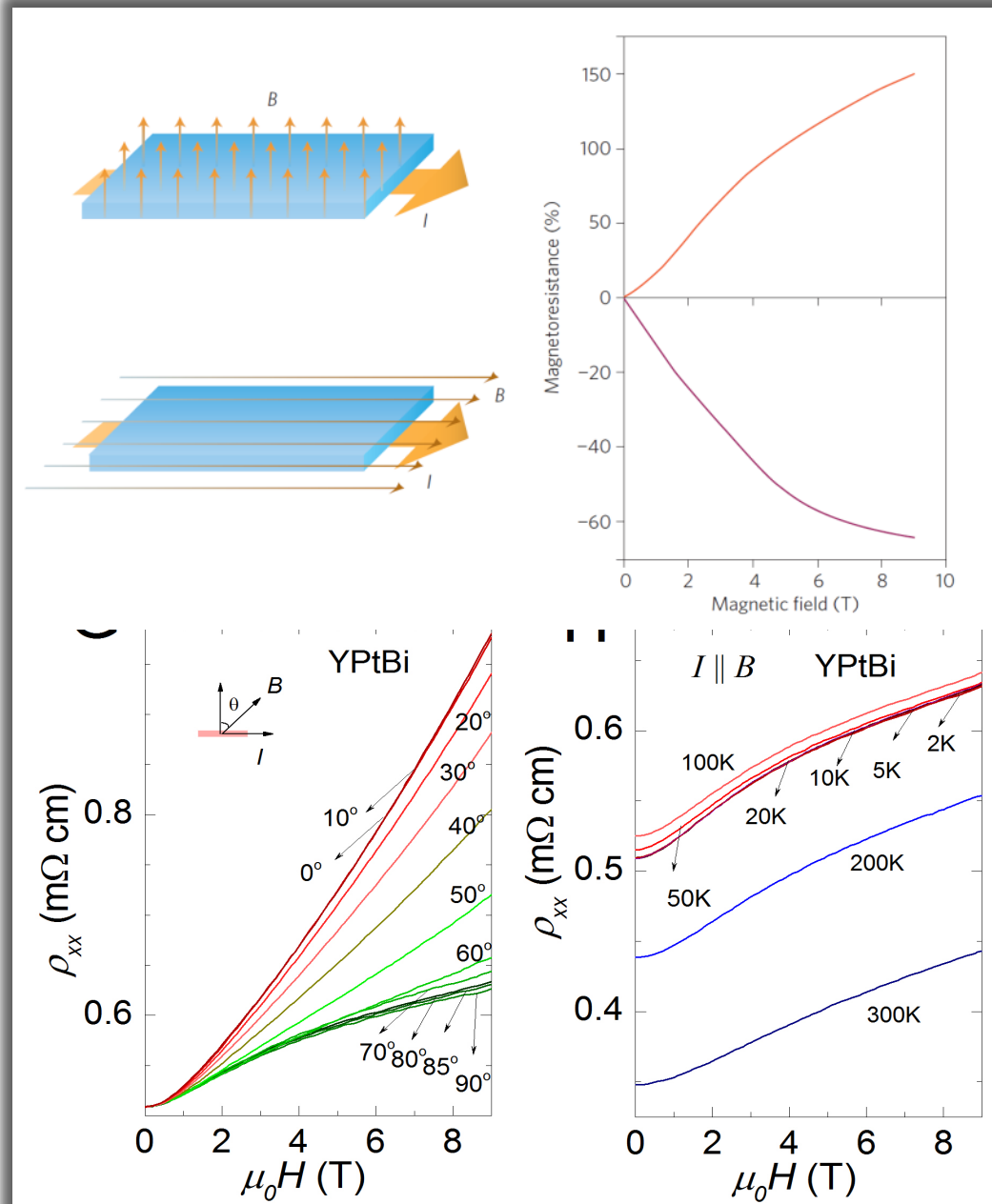


C. Shekhar et al., arXiv:1604.01641, (2016).

M. Hirschberger et al., Nature Mat. Online arXiv:1602.07219, (2016).

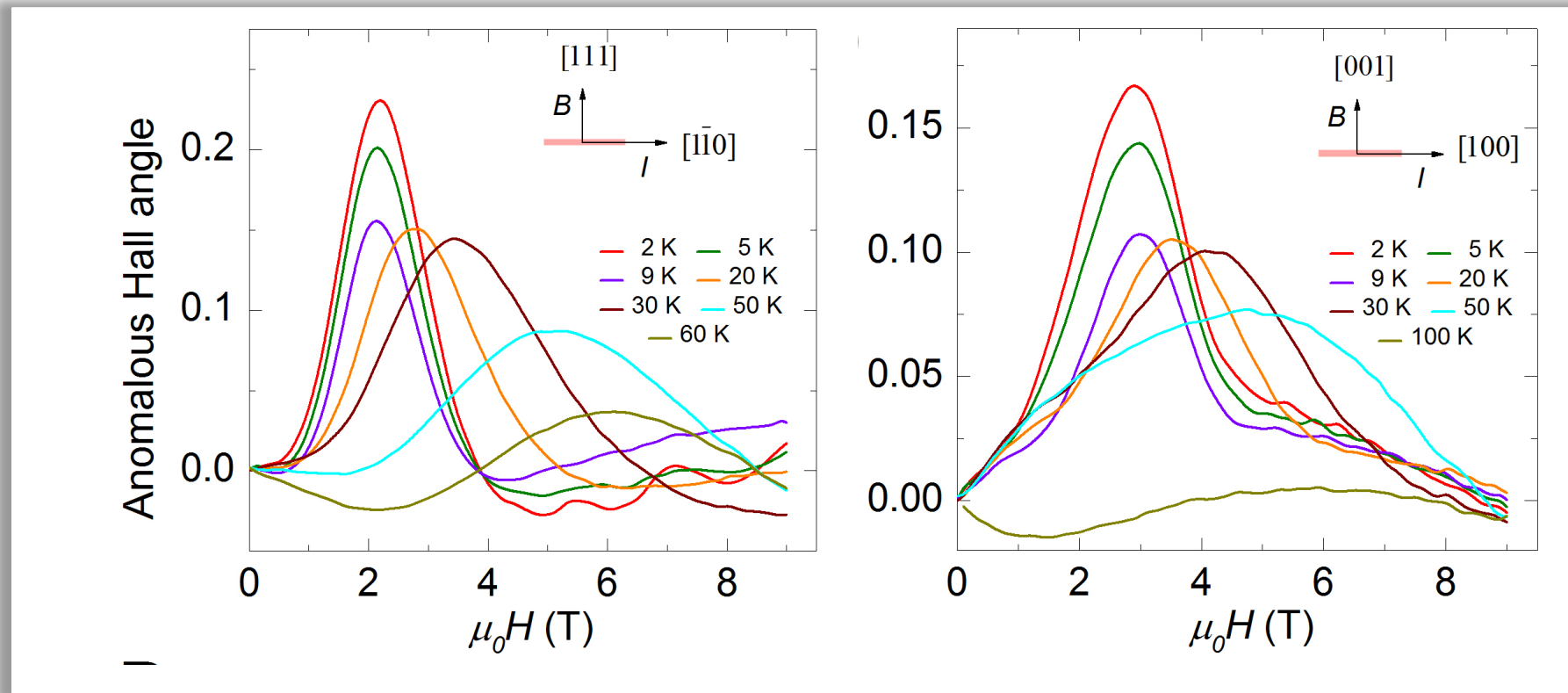


Chiral Anomaly – neg. quadratic MR

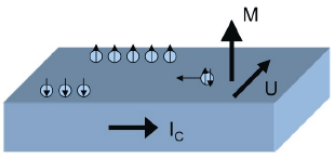




GdPtBi – Anomalous Hall Effect



Anomalous Hall effect
1881



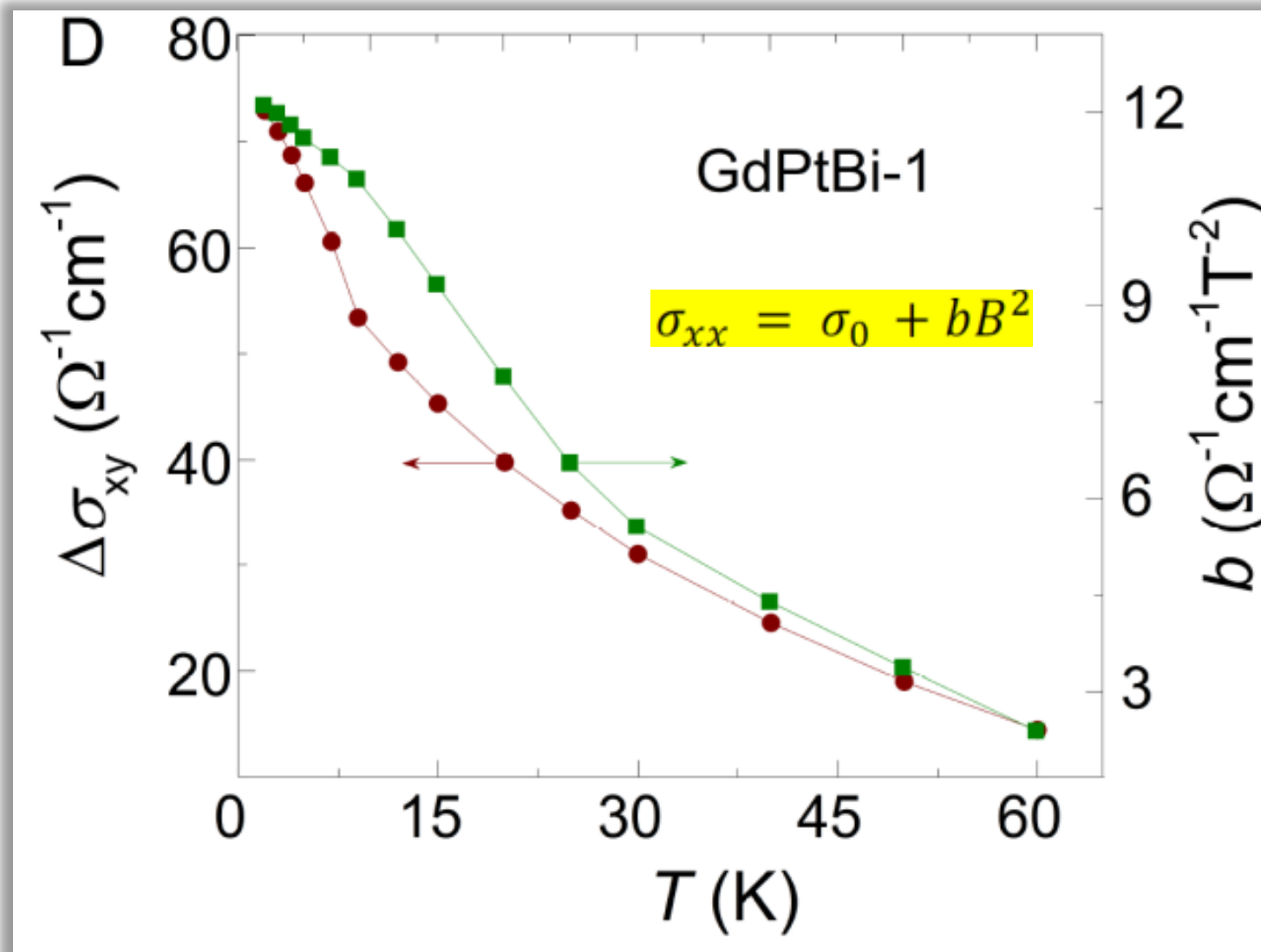
In Ferromagnets an AHE scales with the magnetic moment
Antiferromagnets show no AHE
A Hall angle of 0.2 is exceptional high

Shekhar et al., arXiv:1604.01641, (2016).

T. Suzuki,... & J. G. Checkelsky, Nature Physics (2016) doi:10.1038/nphys3831



Chiral Anomaly – neg. quadratic MR



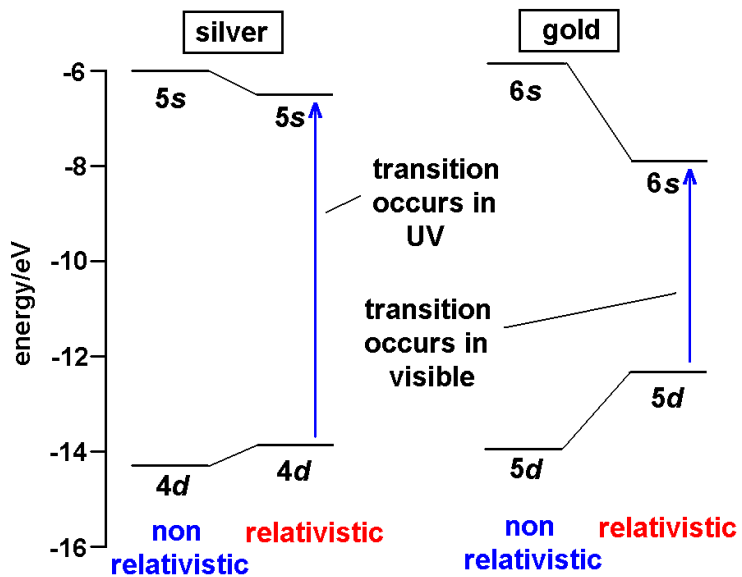
C. Shekhar et al., arXiv:1604.01641, (2016).

Claudia Felser and Binghai Yan, Nature Materials 15 (2016) 1149

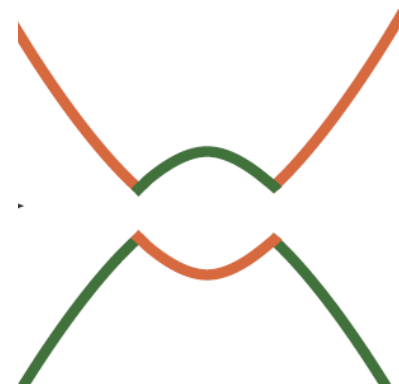
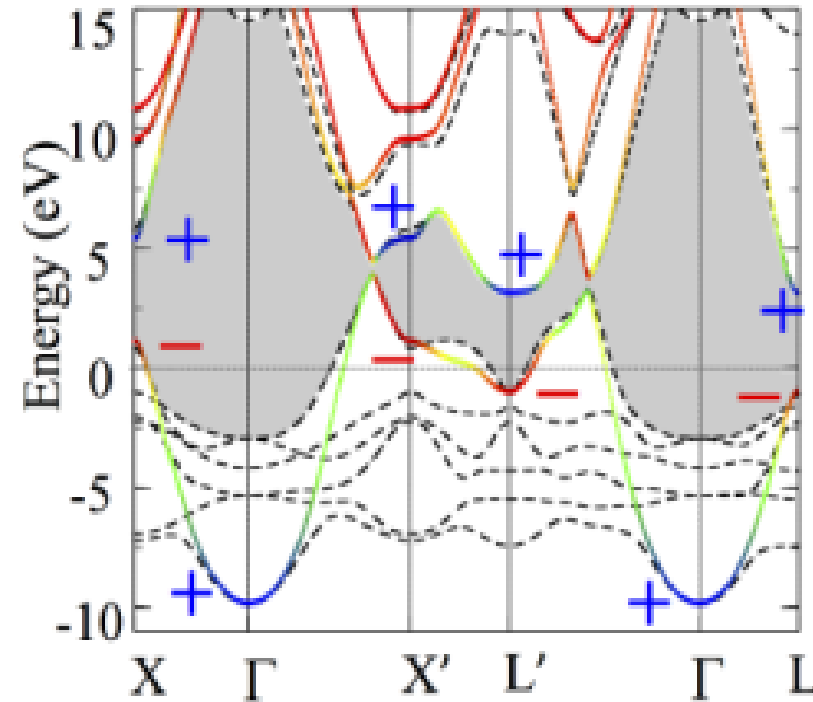
M. Hirschberger et al. Nature Mat. online, arXiv:1602.07219, (2016).



Rewriting the text book: Au



(c) SOC 100%





Rewriting the text book: Au



AUGUST 15, 1939

PHYSICAL REVIEW

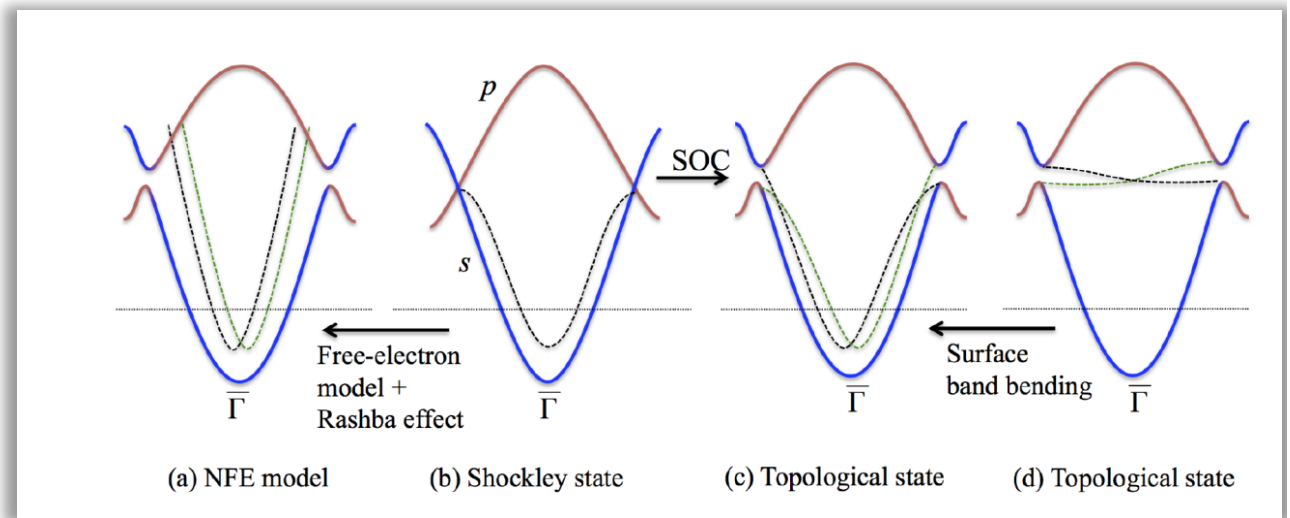
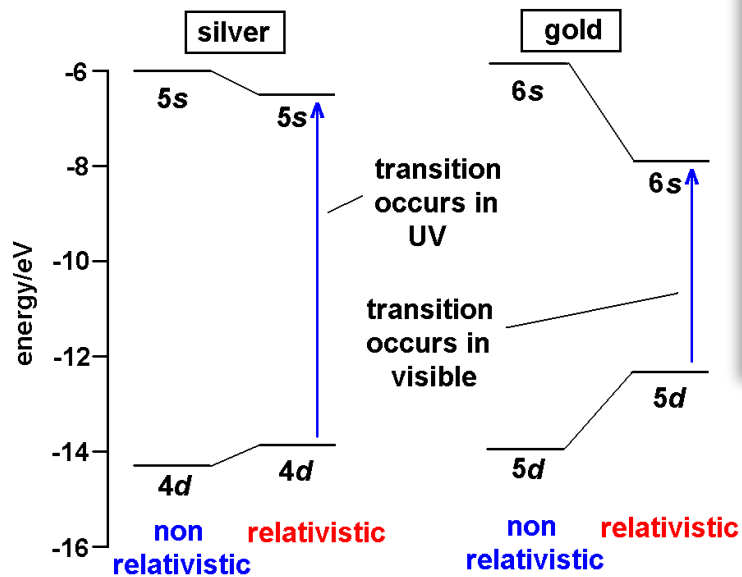
VOLUME 56

On the Surface States Associated with a Periodic Potential

WILLIAM SHOCKLEY

Bell Telephone Laboratories, New York, New York

(Received June 19, 1939)

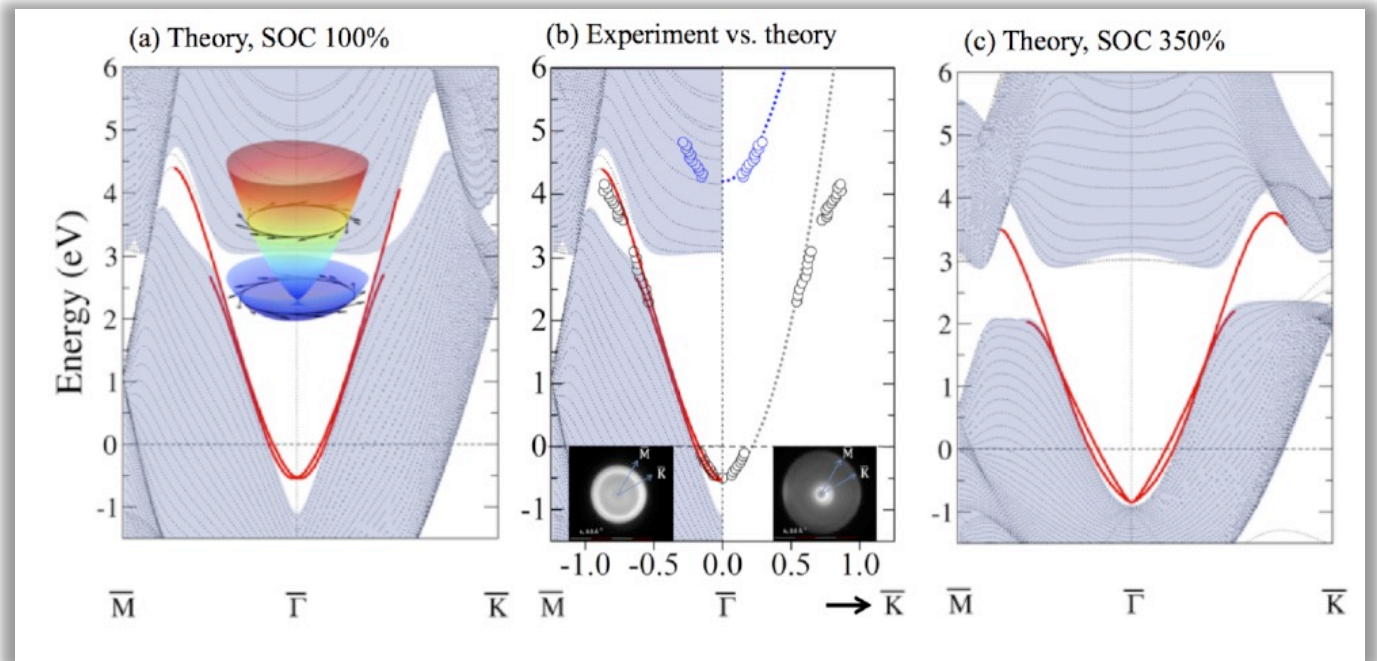
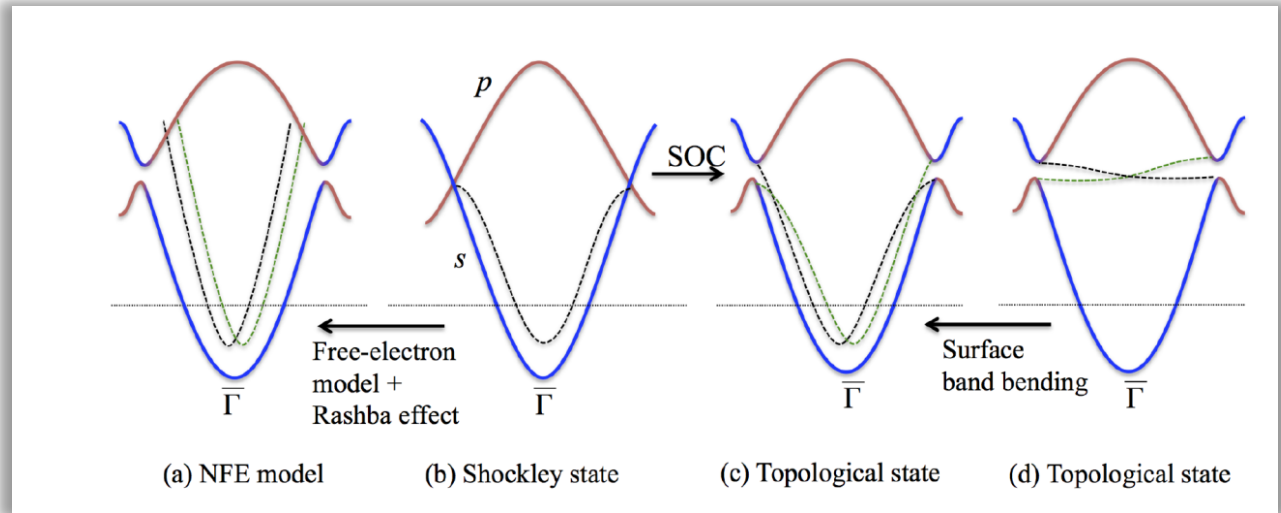
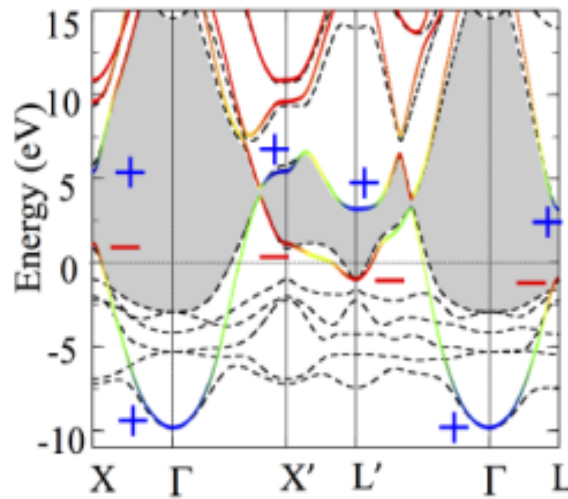




Rewriting the text book: Au



(c) SOC 100%

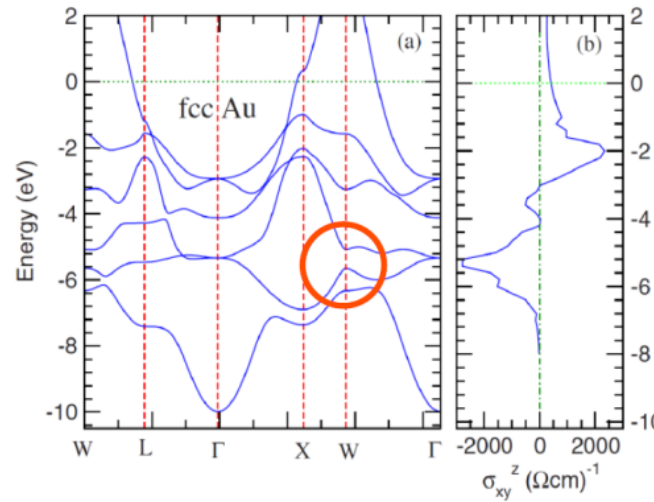
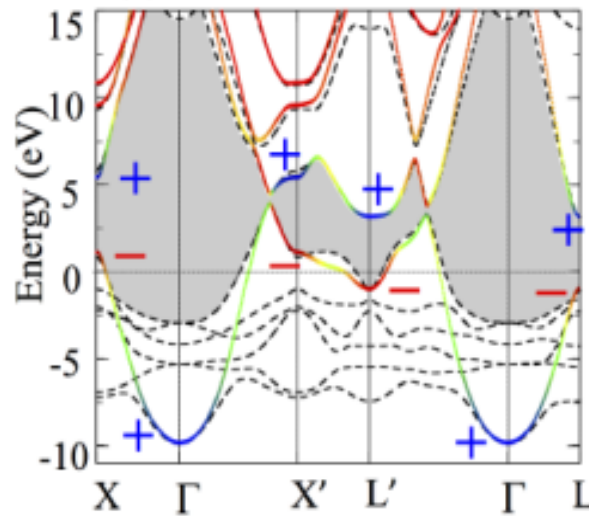


Cs⁺Au⁻

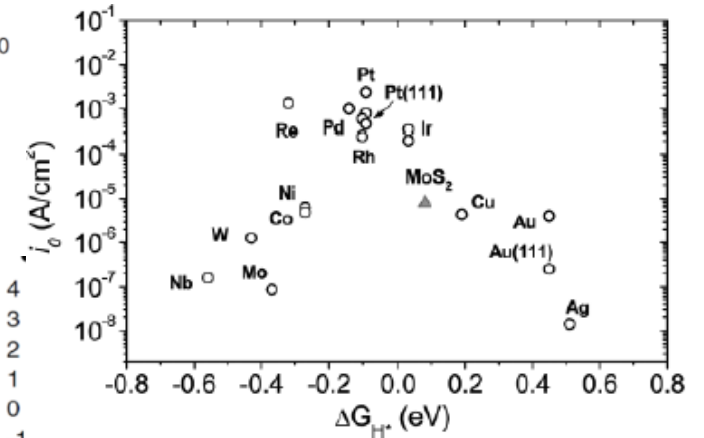


Berry Phase of Au-Pt- Spin Hall Effect

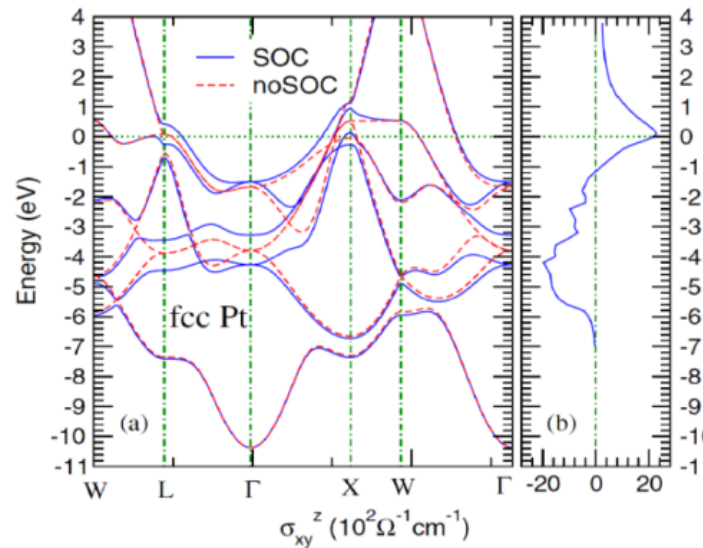
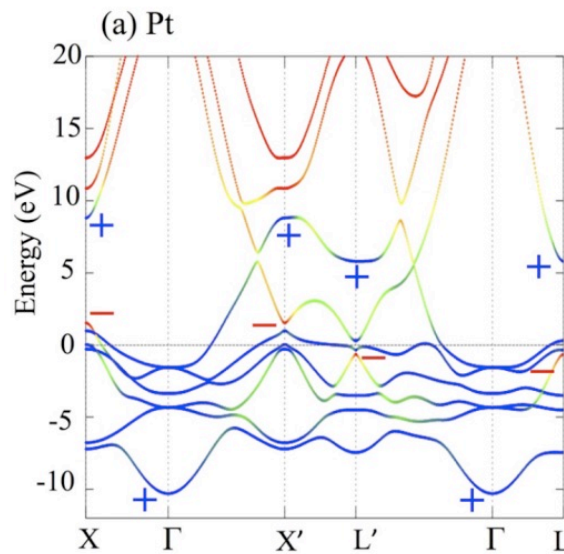
Inert pair effect



Au: 400 $\frac{\hbar}{e} (\Omega \text{ cm})^{-1}$



T. F. Jaramillo et al. Science 317, 100 (2007)



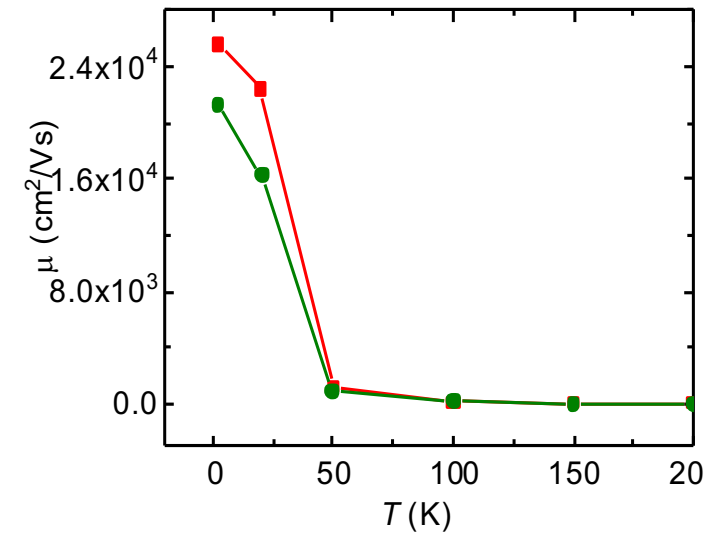
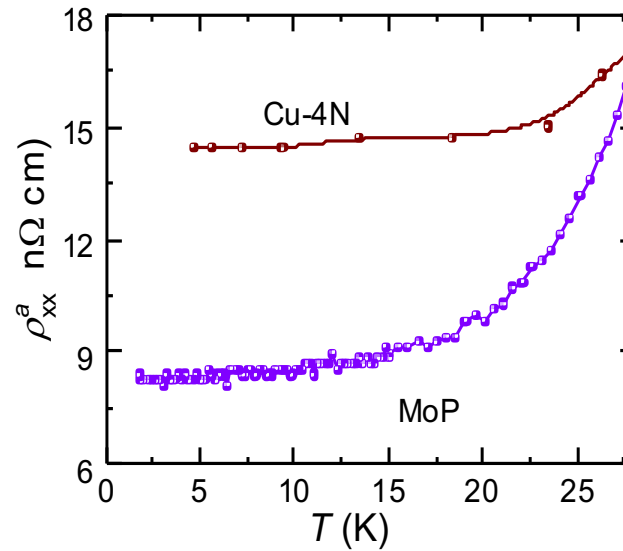
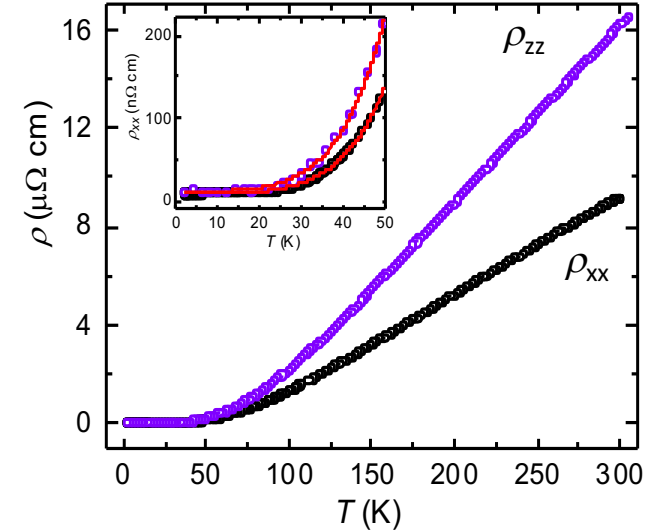
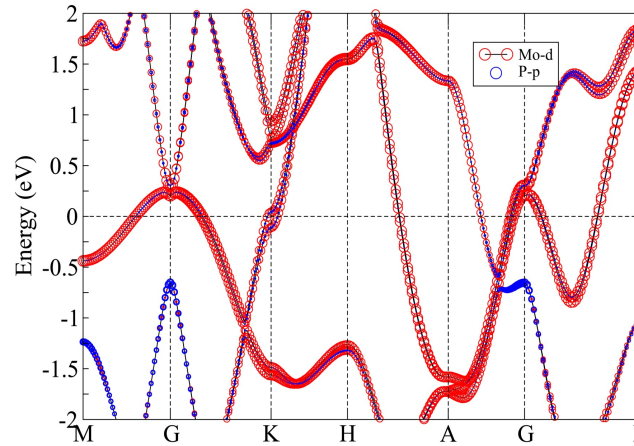
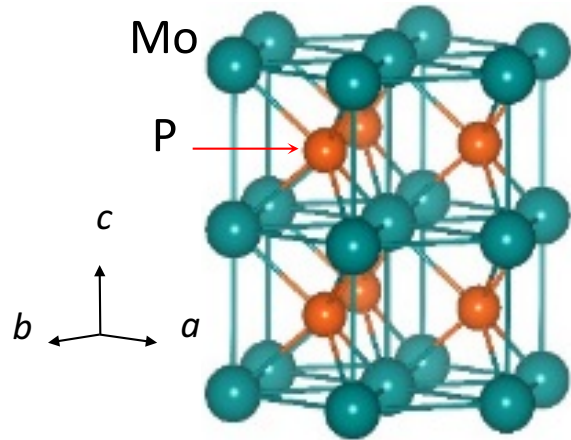
Pt: 2000 $\frac{\hbar}{e} (\Omega \text{ cm})^{-1}$

Guo et al., PRL 100, 096401 (2008)

J. Appl. Phys. 105, 07C701 (2009)

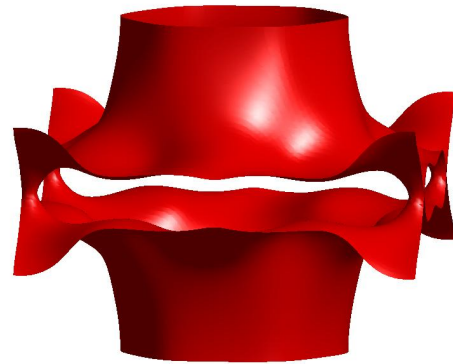
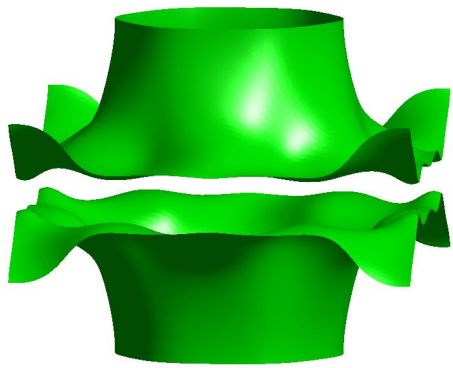


MoP better than Copper

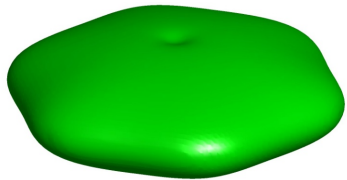




Fermi surfaces



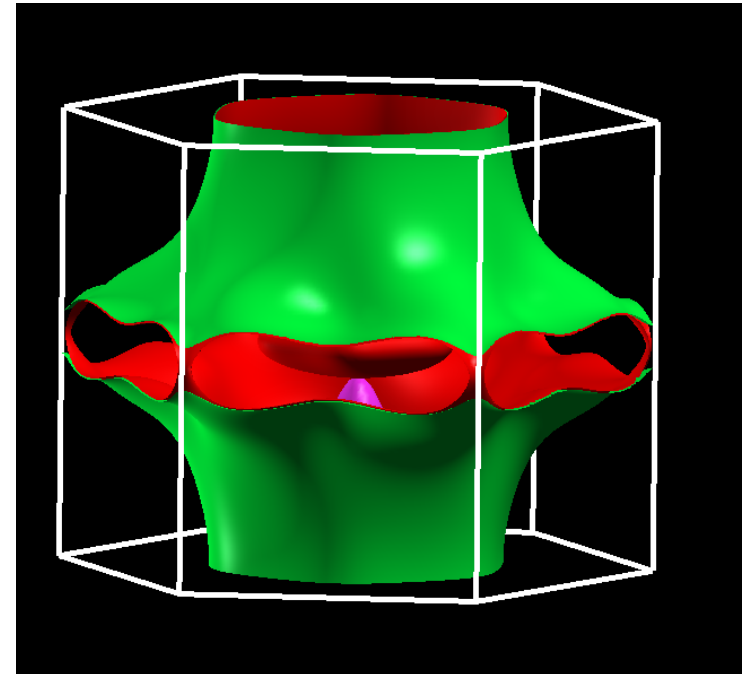
$$2.7 \times 10^{22} \text{ cm}^{-3}$$



$$1.12 \times 10^{21} \text{ cm}^{-3}$$



$$2.57 \times 10^{20} \text{ cm}^{-3}$$



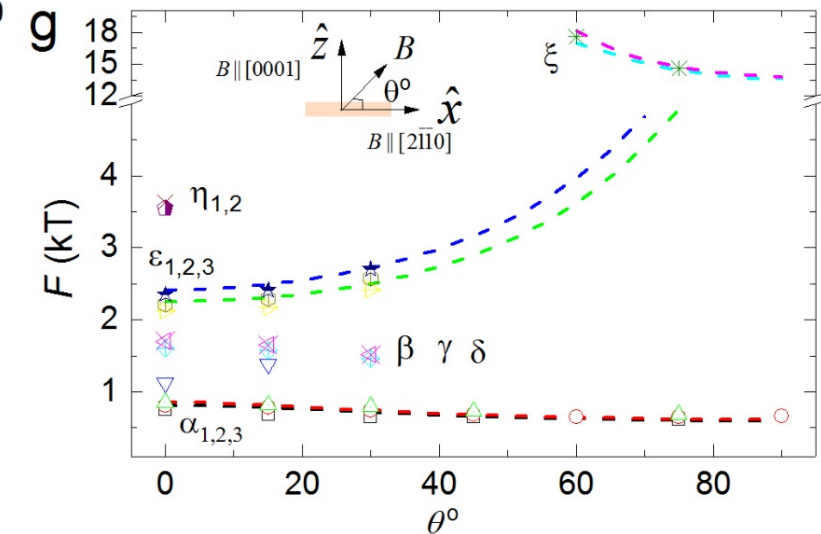
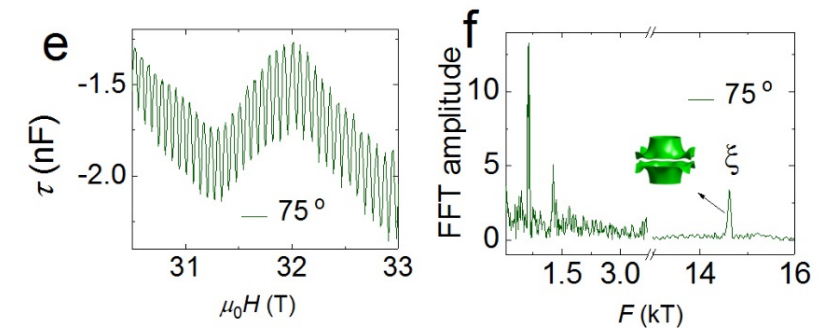
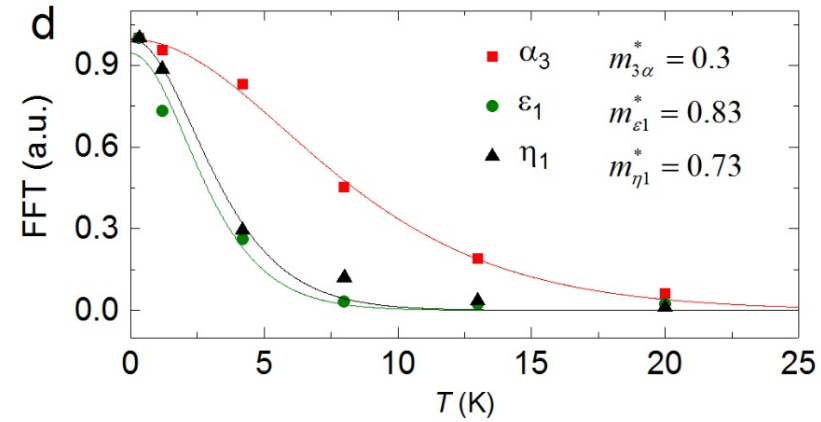
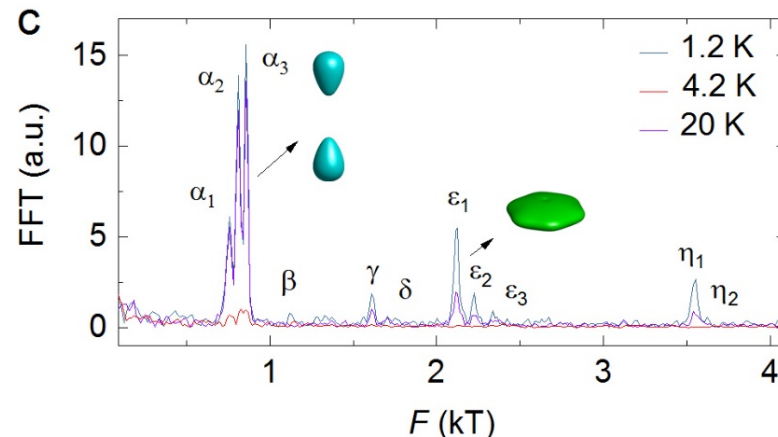
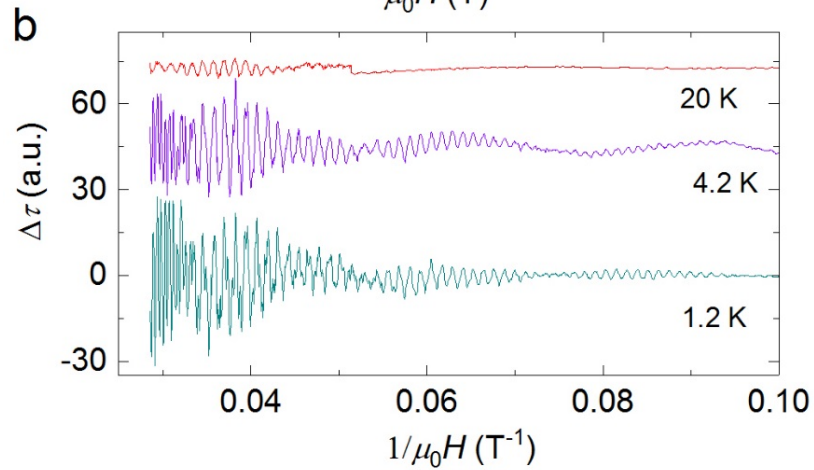
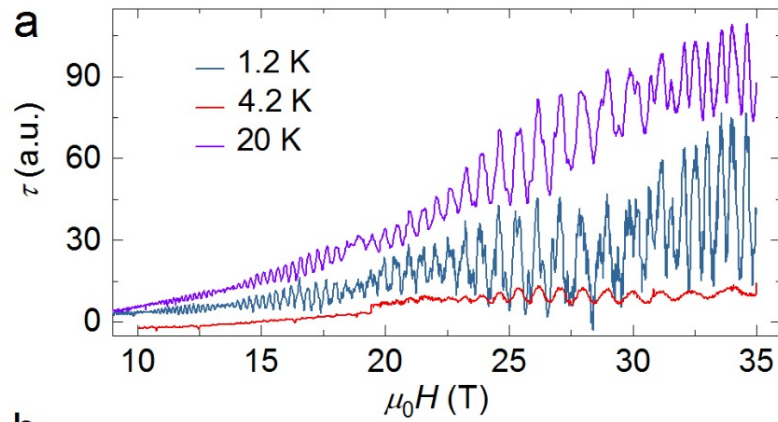
**Charge carriers are mainly
from the open Fermi surface**

Experimental measurement is around
 $3.2 \times 10^{22} \text{ cm}^{-3}$ at 2K

Experiment and calculation have the
same order of magnitude



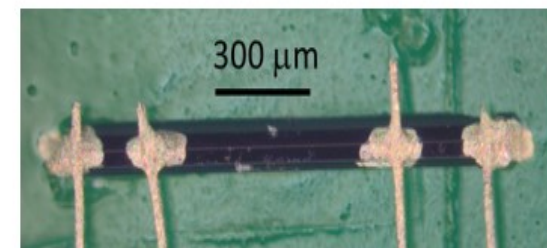
Quantum Oscillations





Macroscopic Mean Free Path

Compound	ρ (Ωcm)	l (μm)	μ ($\text{cm}^2\text{V}^{-1}\text{s}^{-1}$)	n (cm^{-3})
MoP	6×10^{-9}	11	2.4×10^4	2.9×10^{22}
WP ₂	3×10^{-9}	530	4×10^6	5×10^{20}
WC	0.35×10^{-6}		$\sim 1 \times 10^4$	4×10^{20}
PtCoO ₂	40×10^{-9}	5	0.7×10^4	2.2×10^{22}
PdCoO ₂	9×10^{-9}	20	2.8×10^4	2.4×10^{22}

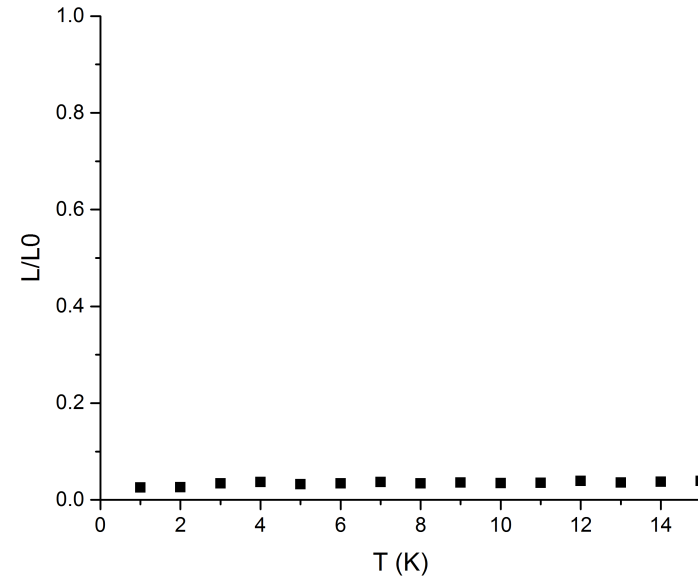
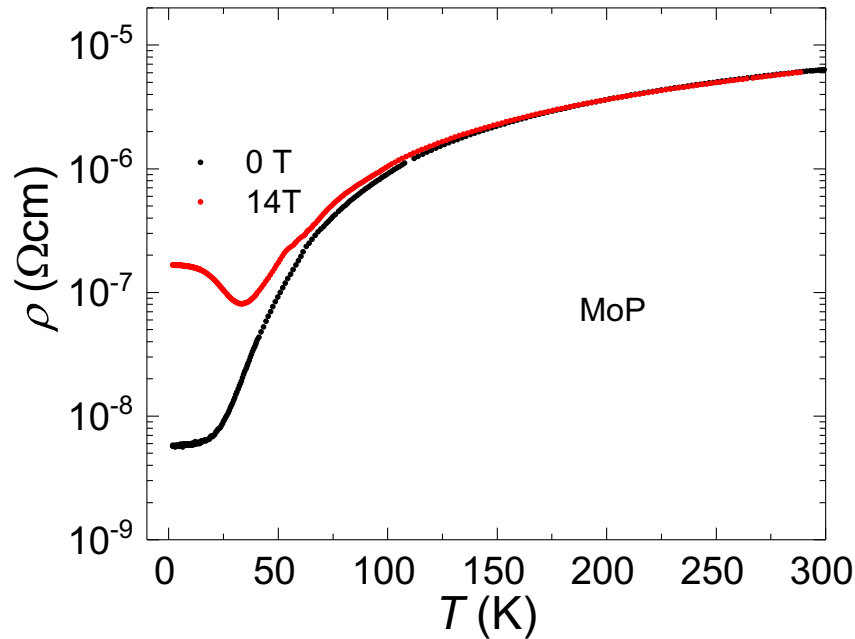


WC J. B. He et al. arXiv:1703.03211
Pallavi Kushwaha, et al. Sci. Adv.1 (2015) e150069
P. Moll Science 351, (2016) 1061

Chandra Shekhar et al. arXiv:1703.03736
Nitesh, et al.; arXiv:1703.04527



Hydrodynamic



- A strong violation of the Wiedemann-Franz law
- The Lorentz

$$L \equiv \frac{\kappa}{\sigma T} = \frac{\pi^2}{3} \equiv L_0$$

Compound	ρ (Ωcm)	l (μm)	μ ($\text{cm}^2\text{V}^{-1}\text{s}^{-1}$)	n (cm^{-3})
MoP	6×10^{-9}	11	2.4×10^4	2.9×10^{22}
WP ₂	3×10^{-9}	530	4×10^6	5×10^{20}
WC	0.35×10^{-6}		$\sim 1 \times 10^4$	4×10^{20}
PtCoO ₂	40×10^{-9}	5	0.7×10^4	2.2×10^{22}
PdCoO ₂	9×10^{-9}	20	2.8×10^4	2.4×10^{22}



What comes next?



RESEARCH

RESEARCH ARTICLE SUMMARY

TOPOLOGICAL MATTER

Beyond Dirac and Weyl fermions: Unconventional quasiparticles in conventional crystals

Barry Bradlyn,* Jennifer Cano,* Zhijun Wang,* M. G. Vergniory, C. Felser, R. J. Cava, B. Andrei Bernevig†

Fermions in condensed-matter systems are not constrained by Poincare symmetry. Instead, they must only respect the crystal symmetry of one of the 230 space groups. Hence, there is the potential to find and classify free fermionic excitations in solid-state systems that have no high-energy counterparts.

What comes next? Magnetic Space groups

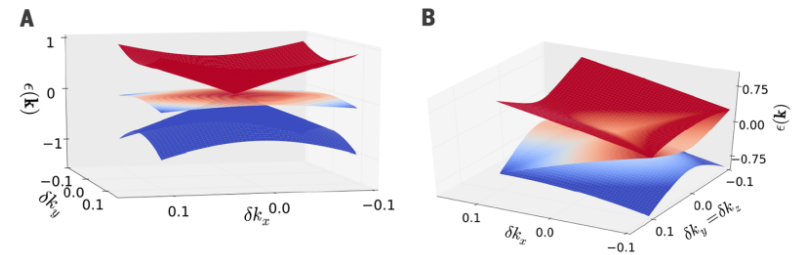
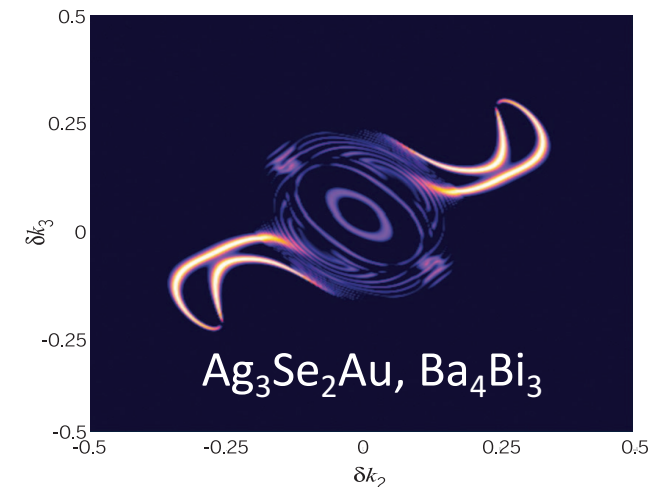
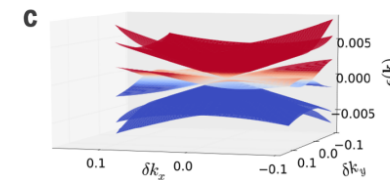
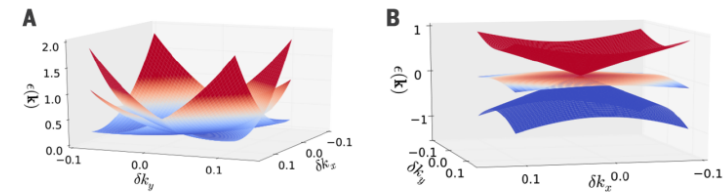


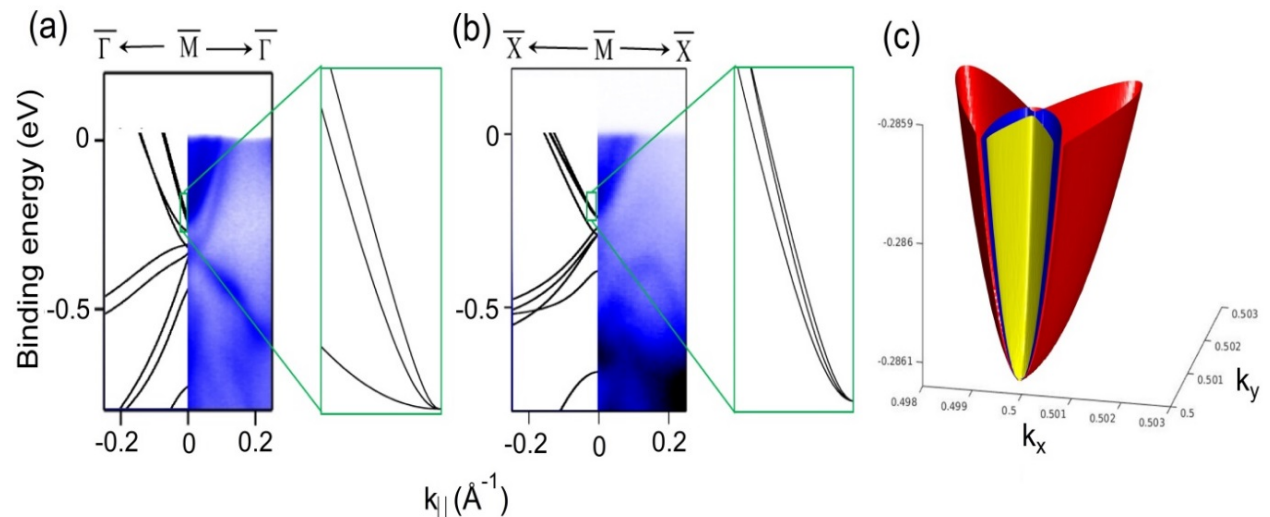
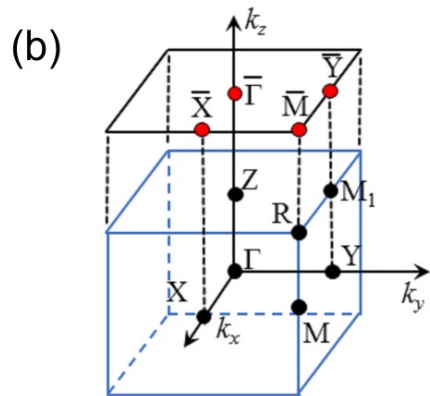
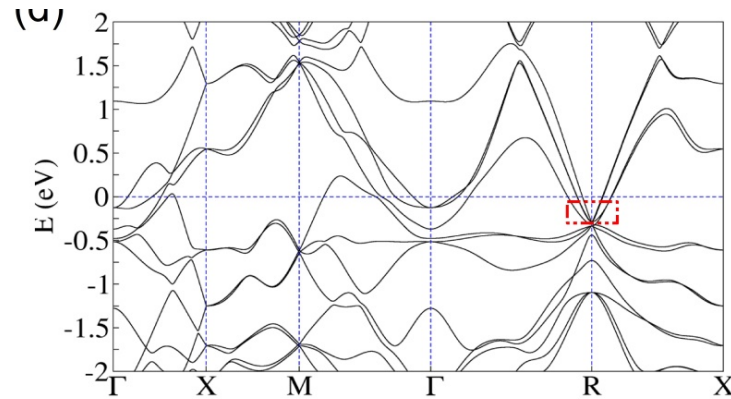
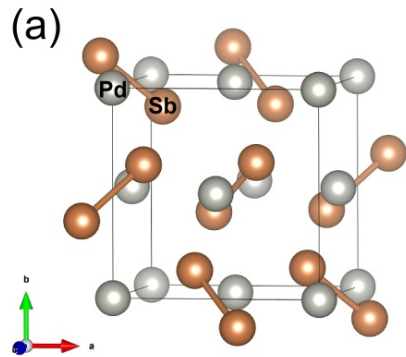
Fig. 1. Energy dispersion near a threefold degeneracy at the P point. (A and B) Shown are threefold degenerate points in (A) SGs 199 and 214 and (B) SG 220. In the latter case, pairs of bands remain degenerate in energy along the high-symmetry lines $|\delta k_x| = |\delta k_y| = |\delta k_z|$.



Science, 353, 6299, (2016)



Example: PdSb₂



6-fold fermions at the R point

Since SG 205 contains inversion symmetry, all bands are doubly degenerate

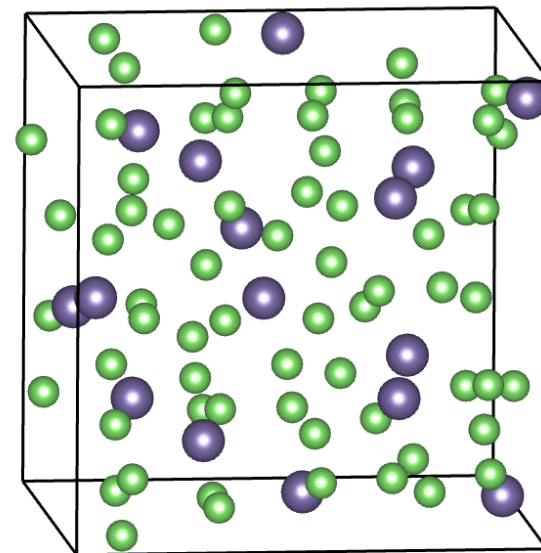
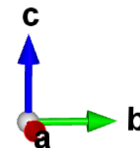
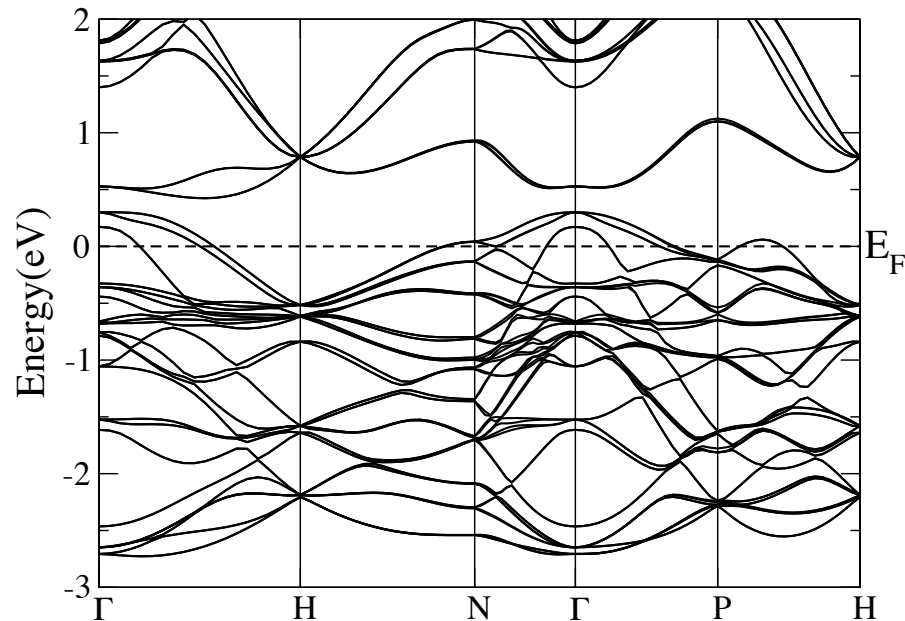


• non-symmorphic: elements with *fractional lattice translations* (157)

- Cubic crystal structure for high degenerations
- Non symmorphic is essential for stabilizing six- and eight-fold degenerate points.

Novel Metals

- SG I-43d (220) has elementary band representations with 16 branches -> 16fold connected metal if topologically trivial
- Filling -1/8 (lowest filling possible in a material is 1/24)
- Examples in the $A_{15}B_4$ material class (Here $Li_{15}Ge_4$)





Universe – applying a lattice



Bringing order to the expanding fermion zoo

Carlo Beenakker Commentary

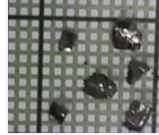
Heisenberg (1930): We observe space as a continuum, but we might entertain the thought that there is an underlying lattice and that space is actually a crystal. Which particles would inhabit such a lattice world? Werner Heisenberg *Gitterwelt* (lattice world) hosted electrons that could morph into protons, photons that were not massless, and more peculiarities that compelled him to abandon “this completely crazy idea”



Topology – interdisciplinary

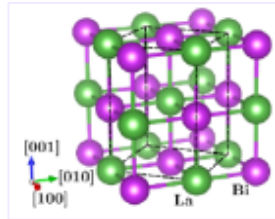
Chemistry

Real space - local
Crystals



LaBi

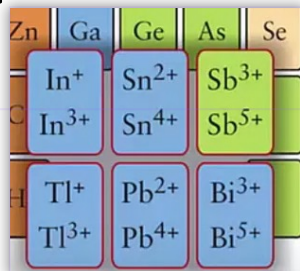
Crystal structure



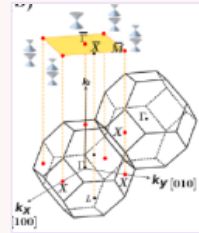
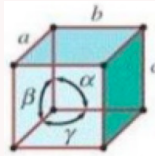
Position of the atoms
Orbitals

Check	WP	Representative
<input type="checkbox"/>	8g	x,y,z
<input type="checkbox"/>	4f	x,1/2,z
<input type="checkbox"/>	4e	x,0,z
<input checked="" type="checkbox"/>	4d	x,x,z
<input checked="" type="checkbox"/>	2c	1/2,0,z
<input type="checkbox"/>	1b	1/2,1/2,z
<input checked="" type="checkbox"/>	1a	0,0,z

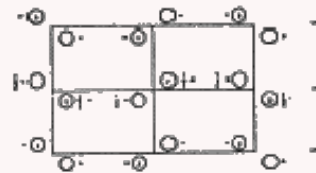
Inert pair effect



Symmetry



Local symmetry

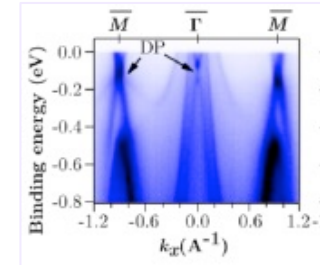
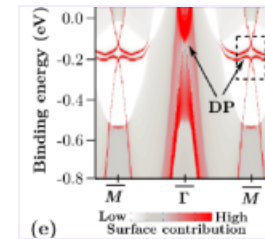


Relativistic effects

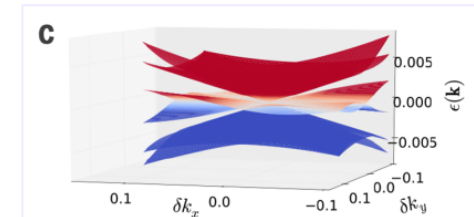
Physics

Recipro. space - delocalized
Brillouin zone

Electronic structure



Band connectivity

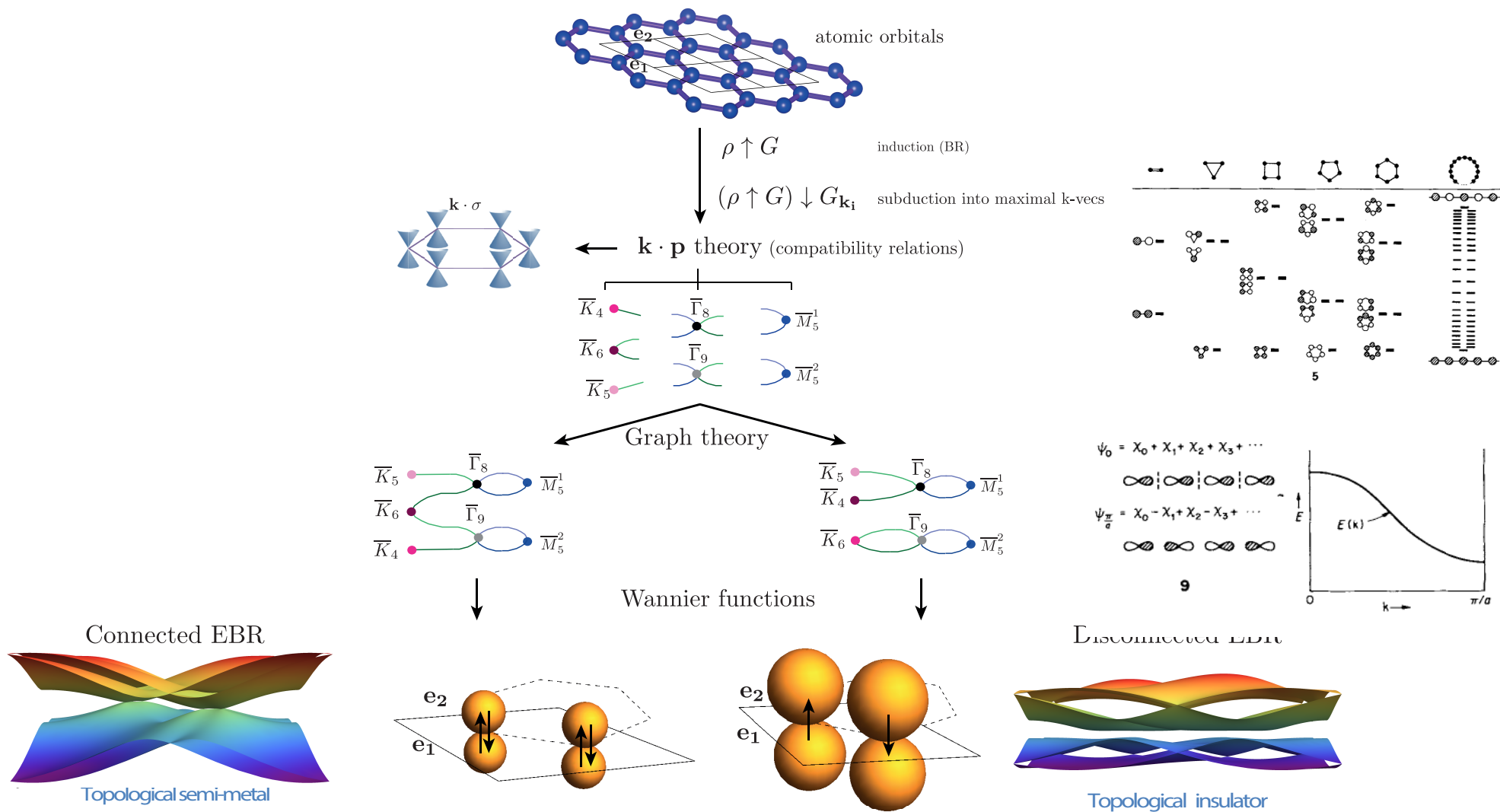


Darwin term

$$H_{\text{Darwin}} = \frac{\hbar^2}{8m_e^2 c^2} (\Delta V)$$

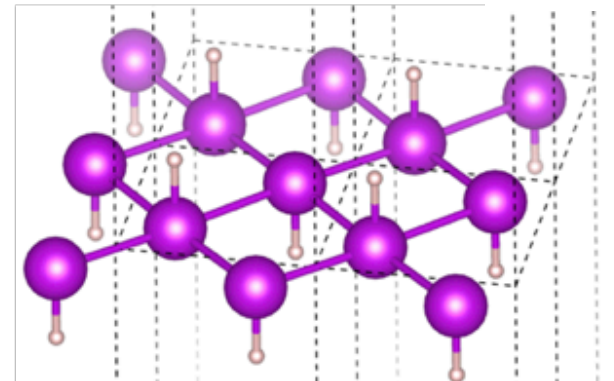
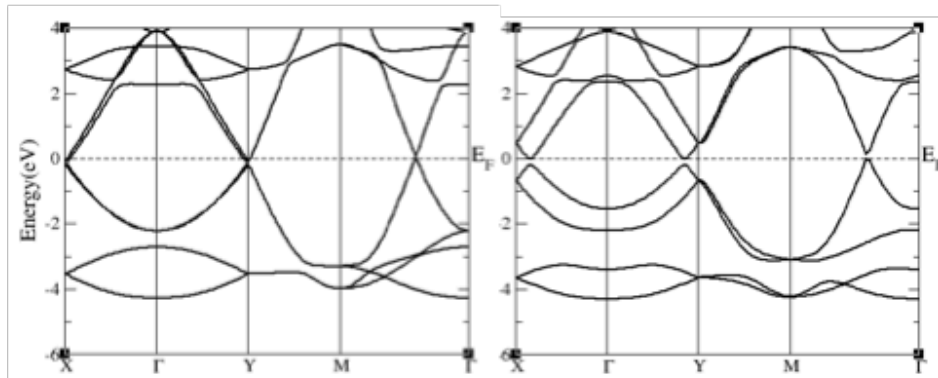
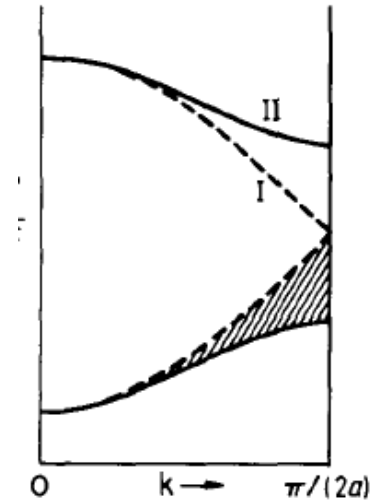
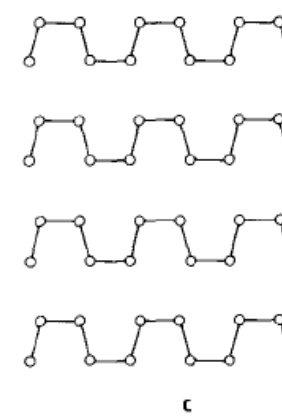
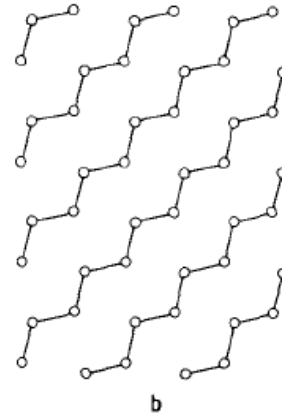
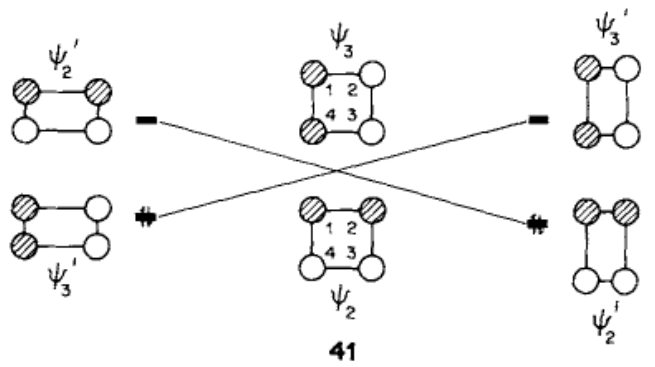


Translation





Square nets of electron doped Bi



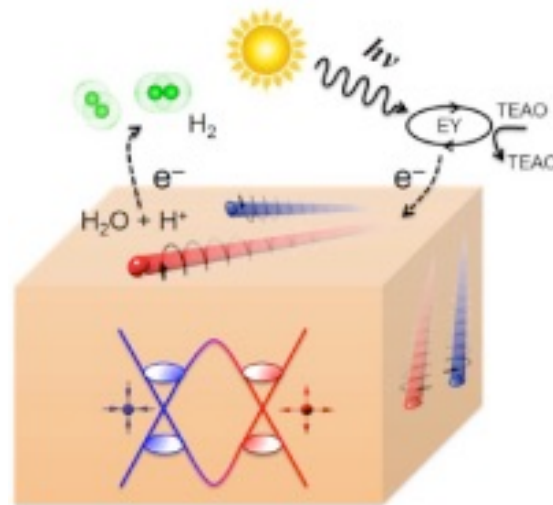
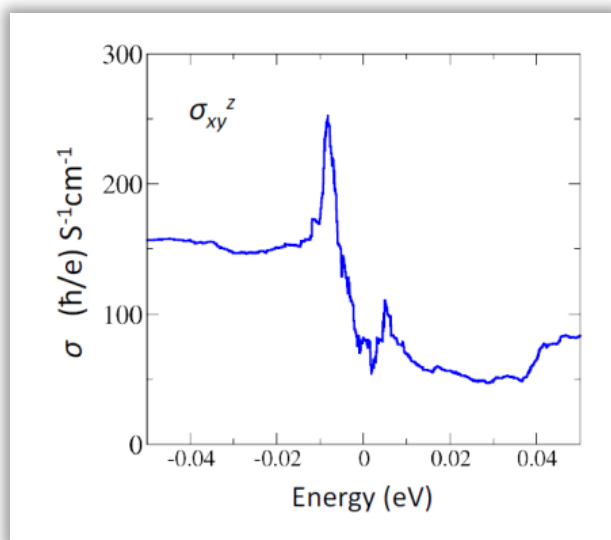
Square Nets of Main Group Elements in Solid-State Materials

Wolfgang Tremel¹ and Roald Hoffmann*

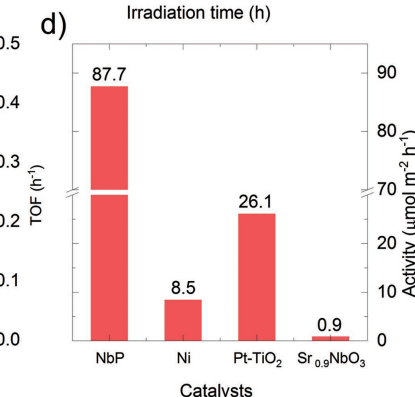
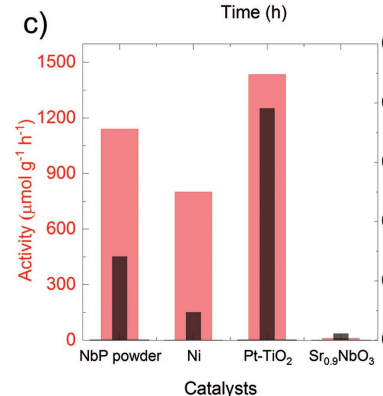
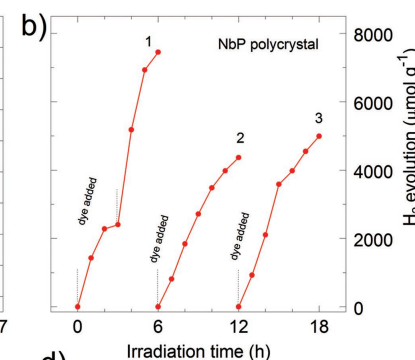
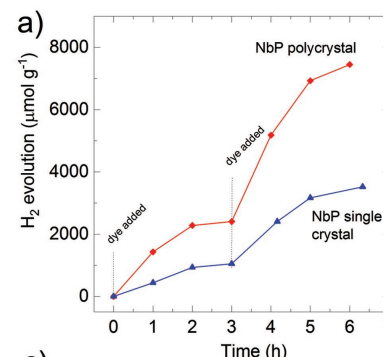
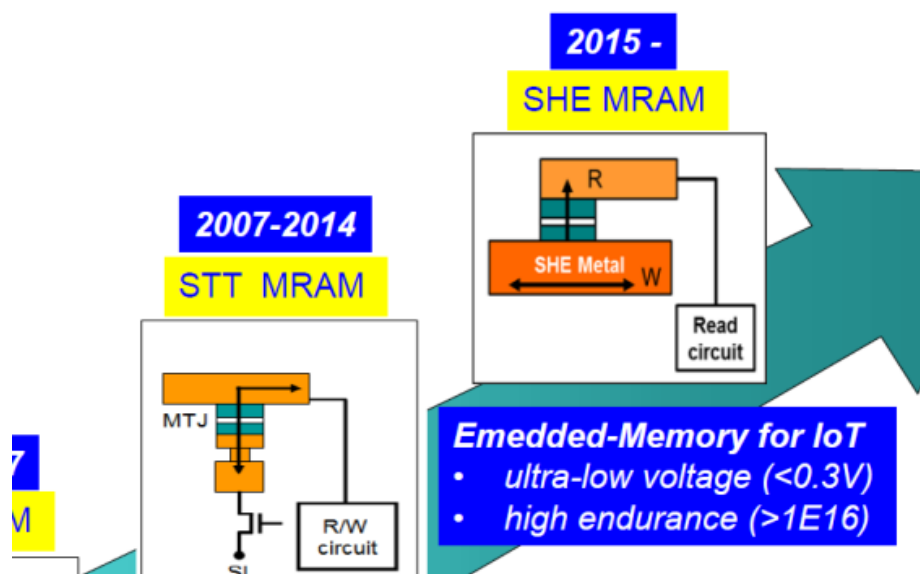
Contribution from the Department of Chemistry and Materials Science Center, Cornell University, Ithaca, New York 14853. Received May 29, 1986



Application Spin Hall Effect and Catalysis



ITRI's MRAM Roadmap



Yang Zhang, et al. PRB **95** (2017) 075128, preprint . arXiv:1610.04034
 Yan Sun, et al. PRL **117** (2016) 146401 preprint arXiv:1604.07167

Catherine R. Rajamathi et al. and C.N.R. Rao, Advanced Materials 2017 preprint arXiv:1608.03783



Summary

Is there a relation between reciprocal and real space Berry curvature

Many materials proposed, only a few made

- More Weyl and Dirac semimetals
- More new Fermions
- High quality single crystals, defect free – or with defects
- Topological insulators in oxides, correlated systems
- Generalization of the concept

Magnetic Fermions

Thin films

Superconductors – Majorana

Chemical reactions

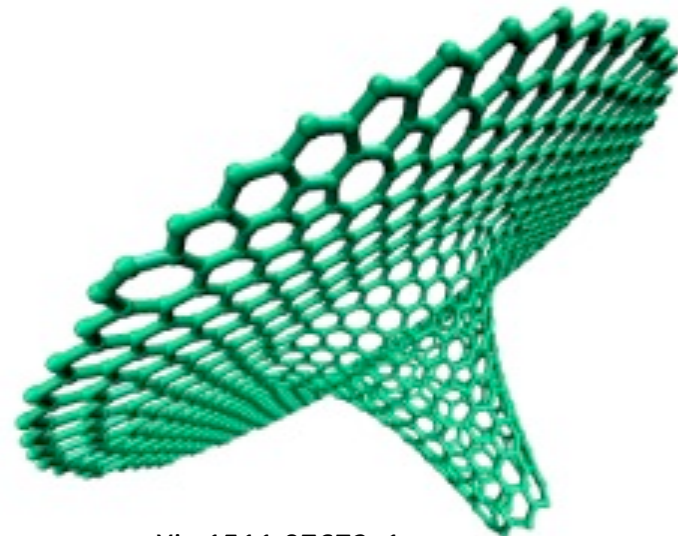
Phase transitions

New properties

- Thermal (magneto) transport
- (Magneto) optical properties ...
- Devices

Applications

- Electronics
- Chemistry (Catalysis) ...



arXiv:1511.07672v1



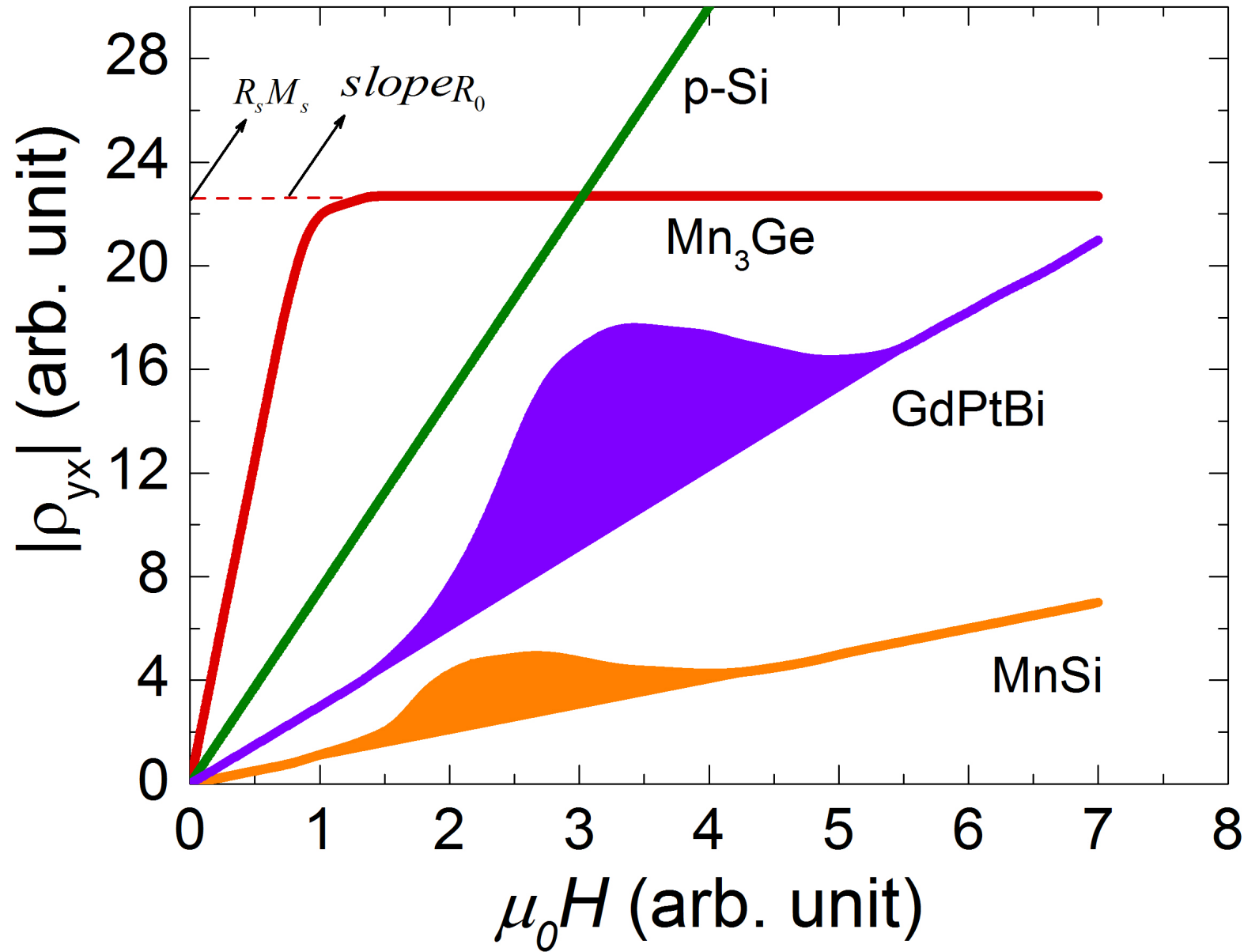
Single Crystals available

BaCr ₂ As ₂	AlPt	MoSe _{2-x} Tex	Ag ₂ Se	YPtBi	YbMnBi ₂
BaCrFeAs ₂	GdAs	MoTe _{2-x} Sex	IrO ₂	NdPtBi	Ni ₂ Mn _{1.4} In _{0.6}
	CoSi	MoTe ₂ (T'/2H)	OsO ₂	GdPtBi	YFe ₄ Ge ₂
CaPd ₃ O ₄			ReO ₂	YbPtBi	
SrPd ₃ O ₄	MoP	PtTe ₂	WP ₂	ScPdBi	Mn _{1.4} PtSn
BaBiO ₃	WP	PtSe ₂	MoP ₂	YPdBi	
		PdTe ₂		ErPdBi	CuMnSb
Bi ₂ Te ₂ Se	TaP	PdSe ₂	VAI ₃	GdAuPb	CuMnAs
Bi ₂ Te ₃	NbP	OsTe ₂	Mn ₃ Ge	TmAuPb	
Bi ₂ Se ₃	NbAs	RhTe ₂	Mn ₃ Ir	AuSmPb	Co ₂ Ti _{0.5} V _{0.5} Sn
BiSbTe ₂ S	TaAs	TaTe ₂	Mn ₃ Rh	AuPrPb	Co ₂ VAI _{0.5} Si _{0.5}
BiTeI	NbP-Mo	NbTe ₂	Mn ₃ Pt	AuNdPb	Co ₂ Ti _{0.5} V _{0.5} Si
BiTeBr	NbP-Cr	WSe ₂	Os	Mn ₃ Si	Mn ₂ CoGa
BiTeCl	TaP-Mo	HfTe ₅	Os	AuLusn	Co ₂ MnGa
	TaAsP	MoTe ₂		AuYSn	Co ₂ Al ₉
LaBi, LaSb		TaS ₂		ErAuSn	Co ₂ MnAl
GdBi, GdSb	CrNb ₃ S ₆	PdSb ₂		EuAuBi	Co ₂ VGa _{0.5} Si _{0.5}
	V ₃ S ₄	CuxWTe ₂			Co ₂ TiSn
HfSiS	Cd ₃ As ₂	FexWTe ₂		CaAgAs	Co ₂ VGa
		WTe ₂			Co ₂ V _{0.8} Mn _{0.2} Ga
Bi ₄ I ₄	MnP	Co _{0,4} Ta ₂ S ₂		KMgSb	CoFeMnSi
	MnAs	Fe _{0,4} Ta ₂ S ₂		KMgBi	
BaSn ₂				KHgSb	
				KHgBi	
				LiZnAs	
				LiZnSb	

Thank you!

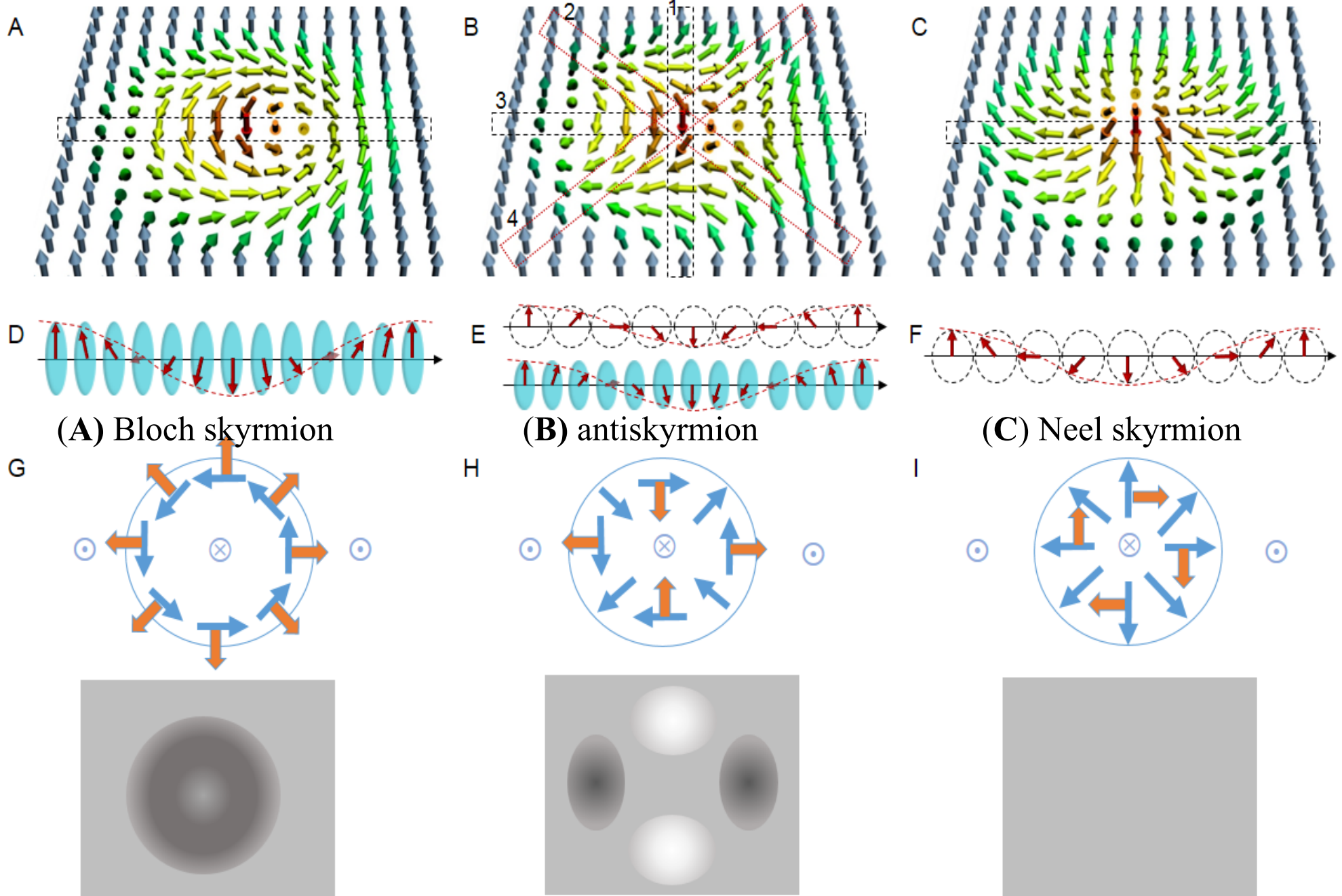


Anomalous Hall effect





Real space topology - Skyrmions





Mn_{1.4}Pt_{0.9}Pt_{0.1}Sn: Anti-Skyrmions

